
Electronic Thesis and Dissertation Repository

8-16-2016 12:00 AM

Controlled Delivery of Angiogenic and Arteriogenic Growth Factors from Biodegradable Poly(ester amide) Electrospun Fibers for Therapeutic Angiogenesis

Somiraa S. Said, *The University of Western Ontario*

Supervisor: Kibret Mequanint, *The University of Western Ontario*

A thesis submitted in partial fulfillment of the requirements for the Doctor of Philosophy degree in Biomedical Engineering

© Somiraa S. Said 2016

Follow this and additional works at: <https://ir.lib.uwo.ca/etd>

 Part of the [Biomaterials Commons](#), [Nanomedicine Commons](#), and the [Polymer Science Commons](#)

Recommended Citation

Said, Somiraa S., "Controlled Delivery of Angiogenic and Arteriogenic Growth Factors from Biodegradable Poly(ester amide) Electrospun Fibers for Therapeutic Angiogenesis" (2016). *Electronic Thesis and Dissertation Repository*. 3951.

<https://ir.lib.uwo.ca/etd/3951>

This Dissertation/Thesis is brought to you for free and open access by Scholarship@Western. It has been accepted for inclusion in Electronic Thesis and Dissertation Repository by an authorized administrator of Scholarship@Western. For more information, please contact wlsadmin@uwo.ca.

Abstract

Therapeutic angiogenesis has emerged as a novel treatment approach for ischemic vascular diseases. It relies on the delivery of exogenous growth factors to stimulate neovessel formation. However, systemic administration of angiogenic factors results in rapid clearance from the site of interest due to their short biological half-life. Mimicking the angiogenesis process is multifaceted; therefore, therapeutic angiogenesis regimens should recapitulate both temporal and spatial presentation of multiple growth factors. In this work, controlled delivery of two growth factors, an angiogenic factor –fibroblast growth factor-2 (FGF2), and an arteriogenic factor –fibroblast growth factor-9 (FGF9), from biodegradable poly(ester amide) (PEA) electrospun fibers towards targeting neovascular formation and maturation, is reported.

FGF2 and FGF9 were dual loaded into PEA fibers using a mixed blend and emulsion electrospinning technique. *In vitro* release kinetics of FGF2/FGF9 dual-loaded PEA fibers over a period of 70 days showed controlled and concurrent release of both factors in a bioactive form. Matrigel tube formation and Boyden chamber transwell assays conducted to evaluate endothelial cell (EC) tube formation, directed smooth muscle cell (SMC) migration, and EC-SMC interaction demonstrated that co-released FGF2 and FGF9 from dual loaded PEA fibers enhanced EC tube formation ($p < 0.05$), directed-migration of SMCs towards PDGF-BB ($p < 0.05$), and EC/SMC tube stabilization. An *ex ovo* chick chorioallantoic membrane (CAM) model coupled with power Doppler ultrasound imaging, and an *in vivo* ischemic hindlimb mouse model were employed to assess the *in vivo* angiogenic capacity of the delivery system. The CAM assay did not show a significant increase in the vascular density of the full CAM surface treated with FGF2/FGF9 dual-loaded fibers ($p > 0.05$); however, the 3D power Doppler volumes displayed enhanced localized angiogenesis underneath the fibrous mats with enhanced blood perfusion and flow, as indicated by a statistically significant increase in vascularization and vascularization flow indices for the dual-loaded PEA fibers group versus the unloaded PEA fibers group ($p < 0.05$).

In order to evaluate the effectiveness of FGF9-loaded PEA fibers *in vivo*, an ischemic hindlimb mouse model was used. Histological analysis of the ischemic tibialis anterior muscle revealed increased percentage of mural cell-covered microvessels in mice treated with FGF9-loaded PEA fibers than those treated with unloaded fibers. Interestingly, CatWalk gait analysis 7 days

post-ischemia did not demonstrate superior restoration of the ischemic hindlimb function for the mice treated with FGF9-loaded PEA fibers, which might be too early for the healing of the injured limb. Taken together, the data in this thesis supports the premise that controlled delivery of fibroblast growth factors from biodegradable PEA electrospun fibers can provide means for minimally invasive revascularization of ischemic tissues as a novel approach for treatment of ischemic vascular diseases.

Keywords

Therapeutic angiogenesis; Controlled release; Angiogenic growth factors; Electrospun poly(ester amide)s (PEAs) fibers; Fibroblast growth factor-2 (FGF2); Fibroblast growth factor-9 (FGF9).

Co-Authorship Statement

The work conducted in this thesis was a collaborative effort. Individual contributions are detailed below:

Chapter 1: Somiraa Said— wrote the chapter, Dr. Kibret Mequanint and Dr. Geoffrey Pickering— revised the chapter.

Chapter 2: A version of this chapter is published as a review article “Somiraa S. Said, J. Geoffrey Pickering and Kibret Mequanint, *Journal of Vascular Research* (2013), 50; 35-51”. Somiraa Said— wrote the first draft, Dr. Kibret Mequanint and Dr. Geoffrey Pickering— revised and edited the manuscript.

Chapter 3: A version of this chapter is published as a research article “Somiraa S. Said, J. Geoffrey Pickering and Kibret Mequanint, *Pharmaceutical Research* (2014), 31(12); 3335-3347”. Somiraa Said— conducted the experimental work, data collection and analysis, and wrote the first draft, Dr. Kibret Mequanint— provided study guidelines and experimental design, revised and edited the manuscript, and Dr. Geoffrey Pickering— revised and edited the manuscript.

Chapter 4: A version of this chapter is published as a research article “Somiraa S. Said, Caroline O’Neil, Hao Yin, Zengxuan Nong, J. Geoffrey Pickering and Kibret Mequanint, *Tissue Engineering Part A* (2016), 22(7-8): 584-596”. Somiraa Said— polymer synthesis, preparation and characterization of the FGF-loaded PEA fibers, *in vitro* studies experimental setup, real-time PCR analysis, phase contrast, confocal and fluorescence microscopy imaging, data collection and analysis, and wrote the first draft, Caroline O’Neil— performed the Matrigel tube formation and Boyden chamber migration assays, Dr. Zengxuan Nong— performed the surgery on the mice and harvested the tissues for histological analysis, Dr. Hao Yin— performed H&E staining for the tissue sections and provided interpretation for the histological data, Dr. Kibret Mequanint and Dr. Geoffrey Pickering— provided study guidelines and experimental design, supervised the study, revised and edited the manuscript.

Chapter 5: A version of this chapter is currently in preparation to be submitted for publication as “Somiraa S. Said, Hao Yin, Mai Elfarnawany, Zengxuan Nong, Caroline O’Neil, Hon

Leong, James Lacefield, Kibret Mequanint and Geoffrey Pickering”. Somiraa Said— polymer synthesis, preparation of the FGF-loaded PEA fibers, experimental setup for the CAM experiments, digital image acquisition for the CAMs and post-analysis using Fiji software, data collection and analysis, and wrote the first draft, Dr. Hao Yin— experimental setup for the mouse ischemic hindlimb experiments, performed the CatWalk assay, H&E and double immunostaining for the tissue sections, and provided interpretation for the histological data, Caroline O’Neil— was responsible for animal handling and care and performed the histological tissue sectioning, Dr. Zengxuan Nong— performed the surgery on the mice and harvested the tissues for histological analysis, Dr. Mai Elfarnawany— performed the power Doppler ultrasound imaging of the CAMs and image processing using a previously developed MATLAB code for vascular quantification, Dr. Hon Leong— provided the CAMs and their handling and care at his lab in St. Joseph’s Hospital, Dr. James Lacefield— provided access to the ultrasound imaging facility at Robarts and supervision to Dr. Elfarnawany, Dr. Kibret Mequanint and Dr. Geoffrey Pickering— provided supervision, revised and edited the manuscript.

Chapter 6: Somiraa Said— wrote the chapter, Dr. Kibret Mequanint and Dr. Geoffrey Pickering— revised the chapter.

This thesis is dedicated to the memory of my grandfather,

El-Said Said.

Acknowledgments

First and foremost, thanks are due to Allah. This thesis would have never come to completion without the support and contributions of many individuals, to each I extend my deepest appreciation.

I would like to acknowledge the guidance and support from my supervisors Dr. Kibret Mequanint and Dr. Geoffrey Pickering, as well as my advisory committee members Dr. Amin Rizkalla and Dr. Stephen Sims. I would also like to thank the Canadian Institutes of Health Research (CIHR) for financial support through the CIHR Strategic Training Program in Vascular Research.

I would like to convey my sincere thanks to all previous and current members of the Mequanint's group, especially Dr. Kalin Penev, for all his constructive feedback and insights in my work specially the statistics. I would like to deeply thank Dr. Darryl Knight for being my mentor through the early years of my PhD studies, giving me such a comprehensive training on all lab equipment and related protocols, the chemical synthesis of poly(ester amide)s, as well as the insightful discussions regarding our scientific research and life in general.

I would like to thank Dr. Pickering's lab members, especially Dr. Hao Yin, Caroline O'Neil, and Dr. Zengxuan Nong for their expert help in conducting the *in vivo* studies including the animal surgery and the subsequent histological processing and analysis. Also, I would like to acknowledge the help of Dr. Hon Leong and Dr. James Lacefield in facilitating the CAM study and the power Doppler ultrasound imaging.

I am deeply thankful to my Engineering buddies, Melissa Salem, Sama Hussein and Dr. Mai Elfarnawany, for making this journey more fun and lifting up my spirits when I am feeling down.

I am extremely indebted to my parents, my sister and my lovely daughter Nada for their unconditional love and their enduring support throughout the years. Special thanks are due to my dear husband, Omar El-Halfawy, for his understanding and his unselfish support along the work in this thesis and for always being my "first go-to reviewer".

Table of Contents

Co-Authorship Statement.....	iii
Acknowledgments.....	vi
Table of Contents.....	vii
List of Tables.....	xii
List of Figures.....	xiii
Chapter 1	1
1 Introduction.....	1
1.1 Overview.....	1
1.2 Hypothesis and Objectives.....	2
1.2.1 Hypothesis.....	2
1.2.2 Objectives.....	3
1.3 Thesis Outline.....	3
1.4 References.....	4
Chapter 2	6
2 Literature Review: Advances in Growth Factor Delivery for Therapeutic Angiogenesis.....	6
2.1 Abstract.....	6
2.2 Introduction.....	7
2.3 Blood Vessel Formation: Vasculogenesis, Angiogenesis and Arteriogenesis.....	8
2.4 Angiogenic Growth Factors.....	10
2.4.1 Vascular Endothelial Growth Factor (VEGF) Family.....	11
2.4.2 Fibroblast growth factor (FGF) family.....	12
2.4.3 Platelet-derived Growth Factor (PDGF).....	13
2.4.4 Other Angiogenic Stimulators.....	14
2.5 Angiogenic Growth Factor Delivery.....	14

2.5.1	Protein <i>versus</i> Gene Therapy	14
2.5.2	Gene Transfer in Therapeutic Angiogenesis.....	15
2.6	Preclinical Studies.....	16
2.6.1	<i>In vivo</i> Studies with Vascular Endothelial Growth Factor.....	16
2.6.2	<i>In vivo</i> Studies with Fibroblast Growth Factor	16
2.7	Clinical Trials in Ischemic Heart Disease.....	17
2.8	Targeting Neovascular Maturation	21
2.8.1	Cues for Functional Blood Vessel Formation.....	21
2.8.2	Co-delivery of Ang-1, PDGF-BB, or HGF with VEGF and FGF-2 for Vascular Stabilization	22
2.8.3	Acquiring Neovasculature Vasoresponsiveness	24
2.9	Angiogenic Growth Factors Delivery Technologies	26
2.9.1	Controlled Delivery of Angiogenic Factors from Polymer-based Systems	26
2.9.2	Electrospun Fibers as Angiogenic Factor Delivery Vehicles	28
2.9.3	Spatio-temporal Controlled Delivery of Angiogenic Factors.....	29
2.10	Safety of Angiogenic Growth Factor Delivery	30
2.11	Conclusions	31
2.12	References	32
Chapter 3	48
3	Controlled Delivery of Fibroblast Growth Factor-9 from Biodegradable Poly(ester amide) Fibers for Building Functional Neovasculature	48
3.1	Abstract.....	48
3.2	Introduction.....	49
3.3	Materials and Methods.....	51
3.3.1	Materials	51
3.3.2	Synthesis of Poly(ester amide) by Interfacial Polymerization.....	52

3.3.3	Fabrication of PEA Electrospun Fibers	52
3.3.4	Characterization of PEA Electrospun Fibers	53
3.3.5	<i>In vitro</i> Degradation Study.....	53
3.3.6	Loading PEA Fibers with Model Protein and Fibroblast Growth Factor-9	54
3.3.7	Determination of Percentage Entrapment Efficiency	55
3.3.8	<i>In vitro</i> Release Study of BSA and FGF9-loaded PEA Electrospun Fibers	55
3.3.9	Bioactivity Assay of the Released Growth Factor	55
3.3.10	Cell Viability and Confocal Microscopy	56
3.3.11	RNA Isolation and Quantitative Real-time PCR Analysis	57
3.3.12	Statistical Analysis.....	58
3.4	Results and Discussion	59
3.4.1	Synthesis of PEA by Interfacial Polymerization	59
3.4.2	Fabrication and Optimization of PEA Electrospun Fibers	60
3.4.3	<i>In vitro</i> Degradation Study.....	63
3.4.4	<i>In vitro</i> Release Study of Loaded PEA Electrospun Fibers	64
3.4.5	Bioactivity Assay of the Released Growth Factor	67
3.4.6	Cell Viability and Confocal Microscopy	68
3.4.7	RNA Isolation and Quantitative Real-time PCR Analysis	71
3.5	Conclusions.....	73
3.6	References.....	73
Chapter 4	78
4	Concurrent and Sustained Delivery of FGF2 and FGF9 from Electrospun Poly(ester amide) Fibrous Mats for Therapeutic Angiogenesis.....	78
4.1	Abstract.....	78
4.2	Introduction.....	79

4.3	Materials and Methods.....	81
4.3.1	Materials	81
4.3.2	Cell Culture and Maintenance	82
4.3.3	Dual-loading of PEA Fibers.....	82
4.3.4	Characterization of PEA Electrospun Fibers	83
4.3.5	<i>In vitro</i> Release Study of Dual-loaded PEA Electrospun Fibers	83
4.3.6	<i>In vitro</i> Angiogenesis Assays: Matrigel Tube Formation Assay	84
4.3.7	Directed Human Coronary Artery Smooth Muscle Cell Migration Assay	85
4.3.8	<i>In vitro</i> Gene Expression of the Inflammatory Marker (Interleukin 8)	86
4.3.9	RNA Isolation and Quantitative Real–time PCR Analysis.....	86
4.3.10	Implantation into Subcutaneous and Tibialis Anterior Muscle Tissues ...	87
4.3.11	Statistical Analysis.....	88
4.4	Results.....	88
4.4.1	Differential Release of FGF2 and FGF9 from Dual-loaded PEA Fibers..	88
4.4.2	Co-released FGF2 and FGF9 from PEA Fibers Enhanced Tube Formation and Directed SMC Migration.....	91
4.4.3	FGF2 and FGF9 Dual-loaded PEA Fibers did not Induce Inflammatory Responses.....	96
4.5	Discussion.....	100
4.6	Conclusions.....	103
4.7	References.....	103
Chapter 5	110
5	<i>In vivo</i> Evaluation of FGF-loaded Electrospun Poly(ester amide) Fibers for Therapeutic Angiogenesis.....	110
5.1	Abstract.....	110
5.2	Introduction.....	111
5.3	Material and Methods	113

5.3.1	Materials	113
5.3.2	Chick Chorioallantoic Membrane (CAM) as an Angiogenesis Screening Platform for FGF2/FGF9 Dual-loaded PEA Fibrous Mats.....	113
5.3.3	Ischemic Hindlimb Mouse Model: <i>In vivo</i> Angiogenesis Assay for FGF9-loaded PEA Fibers	118
5.3.4	Statistical Analysis.....	121
5.4	Results and Discussion	121
5.4.1	FGF2/FGF9 Dual-loaded PEA Fibers Induced Localized Angiogenesis in CAM Model.....	121
5.4.2	Controlled Release of FGF9 from PEA Fibers Stimulated Stable Microvessel Formation in Ischemic Hindlimb Mouse model.....	126
5.5	Conclusion	132
5.6	References.....	132
Chapter 6	137
6	General Discussion and Conclusions.....	137
6.1	Summary.....	137
6.2	Strengths and Limitations	140
6.3	Future Directions	142
6.4	Significance.....	143
6.5	References.....	144
Appendices.....	146
Appendix A: Copyright Permissions	146
Curriculum Vitae	152

List of Tables

Table 2-1: Selected signaling molecules involved in angiogenesis process.....	10
Table 2-2: Major randomized myocardial angiogenesis clinical trials using protein/gene therapy.....	18

List of Figures

Figure 2-1: Major events of the angiogenesis process.....	9
Figure 2-2: FGF9-mediated microvessel maturation.....	25
Figure 2-3: FGF9–stabilization of nascent microvessels through mural cells recruitment to endothelial cell tubes.....	26
Figure 3-1: Chemical structure and corresponding H ¹ -NMR of 8-Phe-4.....	59
Figure 3-2: Optimization of formulation electrospinning parameters.....	61
Figure 3-3: Optimization of process electrospinning parameters.....	62
Figure 3-4: <i>In vitro</i> degradation of PEA electrospun fibers at 37 °C for 28 days.....	63
Figure 3-5: <i>In vitro</i> release study of (A) BSA-loaded PEA fibers and (B) FGF9-loaded PEA fibers, using blend and emulsion electrospinning techniques, in PBS (pH=7.4) at 37 °C (n=3).	66
Figure 3-6: NIH-3T3 cell viability study on 2D PEA films (1% w/v), unloaded and FGF9-loaded 3D PEA emulsion electrospun fibers for 5 days, in Serum+ (5% FBS) and Serum- (serum depleted; 0.05% FBS) conditions, using MTT assay.	69
Figure 3-7: Confocal microscopy images of NIH-3T3, 10T1/2, and HCASMCs.....	70
Figure 3-8: (A) Quantitative real-time PCR analysis of PDGFR-β expression for NIH-3T3 cells seeded on FGF9-loaded emulsion electrospun fibers and PEA fibers with exogenous FGF9 for 24 h.....	72
Figure 4-1: Combined blend and emulsion electrospinning of growth factors facilitate differential release of the loaded proteins.....	90
Figure 4-2: Human coronary artery endothelial metabolic activity study on 3D FGF2/FGF9-loaded PEA fibers, unloaded fibers supplemented with soluble FGF2 and FGF9 as a positive	

control, and TCPS as a negative control, for 5 days using MTT assay. Data represents mean \pm SEM from three independent experiments.	91
Figure 4-3: Co-released FGF2 and FGF9 from PEA fibers increased endothelial cell tube formation. Endothelial cells were treated with co-released FGFs or soluble FGF and cultured on growth factor–reduced Matrigel for 24 h.	92
Figure 4-4: Co-released FGF2 and FGF9 enhanced directed smooth muscle cell migration.	94
Figure 4-5: Co-released FGF2 and FGF9 from dual-loaded PEA fibers stabilize tube formation.	95
Figure 4-6: FGF2/FGF9-loaded PEA electrospun fibers did not induce an inflammatory response <i>in vitro</i>	96
Figure 4-7: Subcutaneous implantation of FGF2/FGF9-loaded PEA electrospun fibers in B6 mice did not induce inflammatory cell infiltration.	98
Figure 4-8: Controlled delivery of FGF9 from PEA fibrous mats resulted in a dose-dependent expansion of mesenchymal progenitor-like cell layers and ECM deposition.	99
Figure 5-1: The <i>ex ovo</i> CAM cultivation protocol steps.	114
Figure 5-2: Steps of digital image pre-processing to produce the final binary CAM image used in percentage vascular density analysis.	116
Figure 5-3: Surgical procedure for induction of hindlimb ischemia by femoral artery ligation in C57BL6/J male mice.	119
Figure 5-4: The effect of FGF2/FGF9 dual-loaded PEA fibers on CAM vasculature.	122
Figure 5-5: The power Doppler 2D images of the control (no fibers), CAMs treated with soluble growth factor, unloaded PEA fibers, and FGF2/FGF9 dual-loaded PEA fibers, acquired at Day 8.	123
Figure 5-6: The power Doppler 3D vessel trees resulting from applying the two-stage signal processing method for power Doppler angiography.	124

Figure 5-7: Vascular quantification of the power Doppler 3D volumes of the control, and CAMs treated with soluble growth factor, unloaded PEA fibers, and FGF2/FGF9 dual-loaded PEA fibers, acquired at Day 8 (n=3), (* $p < 0.05$, *** $p < 0.0001$). 125

Figure 5-8: CatWalk automated quantitative gait analysis for mice treated with unloaded and FGF9-loaded PEA fibrous mats..... 127

Figure 5-9: H&E staining of the histological sections of the TA muscle. 128

Figure 5-10: CD31/SM α -actin double immunostaining of histological sections of the TA muscle at Day 7 and quantitative estimation of SM α -actin+ microvessels at the skin side. 129

Figure 5-11: Endomucin/NG2 double immunostaining of histological sections of the TA muscle at Day 7 and quantitative estimation of NG2+ microvessels at the skin side. 130

Chapter 1

1 Introduction

1.1 Overview

A functional vasculature transports oxygen, nutrients and signals to organs and tissues in both healthy and diseased conditions. Ischemic vascular diseases including coronary heart disease and peripheral arterial disease reduce blood flow and subsequently cause ischemia. Considerable progress has been made in tackling cardiovascular disease in Canada over the past 60 years with death rates declining by more than 75%. This resulted in 165,000 survivors in 2013; each one is a living proof on the importance of research in this area [1]. Despite this encouraging progress, there are 350,000 hospitalizations annually due to heart disease and stroke in Canada. Each year approximately 70,000 heart attacks and 50,000 strokes send Canadians to emergency rooms [2]. Collectively, heart disease and stroke costs the Canadian economy more than \$20.9 billion every year in terms of physician services, hospital costs, lost wages and decreased productivity [1, 3, 4].

Induction of neovessel formation (therapeutic angiogenesis) can offer a promising approach to treat many ischemic vascular conditions, especially coronary and peripheral arterial diseases [5]. Neovascularization can be achieved by three approaches: gene therapy by promoting the expression of angiogenic genes, protein therapy by supplying angiogenic growth factors, and cell therapy through delivering progenitor or stem cells. Protein delivery is the most straightforward strategy and is considered as an ‘off-the-shelf’ treatment. However, systemic administration of the soluble angiogenic growth factors results in their degradation and rapid clearance from the tissue of interest. Since neovessel formation and tissue regeneration usually take from weeks to months [6], unlike bolus delivery that provides a burst and short period of biological effects [5], controlled delivery of the angiogenic factor over a long-term in a sustained manner is needed to protect its bioactivity and prolong its therapeutic effects. Delivery vehicles for angiogenic factors can be developed from natural or synthetic materials. Many natural materials have good biocompatibility and degradability; however, they suffer from source and batch variations that often lead to different biological properties. In addition, large-scale production of

natural materials is challenging. On the other hand, synthetic materials usually offer better quality control. In view of this, the biomaterials field has sufficiently advanced to design biocompatible and biodegradable materials with cell and tissue specificity.

The recent development of a new family of amino acid-based biodegradable poly(ester amide)s (PEAs) that are susceptible to either hydrolytic or enzymatic degradation provides additional resources to fabricate new biodegradable fibers with varying degradation rates for potential biomedical applications, such as drug delivery and vascular tissue engineering [7]. The by-products following degradation of these PEAs will include amino acids, which are found physiologically, limiting their potential systemic toxicity [8, 9]. Moreover, their degradation mechanism is governed by surface erosion [10], which limits the localized accumulation of degradation by-products, supporting cell attachment and proliferation. Unlike polyesters [11], PEA degradation is accompanied by the release of less acidic by-products compared to polyesters, thus avoiding significant pH decrease in the vicinity of the scaffold usually resulting in inflammatory responses. Furthermore, surface eroding PEA scaffolds exhibit linear drug release kinetics, which provides better control of the drug release profile. PEAs successfully synthesized in our laboratory were found to have the potential to promote vascular tissue regeneration owing to their biomimetic properties and favorable degradation profiles [8, 10]. Multiple growth factors can be loaded into PEA delivery vehicles, potentially sustaining their release, enhancing their efficacy and accelerating favorable cell-material interactions. In this work, PEA was used to fabricate biodegradable electrospun fibers for dual and controlled delivery of angiogenic and arteriogenic growth factors to support mature and functional neovessel formation.

1.2 Hypothesis and Objectives

1.2.1 Hypothesis

It is hypothesized that dual and controlled delivery of angiogenic and arteriogenic factors from biodegradable electrospun PEA fibers promotes the assembly of stable and functional neovasculature.

1.2.2 Objectives

In order to test the above hypothesis, the following objectives were formulated:

- Fabrication and optimization of PEA electrospun fibers, to obtain bead-free nanofibers with uniform fiber diameter distribution and loading a model protein (bovine serum albumin; BSA) and the target protein (fibroblast growth factor-9; FGF9).
- Dual loading of the PEA electrospun fibers with fibroblast growth factor-2 (FGF2) and FGF9, and characterization of the delivery system in terms of morphological properties, *in vitro* release kinetics, and bioactivity of the released growth factors.
- *In vitro* study of the effect of the growth factor-loaded PEA electrospun fibrous scaffold on cell viability and proliferation using NIH-3T3 fibroblasts, 10T1/2 cells, and human coronary artery smooth muscle cells (HCASMCs), inflammatory host response using human monocytic cell line (THP-1), directed smooth muscle cell migration and endothelial cell tube formation.
- *In vivo* angiogenesis evaluation of the developed PEA delivery system using an *ex ovo* chick chorioallantoic membrane (CAM) model and ischemic hindlimb mouse model.

1.3 Thesis Outline

This thesis is divided into six chapters. A brief introduction about the clinical motivation of this research (ischemic vascular disease) and the need for new treatment approaches such as therapeutic angiogenesis, together with the hypothesis and objectives are introduced in Chapter 1. A broad literature review of recent advances in growth factor delivery for therapeutic angiogenesis is presented in Chapter 2. The main research findings are presented in Chapters 3-5. Chapter 3 reports the fabrication and optimization of PEA electrospun fibers and loading them with a model protein (BSA) and FGF9 using either blend or emulsion electrospinning technique and their characterization in terms of

morphological properties, *in vitro* release kinetics, and bioactivity of the released growth factor. Chapter 4 discusses dual loading of the PEA electrospun fibers with FGF9 and FGF2 using a mixed blend and emulsion electrospinning technique, *in vitro* angiogenesis assays and evaluating the inflammatory host response using THP-1 human monocytes. Chapter 5 focuses on the *in vivo* angiogenesis evaluation of the FGF-loaded PEA fibers using *ex ovo* chick choriocallantoic membrane model and ischemic hindlimb mouse model. Finally, a general discussion with conclusions outlining the strengths, limitations and future directions are presented in Chapter 6.

1.4 References

1. Heart and Stroke Foundation of Canada - 2014 Report on health - Creating Survivors. [accessed July 2016; Available from: http://www.heartandstroke.com/site/c.ikIQLcMWJtE/b.8968559/k.DE2D/2014_Report_on_health_Creating_Survivors.htm.
2. Statistics Canada. Causes of Death, Canada, 2011. Released January 28, 2014. [accessed July 2016; Available from: <http://www.statcan.gc.ca/daily-quotidien/140128/t140128b001-eng.htm>.
3. Statistics Canada. Morality, Summary List of Causes 2008. Released October 27, 2011. [accessed July 2016; Available from: <http://www.statcan.gc.ca/pub/84f0209x/84f0209x2008000-eng.pdf>.
4. Public Health Agency of Canada. 2006. Tracking Heart Disease and Stroke in Canada. Released June 10, 2009. [accessed July 2016; Available from: <http://www.phac-aspc.gc.ca/publicat/2009/cvd-avc/pdf/cvd-avs-2009-eng.pdf>.
5. Chu, H. and Y. Wang, Therapeutic angiogenesis: controlled delivery of angiogenic factors. *Ther Deliv*, 2012. **3**(6): 693-714.
6. Markkanen, J.E., T.T. Rissanen, A. Kivela, and S. Yla-Herttuala, Growth factor-induced therapeutic angiogenesis and arteriogenesis in the heart--gene therapy. *Cardiovasc Res*, 2005. **65**(3): 656-64.
7. Pang, X. and C.C. Chu, Synthesis, characterization and biodegradation of functionalized amino acid-based poly(ester amide)s. *Biomaterials*, 2010. **31**(14): 3745-54.

8. Knight, D.K., E.R. Gillies, and K. Mequanint, Strategies in Functional Poly(ester amide) Syntheses to Study Human Coronary Artery Smooth Muscle Cell Interactions. *Biomacromolecules*, 2011. **12**(7): 2475-87.
9. Karimi, P., A.S. Rizkalla, and K. Mequanint, Versatile Biodegradable Poly(ester amide)s Derived from α -Amino Acids for Vascular Tissue Engineering. *Materials*, 2010. **3**(4): 2346-2368.
10. Srinath, D., S. Lin, D.K. Knight, A.S. Rizkalla, and K. Mequanint, Fibrous biodegradable l-alanine-based scaffolds for vascular tissue engineering. *J Tissue Eng Regen Med*, 2012. **8**(7): 578-588.
11. Vert, M., S. Li, and H. Garreau, New insights on the degradation of bioresorbable polymeric devices based on lactic and glycolic acids. *Clinical materials*, 1992. **10**(1-2): 3-8.

Chapter 2

2 Literature Review: Advances in Growth Factor Delivery for Therapeutic Angiogenesis*

Overview: This chapter provides background information on natural blood vessel formation, signaling molecules involved in the angiogenesis process, angiogenic growth factor delivery; highlighting the benefits of their controlled delivery and spatiotemporal presentation, and lastly discussing safety concerns of the angiogenic growth factor delivery.

2.1 Abstract

Therapeutic angiogenesis is a new revascularization strategy to induce new vessel formation. The biology and delivery of angiogenic growth factors involved in vessel formation have been extensively studied but success in translating the angiogenic capacity of growth factors into benefits for vascular disease patients is still limited. This could be attributed to issues related to patient selection, growth factor delivery methods or lack of vessel maturation. Comprehensive understanding of the cellular and molecular cross-talk during the different stages of vascular development is needed for the design of efficient therapeutic strategies. The presentation of angiogenic factors either in series or in parallel using a strategy that mimics physiological events, such as concentration and spatio-temporal profiles, is an immediate requirement for functional blood vessel formation. This review provides an overview of the recent delivery strategies of angiogenic factors, and discusses targeting neovascular maturation as a promising approach to induce stable and functional vessels for therapeutic angiogenesis.

Key words: Growth factors; Neovascular maturation; Therapeutic angiogenesis.

* A version of this chapter is published as a review article “Somiraa S. Said, J. Geoffrey Pickering and Kibret Mequanint, *Journal of Vascular Research* (2013), 50; 35-51”. Adapted with permission from KARGER Publishers © 2012.

2.2 Introduction

Notwithstanding rapid advances made in treatment options, cardiovascular diseases remained the leading cause of death in developed countries [1]. In 2008, ischemic heart disease accounted for 7.3 million deaths worldwide [2]. The primary cause of ischemic heart disease is atherosclerosis - a thickening of the lining of the coronary arteries, and the subsequent myocardial ischemia - resulting in functional deficits and infarction. Although considerable progress has been made in preventing and treating atherosclerotic vascular disease (such as thrombolysis, angioplasty, stenting, and surgical bypass), there is no better clinical alternative to the patient's own blood vessels when a coronary artery must be bypassed. However, autologous vein and artery grafts cannot always be used either due to damage, pre-existing disease, or distal coronary arteries that are unsuitable for surgical anastomosis. On the other hand, synthetic grafts can result in immunologic and thrombotic complications [3]. Consequently, nearly 7% of ischemic heart disease patients become ineligible for standard revascularization techniques such as angioplasty or bypass surgery [4]. In these patients, the challenge to improve blood flow to the ischemic heart has led to extensive research and numerous innovative approaches in the field of vascular regenerative medicine [5]. One of the novel strategies in vascular regenerative medicine is therapeutic angiogenesis, which can include the administration of growth factors to induce new vessel formation. This technique has been shown to promote myocardial healing after an infarct in animals demonstrating the functional importance of augmenting the coronary circulation [6, 7]. This, in turn, accelerates the potential of therapeutic angiogenesis as a treatment modality to patients with advanced symptomatic ischemic heart disease, who are ineligible to receive standard invasive revascularization strategies [8, 9]. In this review, an overview of the biology of angiogenesis is provided along with the discussion of the basic characteristics of angiogenic factors, different delivery technologies, and neovascular maturation to form stable and functional vessels through therapeutic angiogenesis strategies.

2.3 Blood Vessel Formation: Vasculogenesis, Angiogenesis and Arteriogenesis

Coronary vasculogenesis, arteriogenesis, and angiogenesis are a spectrum of processes that lead to vessel formation [10]. Vasculogenesis is the *de novo* formation of blood vessels in the embryo from angioblasts or endothelial progenitor cells that migrate, proliferate, and differentiate to form endothelial cells (ECs), and subsequently organize into cord-like structures [11, 12]. It involves both cell-cell and cell-extracellular matrix (ECM) interactions directed spatially and temporally by growth factors [13]. This dynamic process has also been recently suggested to occur in adulthood, where circulating endothelial progenitor cells are recruited to ischemic sites [14]. Arteriolar networks are often remodeled postnatally by the maturation of pre-existing collaterals in response to metabolic demands through the process of arteriogenesis [15]. Angiogenesis, on the other hand, is the process of blood vessel sprouting from pre-existing vasculature and includes subsequent remodeling steps such as pruning, vessel enlargement, and intussusceptions to form stable vessel networks [16, 17]. Angiogenesis is a beneficial process occurring naturally during wound healing, the female monthly reproductive cycle, and pregnancy. Alternatively, angiogenesis can occur as a part of a diseased body where it can aid in cases of ischemia or lead to a disease in the promotion of tumors [18]. During normal function, the body controls the growth of blood vessels using pro-angiogenic factors to stimulate and anti-angiogenic factors to negatively regulate this phenomenon. The events of the angiogenesis process occur in an orderly series (Figure 2-1). It starts by the release of angiogenic growth factors from the ischemic tissues, diffusing into the nearby tissues. The angiogenic growth factors then bind to specific receptors located on the ECs of nearby pre-existing blood vessels. Once growth factors bind to their receptors, the ECs become activated, sending signals from the cells' surface to the nucleus. The EC machinery begins to produce new molecules including enzymes that degrade the basement membrane surrounding existing vessels. ECs begin to proliferate and migrate out and integrins facilitate sprouting of the new blood vessel forward. Additionally matrix metalloproteinases are produced to degrade the ECM in the direction of the sprouting vessel tip in order to accommodate it. As the new vessel extends, the tissue is remodeled around the vessel. Subsequent to this, sprouting ECs

roll up to form a tube. Individual tubes connect to form blood vessels that can circulate blood. Newly formed blood vessel tubes are stabilized by specialized perivascular cells, referred to as mural cells, which can be either vascular smooth muscle cells (VSMCs) or pericytes. Pericytes are thought to stabilize capillaries, whereas VSMCs are critical for the control of vessel conductance which is required for the restoration of blood flow [18]. With continuing flow as well as increasing shear stress and blood pressure over time during vascular development, greater vessel stability is required. Such vessel stability is attained through EC-mural cell interactions and concomitant ECM remodeling including deposition and cross-linking of ECM components (i.e., basement membranes, interstitial matrices, and elastin-rich matrices) at distinct places in the vessel wall [19, 20].

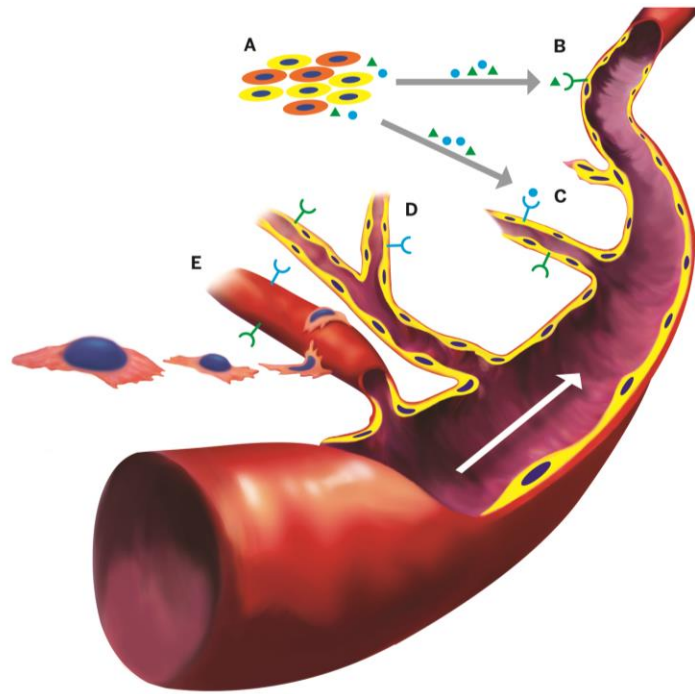


Figure 2-1: Major events of the angiogenesis process.

(A) Angiogenic factor production and release to the surrounding tissue. (B) Paracrine signalling via angiogenic factor-EC receptor binding. (C) Endothelial cell directional migration and tube elongation. (D) Nascent vessel branching. (E) Neovascular maturation and investment of perivascular cells. Modified from the Angiogenesis foundation website [18].

In view of the above, the goal of therapeutic angiogenesis is to enhance the natural process of ischemic revascularization through delivery of angiogenic factors, and to increase blood vessel density and tissue function [3]. Understanding the molecular mechanisms of vascular maturation is essential in developing competent neovascularization strategies. For such complicated developmental process, multiple angiogenic factors are required that act synchronically to form the correct patterning found within a functional blood vessel [3].

2.4 Angiogenic Growth Factors

Ischemia resulting from an arterial occlusion is a natural stimulus for endogenous angiogenesis which induces upregulation of angiogenic growth factors and mobilization of circulating cellular elements collectively enabling the development of an accessory vasculature [5, 21]. In the sections that follow, major angiogenic growth factors are outlined whereas additional factors are listed in Table 2-1.

Table 2-1: Selected signaling molecules involved in angiogenesis process [22].

Signaling molecule	Function(s)
Vascular endothelial growth factors	Involved in angiogenesis and lymphangiogenesis, act specifically on ECs to induce their migration, proliferation, formation of new blood vessels, and induce vascular permeability
Fibroblast growth factors	Involved in angiogenesis, EC proliferation, cord and lumen formation, recruitment of inflammatory cells, pericytes and VSMCs, and vessel maturation
Platelet-derived growth factors	Promote vascular maturation by recruiting VSMCs and pericytes to newly formed vessels, induce inflammatory cell chemotaxis, recruit stem cells from bone marrow, and responsible for the migration of SMC and formation of the neointima

Angiopoietin-1	EC chemotaxis, prevention of excessive vascular permeability, formation of cords and lumens, and vessel stabilization via EC-mural cells interactions
Angiopoietin-2	Vessel destabilization, detachment of VSMCs, and degradation of ECM
Nitric oxide	Vasodilatation, co-factor for VEGFs, FGFs and other angiogenic factors
Granulocyte colony-stimulating factor	Mobilization of bone marrow-derived stem cells, induces proliferation and enhance survival of cardiomyocytes by direct effects on cardiomyocytes, or by the release of proangiogenic mediators
Hypoxia-inducible factor 1a	Upregulation of several genes to promote survival in low-oxygen conditions. These include glycolysis enzymes, which allow ATP synthesis in an oxygen-independent manner, and VEGF, which promotes angiogenesis
Hepatocyte growth factor	It is secreted by mesenchymal cells and acts as a multi-functional cytokine on cells of mainly epithelial origin. Its ability to stimulate mitogenesis, cell motility, and matrix invasion gives it a chief role in angiogenesis and tissue regeneration
Insulin-like growth factor	A key regulator of cellular proliferation and differentiation, promotes physiological cardiac growth, reduces apoptosis and collagen deposition, enhances angiogenesis, and improves cardiac function

2.4.1 Vascular Endothelial Growth Factor (VEGF) Family

Among the many factors implicated in angiogenesis, VEGF is one of the most investigated families of angiogenic growth factors. The VEGF family includes VEGF-A, -B, -C, -D, -

E, -F and placental growth factor (PIGF). VEGF-A is mainly involved in angiogenesis while VEGF-C and VEGF-D are involved in lymphangiogenesis. The human VEGF-A gene is organized into eight exons and alternative exon splicing results in 5 different isoforms (VEGF₁₂₁, VEGF₁₄₅, VEGF₁₆₅, VEGF₁₈₉ and VEGF₂₀₆) [23-25]. VEGF₁₆₅ is the most predominant isoform as well as the most potent in terms of stimulating angiogenesis [3]. VEGF ligands mediate their angiogenic effects by binding to specific VEGF receptors, leading to receptor dimerization and downstream signal transduction. VEGF receptor signalling is detailed elsewhere and the reader is referred to excellent reviews on this subject [26, 27]. VEGF ligands bind to 3 primary receptors (VEGFR-1, VEGFR-2 and VEGFR-3) and 2 co-receptors (neuropilin receptors NP-1 and NP-2). Of the primary receptors, VEGFR-1 and VEGFR-2 are mainly associated with angiogenesis [28]. The third primary receptor, VEGFR-3, is associated with lymphangiogenesis. Endothelial expression of VEGF receptors varies among the 3 primary receptors; VEGFR-2 is expressed on almost all ECs, while VEGFR-1 and -3 are selectively expressed in distinct vascular beds [5]. VEGF acts specifically on ECs to induce their migration, proliferation, and formation of new or large vessels [3]. It also can act in an autocrine manner and increases vascular permeability. VEGF induces vascular permeability, vasodilatation, and upregulates expression of serinoproteases and interstitial collagenases, thereby promoting ECM degradation [29, 30]. VEGF production and subsequent angiogenesis can be triggered by a number of factors in the cellular microenvironment including but not limited to hypoxia, oncogenes, tumor suppressor genes, inflammatory cytokines, and other growth factors [31]. For example, acute myocardial infarction rapidly produces a prolonged over-expression of VEGF and its receptors [32]. Moreover, it has been documented that VEGF increases the number of circulating endothelial progenitor cells in humans after VEGF gene therapy [33].

2.4.2 Fibroblast growth factor (FGF) family

FGFs are another large family of growth factors directly involved in angiogenesis [34]. FGFs are pleiotropic factors that can stimulate and act on different cell types, including

vascular ECs. The FGF gene family is composed of 22 members that bind to seven FGF receptor isoforms (FGFR_{1b}, FGFR_{1c}, FGFR_{2b}, FGFR_{2c}, FGFR_{3b}, FGFR_{3c} and FGFR₄) [35]. The bulk of angiogenic experimental data is focused on FGF-1 (acidic, aFGF) and FGF-2 (basic, bFGF) both of which are potent EC mitogens that also serve as ligands for other cell types, including VSMCs and fibroblasts. FGF binding induces receptor tyrosine kinase (RTK) dimerization, which leads to the activation of signalling pathways involved in cell growth, differentiation, tissue maintenance, and wound repair [35]. FGF induces neovascularisation *in vivo* and is implicated in the growth of new blood vessels during wound healing and embryogenesis. *In vitro*, FGF induces cell proliferation, migration, and production of proteases in ECs by interacting with specific co-receptor systems consisting of tyrosine kinase FGF receptors (FGFRs) and heparin-like glycosaminoglycans (HLGAG) [5, 36]. It has been reported that FGFs act through autocrine, intracrine or paracrine mechanisms to induce angiogenesis in vascular lesions [37]. Although intimate cross-talk takes place between the FGF-2 and VEGF signalling pathways often activating one another to promote angiogenesis, these growth factors, however, have distinct biological effects on ECs [3, 37].

2.4.3 Platelet-derived Growth Factor (PDGF)

PDGF is a pluripotent angiogenic growth factor synthesized by many different cell types in response to external stimuli such as hypoxia or growth factor stimulation, and it has a broad expression pattern [3]. PDGF, together with other growth factors, such as VEGF and FGF, promotes vascular maturation by recruiting VSMCs and pericytes to newly formed vessels [38, 39]. In addition, PDGF mediates collagen production by fibroblasts, regulates lymphatic growth, induces inflammatory cell chemotaxis and recruits stem cells from bone marrow [40].

2.4.4 Other Angiogenic Stimulators

The presence of inflammatory cells like macrophages, monocytes and neutrophils triggers an angiogenic response [29]. In addition to the angiogenic factors discussed in the preceding sections, several other growth factors that impact angiogenesis such as angiopoietins (Ang-1 and Ang-2), monocyte chemoattractant protein-1 (MCP-1), granulocyte macrophage colony-stimulating factor (GM-CSF), hepatocyte growth factor (HGF), leptin, transforming growth factors (TGF- α and TGF- β), tumour necrosis factor alpha (TNF- α), and brain-derived neurotrophic factor (BDNF) have been identified [5]. Furthermore non-peptide molecules, such as nitric oxide (NO), prostaglandins, adenosine and hyaluronic acid have been also reported to have pro-angiogenic properties [29]. However, clinical trials have focused mostly on members of the VEGF and FGF families [6, 8]. Table 2-1 summarizes the role of selected signalling molecules involved in the angiogenic process.

2.5 Angiogenic Growth Factor Delivery

2.5.1 Protein *versus* Gene Therapy

Therapeutic angiogenesis regimens have focused on the administration of a single growth factor, in spite of the complexity of the angiogenesis process, with VEGF-A and FGF 1 and 2 being the most extensively studied angiogenic factors [22]. Growth factor proteins can be administered either directly or via gene-based approaches, employing naked plasmid DNA or a viral vector that encodes the gene to be incorporated by the host ECs [22]. Obvious advantages of gene therapy strategy include longer-term expression of an angiogenic gene and targeting a specific tissue. However, the local concentration of the angiogenic protein is highly dependent on the level of expression of its gene, which is difficult to regulate [41]. Safety concerns usually exist regarding the exposure of patients to foreign genetic material and viral vectors. As well, the effectiveness of gene transfection methods can be compromised by preformed antibodies and inflammatory responses, and the probability of inactivation could increase with re-administration. Protein therapy may arguably be more applicable for clinical use than gene therapy, due to the more predictable

initial dosing of the angiogenic factor, pharmacokinetics and tissue therapeutic levels. Additionally, the use of controlled-release delivery systems can provide prolonged exposure, compensate for the short biological half-life of the angiogenic growth factors, and avoid potential adverse effects of the high plasma concentrations, which is required for adequate myocardial uptake [22]. However, recombinant proteins can be difficult and expensive to produce and may require complicated delivery technologies.

2.5.2 Gene Transfer in Therapeutic Angiogenesis

Early studies of gene therapy utilized plasmid DNA owing to its safety and ease of production. Despite the promising results of VEGF encoding plasmid DNA and other angiogenic factors in preclinical trials and small clinical trials [42, 43], large randomized controlled trials did not support the use of plasmid DNA, due to its low transduction efficacy, lack of a dose response effect, and its transient expression [44, 45]. Although, plasmid DNA is considered safe, it can result in transient fever, inflammation, and sometimes myocardial infarction [44, 46]. Adenovirus (Ad) vectors have demonstrated high transduction efficacy, and more specifically, they are much more efficient than plasmid DNA in the myocardium [47]. Retroviruses were the first vectors to be used for *in vivo* cardiovascular gene transfer, but safety concerns led to reduced interest in them [48]. As an alternative strategy, lentiviruses have been recently used in cardiovascular gene therapy, for the treatment of familial hypercholesterolemia [49], whereas sendai viruses [50] and herpesviruses [51] have also been utilized in some cardiovascular gene therapy applications. Finally, baculoviruses were found to transduce blood vessels transiently with a moderate efficiency [52]. Despite this encouraging data, their advantage is not clear as macrophage-specific immunostaining detected signs of inflammation comparable to adenoviruses.

Adeno-associated virus (AAV) vectors are attractive candidates for cardiovascular gene therapy having a natural tropism towards VSMCs, cardiomyocytes and skeletal muscles. AAV transduces quiescent cells, and drives long-term gene expression lasting several months. It generates only a restricted inflammatory reaction, and the wild-type virus is not

known to cause any diseases in humans [53]. AAV has a long-lasting gene expression pattern with lower maximal gene expression levels than those induced by Ads [54]. Most importantly, the peak expression of AAVs can be achieved in just a few days after the transduction [55].

2.6 Preclinical Studies

2.6.1 *In vivo* Studies with Vascular Endothelial Growth Factor

Animal studies with VEGF have mainly involved VEGF₁₆₅ and VEGF₁₂₁ isoforms. There have been successful results in myocardial ischemia models [56-59]. In one study, the implantation of collagen membrane patch loaded with collagen-binding domain fused to VEGF into infarcted rabbit myocardium, effectively improved left ventricle cardiac function and increased vascular density compared to control group [57]. In a rat model of a resected right ventricular free wall and replaced with the VEGF-immobilized collagen scaffold, Miyagi *et al.* [58] reported that covalently immobilized VEGF-collagen scaffolds improved tissue formation, increased blood vessel density and reduced construct thinning. Controlled delivery of VEGF₁₆₅ from poly(lactic-co-glycolic acid) (PLGA) microparticles in a rat model of myocardial ischemia-reperfusion, resulted in enhanced angiogenesis and arteriogenesis after one month of the treatment [56]. Sustained and localized delivery of VEGF together with insulin-like growth factor-1 from biodegradable gelatin microspheres was proved to attenuate post-myocardial infarction remodeling in a rat model of experimental heart failure [59]. Also, gene transfer of adenoviral VEGF-A₁₆₅ and the mature form of VEGF-D, injected intramyocardially into pigs via a catheter-mediated approach, resulted in transmural angiogenesis induction in porcine heart [60].

2.6.2 *In vivo* Studies with Fibroblast Growth Factor

FGF-1 and FGF-2 have been the most studied of the FGF family. FGF-1 plays a pivotal role in the spontaneous formation of collaterals as it is strongly expressed in ischemic myocardium [22, 61]. Large animal studies using FGF-1 to stimulate angiogenesis initially

produced disappointing results, which can be argued by the short biological half-life (15 minutes at 37°C) of the FGF-1 [62]. Intramyocardial sustained delivery of FGF-2-impregnated gelatin hydrogel microspheres was demonstrated to enhance angiogenesis and ventricular function in a rat myocardial infarcted heart model [63]. Improved myocardial perfusion and cardiac function by controlled-release of FGF-2 using fibrin glue, was reported in a canine acute infarct model - induced by ligation of the left anterior descending coronary artery - with dramatic increase of the total vascular density in comparison with the control group that underwent coronary artery ligation without treatment [64]. In another study, heart failure due to myocardial infarction was induced in pigs followed by intramyocardial administration of biodegradable gelatin microspheres loaded with bFGF 4 weeks after infarction, which resulted in improved left ventricular (LV) function and inhibited LV remodeling compared to the control group [65]. In a preclinical study using a pig model of myocardial ischemia, a single intracoronary infusion of adenovirus 5 fibroblast growth factor-4 (Ad5FGF-4), improved cardiac contractile function and regional blood flow in the ischemic region during stress [66].

2.7 Clinical Trials in Ischemic Heart Disease

After preclinical studies had established a proof of concept for therapeutic angiogenesis, investigators sought to extrapolate these findings to patients with myocardial ischemia. Patients included in the clinical trials of therapeutic myocardial angiogenesis, suffered from severe angina unresponsive to medical therapy and were unsuitable for standard revascularization techniques [5]. Major therapeutic angiogenesis clinical trials for myocardial ischemia using protein/gene therapy are summarised in Table 2-2.

Most of these clinical trials showed little success in translating the angiogenic capacity of growth factors into benefits to ischemic heart disease patients either through gene or protein therapy. The potential reasons for such poor results include the limited duration of the therapy achieved with bolus delivery of recombinant proteins or gene delivery vectors, the high costs associated with protein therapy because of the need for large doses and complicated delivery technologies, issues with patient selection, and the generation of

immature and unstable blood vessels that regress over time. Potential strategies to overcome these challenges include the use of controlled delivery systems that allow prolonged angiogenic stimulation and the use of growth factor combinations to stimulate the generation of mature and stable blood vessels. Ultimately, the key is acquiring a neovasculature that can effectively deliver flow via vasoresponsiveness - the dynamic regulation of the luminal diameter of arterioles, which is crucial for controlling the metabolic needs of the tissues.

Table 2-2: Major randomized myocardial angiogenesis clinical trials using protein/gene therapy.

Growth factor	Route and dose	n	Results	Reference
Granulocyte-macrophage colony stimulating factor (GM-CSF)	40 µg intracoronary (IC) once and 10 µg/kg subcutaneous (SC) for 2 weeks	21	Short-term administration protocol of GM-CSF showed significant improvement of collateral flow index ($p < 0.05$) and ECG signs ($p = 0.04$) after vascular balloon occlusion.	Seiler <i>et al.</i> [67]
GM-CSF	10 µg/kg SC for 2 weeks	14	Subcutaneous short-term protocol of GM-CSF significantly promotes coronary collateral artery growth among patients with CAD. However, two cases of acute coronary syndromes in the treatment group were reported.	Zbinden <i>et al.</i> [68]
Granulocyte colony stimulating factor (G-CSF)	10 µg/kg SC for 5 d after percutaneous coronary intervention (PCI) for acute myocardial infarction (AMI)	114	Stem cell mobilization by G-CSF therapy in patients with acute myocardial infarction had no significant influence on infarct size, left ventricular function, or coronary restenosis.	Zohlhofer <i>et al.</i> [69]

G-CSF	10 µg/kg SC for 6 days after PCI for AMI	78	Bone marrow stem cell mobilization with subcutaneous G-CSF did not lead to significant improvement in ventricular function after acute myocardial infarction.	Ripa <i>et al.</i> [70]
FGF-2	10 or 100 µg delivered via sustained-release heparin-alginate microcapsules implanted in ischemic myocardial territories during coronary artery bypass graft (CABG)	24	Magnetic resonance assessment of the target ischemic zone showed significant improvement of myocardial perfusion and reduction in the target ischemic area in the 100 µg bFGF group, 3 months after CABG.	Laham <i>et al.</i> [71]
Recombinant FGF-2	0, 0.3, 3, 30 µg/kg IC	337	A single IC infusion of rFGF-2 showed no significant difference of exercise tolerance or myocardial perfusion. But does show trends toward symptomatic improvement at 90 days but not at 180 days due to the continued improvement in the placebo group.	Simons <i>et al.</i> [72]
Adenovirus5F GF-4 (Ad5FGF-5)	5 ascending doses IC	79	A trend towards clinical improvement in exercise treadmill testing. Single intracoronary administration of Ad5-FGF4 was safe and well tolerated with no immediate adverse events.	Grines <i>et al.</i> [73]
Recombinant VEGF-A₁₆₅	17 ng/kg/min IC and intravenous (IV) or	178	rhVEGF offered no improvement beyond placebo in all measurements	Henry <i>et al.</i> [74]

	50 ng/kg/min IC and IV		by Day 60. High-dose rhVEGF resulted in significant improvement in angina class and non-significant improvement in exercise tolerance time and angina frequency at 120 days compared to placebo.	
AdVEGF₁₆₅ or naked plasmid	(2 × 10 ¹⁰ pfu or 2 mg DNA) IC during percutaneous transluminal coronary angioplasty	103	Significant improvement of myocardial perfusion in the adenoviral VEGF group at 6 months. No difference in vessel restenosis rates.	Hedman <i>et al.</i> [44]
AdVEGF₁₂₁	2 × 10 ¹⁰ pfu intramyocardial injection via mini-thoracotomy	67	Improvement in exercise-induced ischemia at 26 weeks.	Stewart <i>et al.</i> [75]
Naked VEGF₁₆₅ plasmid	0.5 mg percutaneous intramyocardial injection	80	No significant improvement of stress-induced myocardial perfusion. However, regional wall motion was significantly improved.	Kastrup <i>et al.</i> [45]
Plasmid VEGF₁₆₅	2.0 mg intramyocardial injection	93	No improvement in myocardial perfusion; significant reduction in the ischemic area, increase in exercise test time and improvement in angina class.	Stewart <i>et al.</i> [76]
AdGV-VEGF₁₂₁	intramyocardial injection	17	No significant difference in myocardial perfusion and exercise capacity at 52 weeks. Premature study termination.	Kastrup <i>et al.</i> [77]

2.8 Targeting Neovascular Maturation

2.8.1 Cues for Functional Blood Vessel Formation

Pericyte and VSMC recruitment to nascent vessels is pivotal for vessel maturation [78]. Absence of perivascular cell coverage subjects newly formed vessels to regression and they become dependent upon ongoing growth factor stimulation from the environment for their survival [79]. However, nascent vessels are stabilized and become resistant to regression once they are invested with pericytes. Basement membrane matrices are one of the key ECM components facilitating EC tube stabilization. They are in direct contact with the ECs layer on its abluminal surface and provide important signals that control the stability of this layer. Despite the substantial information which exists on the signalling properties of basement membrane components toward different cell types, much remains to be learned concerning how such components affect EC behaviour at distinct stages of vascular morphogenesis and stabilization in embryonic and postnatal life [80]. The importance of pericyte recruitment to EC-lined tubes *in vitro* and *in vivo*, has been demonstrated to be essential to stimulate vascular basement membrane matrix assembly, which is considered a key step in vascular maturation and stabilization [81]. Not surprisingly, stimulation of cell migration for vascular maturation is growth factor dependent. This is exemplified by Regranex[®], a genetically engineered PDGF based commercial product developed for the recruitment of cells in wound healing [82]. Although its reported mechanism of action is through mesenchymal cell proliferation and matrix production, there is a probability that part of PDGF's mechanism of action in chronic wound healing may also be due to improvement of neovascular maturation [83].

The endothelial basement membrane is unique in its accumulation of the protein von Willebrand Factor (vWF), which is derived from endothelial Weibel-Palade body secretions [84]. Following the formation of a quiescent vasculature, vWF plays an essential role in haemostasis. In addition to its role in the recruitment, adhesion, and migration of leukocytes, vWF has been recently shown to play a role in vessel patterning [85]. Although multiple cell types, secreted proteins, and growth factors collectively and in coordination regulate angiogenesis and vessel stabilization, the Notch signalling pathway is unique in

its involvement in multiple stages of angiogenesis, from initial vascular plexus formation and patterning, to VSMC recruitment and vascular remodeling [86]. Scheppke *et al.* [86] reported that VSMC recognition of the Notch ligand (Jagged1) on ECs leads to expression of integrin $\alpha\beta3$ on VSMCs. Once expressed, integrin $\alpha\beta3$ facilitates VSMC adhesion to vWF in the endothelial basement membrane of developing retinal arteries, leading to vessel maturation. Their conclusions were based on the notion that genetic or pharmacological disruption of Jagged1, Notch, $\alpha\beta3$, or vWF suppresses VSMC coverage of nascent vessels and arterial maturation during vascular development [86].

2.8.2 Co-delivery of Ang-1, PDGF-BB, or HGF with VEGF and FGF-2 for Vascular Stabilization

Given the lack of clear benefits of VEGF gene therapy in two major clinical trials [45, 76], targeting neovascular maturation is an attractive alternative or supplementary strategy to ensure efficient therapeutic angiogenesis. Although, VEGF directly stimulates EC proliferation and migration, it has been reported that it can act as an inhibitor of neovascularization on the basis of its capacity to disrupt VSMC function [87]. Specifically, under conditions of PDGF-mediated angiogenesis, VEGF ablates pericyte coverage of nascent vascular sprouts, leading to vessel destabilization [87]. Perivascular nascent vessel maturation process is a natural feature of blood vessel development in the embryo [88]; however, there are no strategies for promoting an equivalent vascular maturation process in ischemic adult tissues. Such strategies could also be important to the viability of tissue-engineered substitutes, which can be compromised by inefficient vascularization and oxygen delivery [89]. Evidently, the formation of a mature vasculature requires precise spatial and temporal regulation of a large number of angiogenic stimulators and inhibitors. The complexity and heterogeneity of the factors involved in vascular maturation suggest the use of a co-delivery or sequential delivery approach, to overcome the drawbacks of single growth factor delivery. For example, systemic co-administration of Ang-1 and VEGF through intravenous adenoviral delivery has been shown to protect adult vasculature from lethal vascular leakage induced by systemic VEGF expression [90]. Local co-expression of VEGF and Ang-1 has been reported to reduce VEGF-induced leakage in rat

hind limb ischemia [91]. Temporally separated delivery of VEGF and Ang-1 gene therapy also resulted in sustained and functional neovascularization in unilateral hind limb ischemia rat model [92]. Moreover, adenoviral delivery of VEGF and Ang-1 induced vessels that were more mature and persisted after 4 weeks compared to VEGF alone [93]. Adeno-associated viral vectors expressing cardiac-specific and hypoxia-inducible VEGF [AAV-myosin light chain-2v (MLC)VEGF] and Ang1 (AAV-MLCAng1) were co-injected in a porcine myocardial infarcted heart model [94]. Cardiac-specific and hypoxia-induced co-expression of VEGF and Ang1 was found to improve the perfusion and function of porcine myocardial infarcted heart through the induction of angiogenesis and cardiomyocyte proliferation [94].

Similarly the approach of co-delivering PDGF-BB with VEGF is justified by the suggestion that increasing the recruitment of pericytes could provide a comprehensive stimulation of several pathways in a co-ordinated fashion, and hence better simulation of the physiological process. Delivery of recombinant VEGF and PDGF-BB proteins from a PLGA scaffold has been shown to induce larger and more mature vessels compared with VEGF alone subcutaneously and in ischemic skeletal muscle [95]. The combination of recombinant PDGF-BB with FGF-2 has been reported to increase vascular stabilization in the mouse cornea and in rat and rabbit hind limb ischemia models [38]. However, the co-delivery of PDGF-BB was found not to correct VEGF induced abnormalities in the cornea. Thus, it was not pursued further in the more clinically relevant muscular tissue. Co-delivery of the VEGF and PDGF-BB genes to ischemic myocardium by venous retroinfusion of adeno-associated viral vector has recently been found to significantly improve perfusion and collateral arteriogenesis [96]. It is worth mentioning that PDGF together with other factors, originating from the aggregating platelets, mononuclear cells, endothelial cells, and VSMCs themselves at the site of injury, act as a proliferating agent and are responsible for the migration of the VSMCs and the process of restenosis [97]. Given the beneficial effect of VEGF and PDGF co-delivery in prior studies [38, 95], the suggestion that PDGF causes restenosis requires further investigation.

In addition to Ang-1 and PDGF-BB, co-delivery of HGF was reported to potently induce arteriogenesis and reduce cardiac fibrosis. Intramyocardial delivery of cross-linked

albumin-alginate microcapsules that sequentially release FGF-2 and HGF was investigated in a rat model with chronic heart failure induced by coronary ligation [98]. Data from the study indicated that dual delivery stimulated angiogenesis and prevented cardiac hypertrophy and fibrosis, leading to improved cardiac perfusion after 3 months.

2.8.3 Acquiring Neovasculature Vasoresponsiveness

Although stimulating angiogenesis using growth factors is an essential first step, it is not a sufficient condition for its efficiency. It has become recognized that angiogenic growth factors cannot generate vasoreactive neovessels by themselves [99]. Vasoreactivity is the dynamic regulation of the luminal diameter of arterioles and arteries and it is vital to controlling flow into capillary beds, and consequently, to meeting the oxygen and metabolic needs of tissues. Frontini *et al.* [99] reported that the delivery of fibroblast growth factor-9 (FGF-9) imparts stability, longevity and the ability to regulate blood flow through vasoresponsiveness of the newly formed microvessels. In this cited work, it was found that mural cell exposure to FGF-9 activated FGF receptor signalling, promoted cell elongation, decreased apoptosis, increased the expression of PDGFR β and Sonic Hedgehog (SHH), and augmented the mural cell chemotactic response to PDGF-BB (Figure 2-2) . Unlike FGF-2, FGF-9 was found not to stimulate angiogenesis in subcutaneous implants, but instead it drives muscularization of angiogenic sprouts within the implant and enhances the ability of the microvasculature to receive flow and resist regression [99].

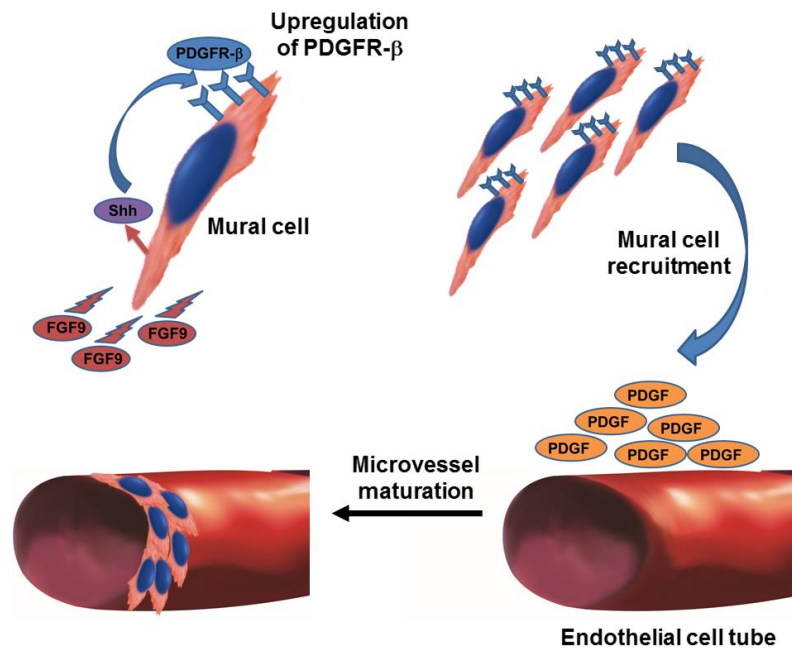
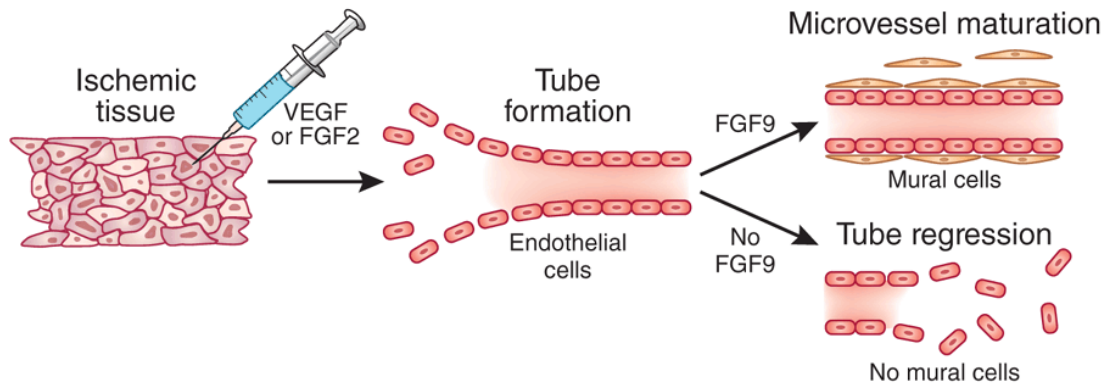


Figure 2-2: FGF9-mediated microvessel maturation.

FGF9 stimulates mural cells to express Sonic Hedgehog, which signals the upregulation of PDGFR- β in an autocrine manner. PDGF-BB, the ligand of this receptor, which is synthesized by the endothelial cell tubes, enhances the recruitment of FGF9-stimulated mural cells. Hence, the FGF9-SHH-PDGFR β axis mediates the migration of mural cells to endothelial tubes resulting in microvessel maturation.

Figure 2-3 illustrates FGF-9–stabilization of nascent microvessels through mural cell recruitment to ECs tubes. FGF-9 increases smooth muscle cell expression of the PDGF receptor, through the SHH pathway, thereby enhancing the recruitment of smooth muscles to nascent vessels. When FGF-9 was infused into ischemic mouse hind limb, the resulting microvessels were found to be invested with more VSMCs than those generated in the absence of FGF-9. In addition, FGF-9 injection had led to accelerated re-growth of muscle mass, along with improved limb function, compared to control vehicle [83].



Katie Vicari

Figure 2-3: FGF9—stabilization of nascent microvessels through mural cells recruitment to endothelial cell tubes.

Used with permission from Macmillan Publishers Ltd: [Nat Biotechnol][83].

2.9 Angiogenic Growth Factors Delivery Technologies

The use of recombinant protein growth factors may be a preferred therapeutic strategy compared with gene therapy [100]. Angiogenic growth factors have been delivered either by bolus injection or infusion into systemic circulation or the tissues of interest. The short half-life of these proteins results in low local availability that do not meet the spatial and temporal design criteria [17, 101-103]. One approach to overcome such limitations is the localized and sustained delivery of growth factors at the desired site from polymer-based delivery systems.

2.9.1 Controlled Delivery of Angiogenic Factors from Polymer-based Systems

Biodegradable polymer vehicles incorporating growth factors can provide sustained release into the site of interest yielding concentrations within the therapeutic range over a period of days to months [17, 104]. Moreover, polymer properties can be readily tailored to change the temporal and spatial release profiles, making polymer-based delivery systems promising candidates for therapeutic angiogenesis [17, 105-107]. Polymers used in controlled delivery of angiogenic factors include synthetic polymers such as poly(glycolic

acid) (PGA), poly(lactic acid) (PLA), and their copolymer (PLGA) [104, 108, 109]. In addition, natural polymers such as fibrin [110], collagen [111], alginate [112], chitosan [113], gelatin [114], and other hydrogels [115] can be used in the fabrication of controlled delivery systems. Delivery systems often comprise porous scaffolds, hydrogels or microspheres according to the desired application [105, 116]. The fabrication method used to produce the scaffold or vehicle can denature or inactivate the incorporated angiogenic factors. Electrospinning together with gas-foaming techniques were reported to produce vehicles that retain the bioactivity of incorporated and released growth factors [117-120]. Fibrin gel has been used as delivery system of growth factors such as nerve growth factor [121], bFGF [122], VEGF [123], and transforming growth factor-beta [124]. Despite positive results, the release kinetics from such fibrin delivery matrix remained uncontrolled [3]. On the other hand, incorporation of thrombin and fibrinogen together with heparin in fibrin gels demonstrated better control of the release rate of heparin-binding growth factors, such as VEGF and FGF-2 [125], which can be explained by the fact that many angiogenic growth factors are found associated with heparin in native ECM. Moreover, photoreactive combinations of gelatin and heparin have also been employed to localize VEGF and FGF-2 to polyurethane grafts [126]. Collagen and its derivative gelatin often have poor loading capacity for growth factors. Heparin has been covalently attached to collagen to enhance the capture of angiogenic growth factors in the matrix. The addition of glycosaminoglycans alters the cross-linking density of the matrix and decreases the pore size limiting the burst release of entrapped growth factors [3, 111]. Alginate microspheres can be employed for sustained release of entrapped proteins. Protein loss during bead preparation has been a major challenge for efficient drug delivery [3]. Microspheres of PLGA and poly(ethylene glycol) have been formulated for controlled release of VEGF with subsequent evaluation *in vitro* [104]. As with alginate microspheres, the exact processing parameters and subsequent retention of bioactivity remains challenging. VEGF has also been delivered from hydrocarbon stent coatings, which demonstrated increased EC growth [127]. Immobilization of growth factors has been adopted to induce specific and localized effect. It can protect against cellular inactivation and digestion [128]. Immobilized bFGF onto poly(ethylene glycol) diacrylate hydrogels has been reported to induce VSMC proliferation and migration [129].

2.9.2 Electrospun Fibers as Angiogenic Factor Delivery Vehicles

Electrospinning is an established technique for scaffold fabrication that can prolong the angiogenic factor release and overcome difficulties encountered with angiogenic factor incorporation within conventional scaffolds, such as controlling the release profile and retaining growth factor bioactivity. In the electrospinning process, a high voltage is applied to the droplet of polymer solution to overcome the surface tension and enable the formation of fibers with an average diameter ranging from the micrometer to the sub-micrometer range. Desirable release profiles can be achieved by controlling the chemical nature of polymers and bioactive molecules, size and morphology of fibers, porosity of fibrous structure and their degradation rate, and initial drug-loading [130]. An appropriately sustained growth factor release profile in combination with a nanofibrous scaffold could positively influence stem cell behavior and fate [119]. Sahoo *et al.* [119] reported that PLGA nanofibers incorporated with bFGF favored bone marrow stem cell attachment and subsequent proliferation. In this case, cells cultured on coaxial electrospun fibrous scaffolds demonstrated increased collagen production and upregulated gene expression of specific ECM proteins, indicating fibroblastic differentiation. Casper *et al.* [131] used a low molecular weight heparin (LMWH) grafted to poly (ethylene glycol) and electrospun this conjugate within PLGA for bFGF delivery. Heparin retention within the graft structure was increased as well as FGF retention with the conjugation versus LMWH alone. It has been proposed that the resulting nanoscale features, that are achievable with electrospinning, may be ideal for growth factor localization. Heparinized electrospun fibers were reported to efficiently bind bFGF, sustaining its release and preserving its bioactivity [120]. Chitosan/poly(vinyl alcohol) conjugated nerve growth factor scaffolds for potential neural tissue engineering purposes were prepared using electrospinning and reported to support cell attachment and proliferation [132]. Co-axial electrospun fibers offered both topographical and biochemical cues for regenerative medicine applications. The plasma factor VIII-releasing co-axial electrospun poly(urethane) fibers facilitated sustained treatment of hemophilia via a non-viral tissue engineering approach [118]. Emulsion electrospinning was adopted to embed bFGF into poly(ethylene glycol)-poly(DL-lactide) ultrafine fibers with a core-sheath structure to promote the wound healing process [133].

Moreover, bFGF was physically immobilized within gelatin electrospun scaffolds with aligned or random fiber orientations. EC adhesion and orientation was found to be highly dependent on scaffold fiber orientation and morphology, where the cells expressed synthetic phenotype when seeded onto the aligned scaffolds, which is of a particular importance in new blood vessel formation [134].

A family of biodegradable poly(ester amide)s (PEA)s was explored in our laboratory to fabricate electrospun nanofibers [135, 136]. The rationale for exploring PEAs is that they combine the favorable properties of both polyesters and polyamides – the tunability in the degradation rate via the ester groups and mechanical strength via the hydrogen bonding of the amide groups. The ester and amide linkages promote both hydrolytic and enzymatic degradation, which should ensure a surface degradation mechanism [137], and this provides better prediction and control over the release profile. In addition, PEAs with tailored degradation rates can be synthesized with the careful selection of the monomers. Their degradation by-products include amino acids, which are found physiologically, limiting their potential systemic toxicity [138]. Unlike polyesters, PEA degradation results in less acidic by-products, avoiding significant pH decrease in the tissues and thus decreased host immune responses [139]. In this thesis, a PEA derived from the α -amino acid, L-phenylalanine, was utilized to fabricate dual-loaded electrospun fibers for therapeutic angiogenesis application.

2.9.3 Spatio-temporal Controlled Delivery of Angiogenic Factors

Local concentration of angiogenic growth factors delivered by polymer-based delivery systems can be tuned by modifying the physical or chemical properties of these systems. The release of encapsulated growth factors is controlled by porosity, pore size, inter-pore distance, the degree of cross-linking, and degradation rate of the delivery system [17]. Pore size and porosity have also been found to affect host inflammation and angiogenesis [140]. Mooney and coworkers [141] reported that altering the composition of synthetic polymer such as PLGA can control the degradation rate to produce differential VEGF release profiles. Delivery systems can be designed to release angiogenic growth factors in

response to specific signals from the cellular environment, including enzymes such as cell secreted proteinases [142, 143] and mechanical stimulation [144]. Polymer-based systems permitting sequential growth factors delivery; such as VEGF and PDGF-BB [95], VEGF and Angiopoietin-1 [145], or FGF-2 and PDGF-BB [38], have been demonstrated to promote mature and stable vessel formation more effectively than simultaneous delivery of the growth factors.

Spatial gradients of growth factors in tissues of interest can be achieved by changing the placement of polymer vehicles, immobilizing insoluble ligands to localize cells of interest, or designing delivery systems to provide spatially distinct signals [17]. For example, a porous bi-layered PLG scaffold system locally presenting VEGF alone in one spatial region, and VEGF and PDGF-BB in an adjacent region was reported to produce spatially different vessel morphologies [146]. Accordingly, presenting pro- and anti-angiogenic factors at different sites in the polymer scaffold may produce diverse vascular structures [17]. Coupling of cell adhesive ligands such as Arg-Gly-Asp (RGD) to the site of interest can also be used to control the region of vessels formation [147], and the nano-scale organization of RGD can affect EC adhesion and motility [148]. Novel 3D fabrication techniques can offer more opportunities to control the geometry and design of polymer-based scaffolds [149], consequently making it possible to incorporate angiogenic growth factor releasing vehicles into micro or nano-scale electromechanical devices to have more accurate control over spatial and temporal presentation of these growth factors [150, 151]. Integrating therapeutic angiogenesis with nanomedicine strategies may also offer more promising applications in regenerative medicine [152].

2.10 Safety of Angiogenic Growth Factor Delivery

Several safety concerns can arise from the delivery of angiogenic growth factors to induce therapeutic angiogenesis for treatment of ischemic cardiovascular disease. These concerns focus on the potential for pathological angiogenesis and the side effects of the delivered factor [153]. Animal studies and early clinical trials suggested several typical side effects associated with exposure to FGF-2 and VEGF. VEGF and FGF-2 are known to be

associated with systemic hypotension that occurs in a dose-dependent fashion; in this regard, the doses of FGF-2 leading to hypotension are substantially higher than for VEGF [154, 155]. It can be attributed to the upregulation of nitric oxide synthase and increased vessel wall permeability [156]. This has been shown in phase I trials at high doses or with rapid infusion of the angiogenic factors. FGF-2 has also been associated with proliferative membranous nephropathy leading to proteinuria in mice, but this has not been observed in clinical studies [157]. It is probably related to FGF-2 deposition in the heparan sulphate rich glomerular membrane [158]. For that reason, FGF-2 is not preferred to be used in patients with decreased creatinine clearance. Also, the adverse effects of VEGF and FGF include local oedema, anaemia, and thrombocytopenia [159, 160]. Growth factor gene therapy is usually accompanied with concerns of inflammatory responses due to exposure of patients to foreign genetic material and viral vectors [44, 46]. Over-expression of VEGF in mice has been associated with the formation of angiomas and vascular tumors [161, 162]. The major concern is that the induction of angiogenesis may increase the risk of cancer. This concern arises from the well documented role of angiogenesis in tumor growth and metastasis [163]. To date, neither *in vitro* nor *in vivo* data exists to suggest that methods of therapeutic angiogenesis increase the risk of neoplastic growth or metastases. Oncogenic effects are not likely to occur with short-term dosing, appropriate patient selection, and localized delivery [74, 164, 165].

2.11 Conclusions

Ischemic heart disease causes millions of deaths worldwide. Data in the literature suggest that therapeutic angiogenesis may offer hope for ischemic heart disease patients who are ineligible to standard revascularization techniques. Moreover, if this proves to be the case, then expanded indications for therapeutic angiogenesis might then follow. Comprehensive understanding of the basic biology of neovascularization in physiological and pathological conditions will provide important information for the design of optimal delivery systems in terms of growth factor concentration, spatial and temporal release profiles, and their simultaneous or sequential presentation. Moreover, increased knowledge of the biological

mechanisms that regulate blood vessels growth and maturation, which highlights the complexity of molecular and cellular interactions taking place within the angiogenic microenvironment, is essential for targeting both neovascular induction and maturation. The combination of therapeutic angiogenesis with controlled delivery strategies could provide a minimally invasive revascularisation strategy that may be a major advance in the treatment of ischemic heart disease.

2.12 References

1. Roger, V.L., A.S. Go, D.M. Lloyd-Jones, E.J. Benjamin, J.D. Berry, W.B. Borden, D.M. Bravata, S. Dai, E.S. Ford, C.S. Fox, H.J. Fullerton, C. Gillespie, S.M. Hailpern, J.A. Heit, V.J. Howard, B.M. Kissela, S.J. Kittner, D.T. Lackland, J.H. Lichtman, L.D. Lisabeth, D.M. Makuc, G.M. Marcus, A. Marelli, D.B. Matchar, C.S. Moy, D. Mozaffarian, M.E. Mussolino, G. Nichol, N.P. Paynter, E.Z. Soliman, P.D. Sorlie, N. Sotoodehnia, T.N. Turan, S.S. Virani, N.D. Wong, D. Woo, and M.B. Turner, Heart disease and stroke statistics--2012 update: a report from the American Heart Association. *Circulation*, 2012. **125**(1): e2-e220.
2. Gaziano, T.A., A. Bitton, S. Anand, S. Abrahams-Gessel, and A. Murphy, Growing epidemic of coronary heart disease in low- and middle-income countries. *Curr Probl Cardiol*, 2010. **35**(2): 72-115.
3. Zhang, G. and L.J. Suggs, Matrices and scaffolds for drug delivery in vascular tissue engineering. *Adv Drug Deliv Rev*, 2007. **59**(4-5): 360-73.
4. Williams, B., M. Menon, D. Satran, D. Hayward, J.S. Hodges, M.N. Burke, R.K. Johnson, A.K. Poulouse, J.H. Traverse, and T.D. Henry, Patients with coronary artery disease not amenable to traditional revascularization: prevalence and 3-year mortality. *Catheter Cardiovasc Interv*, 2010. **75**(6): 886-91.
5. Mitsos, S., K. Katsanos, E. Koletsis, G.C. Kagadis, N. Anastasiou, A. Diamantopoulos, D. Karnabatidis, and D. Dougenis, Therapeutic angiogenesis for myocardial ischemia revisited: basic biological concepts and focus on latest clinical trials. *Angiogenesis*, 2012. **15**(1): 1-22.
6. Losordo, D.W. and S. Dimmeler, Therapeutic angiogenesis and vasculogenesis for ischemic disease. Part I: angiogenic cytokines. *Circulation*, 2004. **109**(21): 2487-91.
7. Losordo, D.W. and S. Dimmeler, Therapeutic angiogenesis and vasculogenesis for ischemic disease: part II: cell-based therapies. *Circulation*, 2004. **109**(22): 2692-7.

8. Gupta, R., J. Tongers, and D.W. Losordo, Human studies of angiogenic gene therapy. *Circ Res*, 2009. **105**(8): 724-36.
9. Lekas, M., P. Lekas, D.A. Latter, M.B. Kutryk, and D.J. Stewart, Growth factor-induced therapeutic neovascularization for ischaemic vascular disease: time for a re-evaluation? *Curr Opin Cardiol*, 2006. **21**(4): 376-84.
10. Robich, M.P., L.M. Chu, S. Oyamada, N.R. Sodha, and F.W. Sellke, Myocardial therapeutic angiogenesis: a review of the state of development and future obstacles. *Expert Rev Cardiovasc Ther*, 2011. **9**(11): 1469-79.
11. Conway, E.M., D. Collen, and P. Carmeliet, Molecular mechanisms of blood vessel growth. *Cardiovasc Res*, 2001. **49**(3): 507-21.
12. Lutun, A. and P. Carmeliet, De novo vasculogenesis in the heart. *Cardiovasc Res*, 2003. **58**(2): 378-89.
13. Adair, T.H. and J.P. Montani, Angiogenesis, in *Integrated Systems Physiology: from Molecule to Function to Disease*, D.N. Granger and J.P. Granger, Editors. 2010, Morgan & Claypool Life Sciences. 1-84.
14. Li, B., E.E. Sharpe, A.B. Maupin, A.A. Teleron, A.L. Pyle, P. Carmeliet, and P.P. Young, VEGF and PlGF promote adult vasculogenesis by enhancing EPC recruitment and vessel formation at the site of tumor neovascularization. *FASEB J*, 2006. **20**(9): 1495-7.
15. Schaper, W., Collateral circulation: past and present. *Basic Res Cardiol*, 2009. **104**(1): 5-21.
16. Ferrara, N. and R.S. Kerbel, Angiogenesis as a therapeutic target. *Nature*, 2005. **438**(7070): 967-74.
17. Cao, L. and D.J. Mooney, Spatiotemporal control over growth factor signaling for therapeutic neovascularization. *Adv Drug Delivery Rev*, 2007. **59**(13): 1340-50.
18. Understanding Angiogenesis: Angiogenesis process. [accessed July 2016; Available from: <http://www.angio.org/ua.php>.
19. Davis, G.E., A.N. Stratman, A. Sacharidou, and W. Koh, Molecular basis for endothelial lumen formation and tubulogenesis during vasculogenesis and angiogenic sprouting. *Int Rev Cell Mol Biol*, 2011. **288**: 101-65.
20. Stratman, A.N. and G.E. Davis, Endothelial cell-pericyte interactions stimulate basement membrane matrix assembly: influence on vascular tube remodeling, maturation, and stabilization. *Microsc Microanal*, 2012. **18**(1): 68-80.

21. Forsythe, J.A., B.H. Jiang, N.V. Iyer, F. Agani, S.W. Leung, R.D. Koos, and G.L. Semenza, Activation of vascular endothelial growth factor gene transcription by hypoxia-inducible factor 1. *Mol Cell Biol*, 1996. **16**(9): 4604-13.
22. Ruel, M. and F.W. Sellke, Angiogenic protein therapy. *Semin Thorac Cardiovasc Surg*, 2003. **15**(3): 222-35.
23. Tammela, T., B. Enholm, K. Alitalo, and K. Paavonen, The biology of vascular endothelial growth factors. *Cardiovasc Res*, 2005. **65**(3): 550-63.
24. Roy, H., S. Bhardwaj, and S. Yla-Herttuala, Biology of vascular endothelial growth factors. *FEBS Lett*, 2006. **580**(12): 2879-87.
25. Yla-Herttuala, S., T.T. Rissanen, I. Vajanto, and J. Hartikainen, Vascular endothelial growth factors: biology and current status of clinical applications in cardiovascular medicine. *J Am Coll Cardiol*, 2007. **49**(10): 1015-26.
26. Olsson, A.K., A. Dimberg, J. Kreuger, and L. Claesson-Welsh, VEGF receptor signalling - in control of vascular function. *Nat Rev Mol Cell Biol*, 2006. **7**(5): 359-71.
27. Bruce, D. and P.H. Tan, Vascular endothelial growth factor receptors and the therapeutic targeting of angiogenesis in cancer: where do we go from here? *Cell Commun Adhes*, 2011. **18**(5): 85-103.
28. Shibuya, M., Differential roles of vascular endothelial growth factor receptor-1 and receptor-2 in angiogenesis. *J Biochem Mol Biol*, 2006. **39**(5): 469-78.
29. Tabibiazar, R. and S.G. Rockson, Angiogenesis and the ischaemic heart. *Eur Heart J*, 2001. **22**(11): 903-18.
30. Unemori, E.N., N. Ferrara, E.A. Bauer, and E.P. Amento, Vascular endothelial growth factor induces interstitial collagenase expression in human endothelial cells. *J Cell Physiol*, 1992. **153**(3): 557-62.
31. Costa, C., R. Soares, J.S. Reis-Filho, D. Leitao, I. Amendoeira, and F.C. Schmitt, Cyclo-oxygenase 2 expression is associated with angiogenesis and lymph node metastasis in human breast cancer. *J Clin Pathol*, 2002. **55**(6): 429-34.
32. Li, J., L.F. Brown, M.G. Hibberd, J.D. Grossman, J.P. Morgan, and M. Simons, VEGF, flk-1, andflt-1 expression in a rat myocardial infarction model of angiogenesis. *Am J Physiol*, 1996. **270**(5 Pt 2): H1803-11.
33. Kalka, C., H. Masuda, T. Takahashi, R. Gordon, O. Tepper, E. Gravereaux, A. Pieczek, H. Iwaguro, S.I. Hayashi, J.M. Isner, and T. Asahara, Vascular endothelial growth factor(165) gene transfer augments circulating endothelial progenitor cells in human subjects. *Circ Res*, 2000. **86**(12): 1198-202.

34. Presta, M., P. Dell'Era, S. Mitola, E. Moroni, R. Ronca, and M. Rusnati, Fibroblast growth factor/fibroblast growth factor receptor system in angiogenesis. *Cytokine Growth Factor Rev*, 2005. **16**(2): 159-78.
35. Itoh, N. and D.M. Ornitz, Fibroblast growth factors: from molecular evolution to roles in development, metabolism and disease. *J Biochem*, 2011. **149**(2): 121-30.
36. Venkataraman, G., R. Raman, V. Sasisekharan, and R. Sasisekharan, Molecular characteristics of fibroblast growth factor-fibroblast growth factor receptor-heparin-like glycosaminoglycan complex. *Proc Natl Acad Sci U S A*, 1999. **96**(7): 3658-63.
37. Distler, J.H., A. Hirth, M. Kurowska-Stolarska, R.E. Gay, S. Gay, and O. Distler, Angiogenic and angiostatic factors in the molecular control of angiogenesis. *Q J Nucl Med*, 2003. **47**(3): 149-61.
38. Cao, R., E. Brakenhielm, R. Pawliuk, D. Wariaro, M.J. Post, E. Wahlberg, P. Leboulch, and Y. Cao, Angiogenic synergism, vascular stability and improvement of hind-limb ischemia by a combination of PDGF-BB and FGF-2. *Nat Med*, 2003. **9**(5): 604-13.
39. Wang, X.T., P.Y. Liu, and J.B. Tang, PDGF gene therapy enhances expression of VEGF and bFGF genes and activates the NF-kappaB gene in signal pathways in ischemic flaps. *Plast Reconstr Surg*, 2006. **117**(1): 129-37; discussion 138-9.
40. Alvarez, R.H., H.M. Kantarjian, and J.E. Cortes, Biology of platelet-derived growth factor and its involvement in disease. *Mayo Clin Proc*, 2006. **81**(9): 1241-57.
41. Sellke, F.W. and M. Ruel, Vascular growth factors and angiogenesis in cardiac surgery. *Ann Thorac Surg*, 2003. **75**(2): S685-90.
42. Tsurumi, Y., S. Takeshita, D. Chen, M. Kearney, S.T. Rossow, J. Passeri, J.R. Horowitz, J.F. Symes, and J.M. Isner, Direct intramuscular gene transfer of naked DNA encoding vascular endothelial growth factor augments collateral development and tissue perfusion. *Circulation*, 1996. **94**(12): 3281-90.
43. Vale, P.R., D.W. Losordo, C.E. Milliken, M.C. McDonald, L.M. Gravelin, C.M. Curry, D.D. Esakof, M. Maysky, J.F. Symes, and J.M. Isner, Randomized, single-blind, placebo-controlled pilot study of catheter-based myocardial gene transfer for therapeutic angiogenesis using left ventricular electromechanical mapping in patients with chronic myocardial ischemia. *Circulation*, 2001. **103**(17): 2138-43.
44. Hedman, M., J. Hartikainen, M. Syvanne, J. Stjernvall, A. Hedman, A. Kivela, E. Vanninen, H. Mussalo, E. Kauppila, S. Simula, O. Narvanen, A. Rantala, K. Peuhkurinen, M.S. Nieminen, M. Laakso, and S. Yla-Herttuala, Safety and feasibility of catheter-based local intracoronary vascular endothelial growth factor gene transfer in the prevention of postangioplasty and in-stent restenosis and in the

treatment of chronic myocardial ischemia: phase II results of the Kuopio Angiogenesis Trial (KAT). *Circulation*, 2003. **107**(21): 2677-83.

45. Kastrup, J., E. Jorgensen, A. Ruck, K. Tagil, D. Glogar, W. Ruzyllo, H.E. Botker, D. Dudek, V. Drvota, B. Hesse, L. Thuesen, P. Blomberg, M. Gyongyosi, and C. Sylven, Direct intramyocardial plasmid vascular endothelial growth factor-A165 gene therapy in patients with stable severe angina pectoris A randomized double-blind placebo-controlled study: the Euroinject One trial. *J Am Coll Cardiol*, 2005. **45**(7): 982-8.
46. McMahon, J.M., K.E. Wells, J.E. Bamfo, M.A. Cartwright, and D.J. Wells, Inflammatory responses following direct injection of plasmid DNA into skeletal muscle. *Gene Ther*, 1998. **5**(9): 1283-90.
47. Wright, M.J., L.M. Wightman, C. Lilley, M. de Alwis, S.L. Hart, A. Miller, R.S. Coffin, A. Thrasher, D.S. Latchman, and M.S. Marber, In vivo myocardial gene transfer: optimization, evaluation and direct comparison of gene transfer vectors. *Basic Res Cardiol*, 2001. **96**(3): 227-36.
48. Laitinen, M., T. Pakkanen, E. Donetti, R. Baetta, J. Luoma, P. Lehtolainen, H. Viita, R. Agrawal, A. Miyanojara, T. Friedmann, W. Risau, J.F. Martin, M. Soma, and S. Yla-Herttuala, Gene transfer into the carotid artery using an adventitial collar: comparison of the effectiveness of the plasmid-liposome complexes, retroviruses, pseudotyped retroviruses, and adenoviruses. *Hum Gene Ther*, 1997. **8**(14): 1645-50.
49. Kankkonen, H.M., E. Vahakangas, R.A. Marr, T. Pakkanen, A. Laurema, P. Leppanen, J. Jalkanen, I.M. Verma, and S. Yla-Herttuala, Long-term lowering of plasma cholesterol levels in LDL-receptor-deficient WHHL rabbits by gene therapy. *Mol Ther*, 2004. **9**(4): 548-56.
50. Masaki, I., Y. Yonemitsu, K. Komori, H. Ueno, Y. Nakashima, K. Nakagawa, M. Fukumura, A. Kato, M.K. Hasan, Y. Nagai, K. Sugimachi, M. Hasegawa, and K. Sueishi, Recombinant Sendai virus-mediated gene transfer to vasculature: a new class of efficient gene transfer vector to the vascular system. *Faseb J*, 2001. **15**(7): 1294-6.
51. Coffin, R.S., M.K. Howard, D.V. Cumming, C.M. Dollery, J. McEwan, D.M. Yellon, M.S. Marber, A.R. MacLean, S.M. Brown, and D.S. Latchman, Gene delivery to the heart in vivo and to cardiac myocytes and vascular smooth muscle cells in vitro using herpes virus vectors. *Gene Ther*, 1996. **3**(7): 560-6.
52. Airene, K.J., M.O. Hiltunen, M.P. Turunen, A.M. Turunen, O.H. Laitinen, M.S. Kulomaa, and S. Yla-Herttuala, Baculovirus-mediated periadventitial gene transfer to rabbit carotid artery. *Gene Ther*, 2000. **7**(17): 1499-504.

53. Rissanen, T.T. and S. Yla-Herttuala, Current status of cardiovascular gene therapy. *Mol Ther*, 2007. **15**(7): 1233-47.
54. Gruchala, M., S. Bhardwaj, K. Pajusola, H. Roy, T.T. Rissanen, I. Kokina, I. Kholova, J.E. Markkanen, J. Rutanen, T. Heikura, K. Alitalo, H. Bueler, and S. Yla-Herttuala, Gene transfer into rabbit arteries with adeno-associated virus and adenovirus vectors. *J Gene Med*, 2004. **6**(5): 545-54.
55. Su, H., Y. Huang, J. Takagawa, A. Barcena, J. Arakawa-Hoyt, J. Ye, W. Grossman, and Y.W. Kan, AAV serotype-1 mediates early onset of gene expression in mouse hearts and results in better therapeutic effect. *Gene Ther*, 2006. **13**(21): 1495-502.
56. Formiga, F.R., B. Pelacho, E. Garbayo, G. Abizanda, J.J. Gavira, T. Simon-Yarza, M. Mazo, E. Tamayo, C. Jauquicoa, C. Ortiz-de-Solorzano, F. Prosper, and M.J. Blanco-Prieto, Sustained release of VEGF through PLGA microparticles improves vasculogenesis and tissue remodeling in an acute myocardial ischemia-reperfusion model. *J Control Release*, 2010. **147**(1): 30-7.
57. Gao, J., J. Liu, Y. Gao, C. Wang, Y. Zhao, B. Chen, Z. Xiao, Q. Miao, and J. Dai, A myocardial patch made of collagen membranes loaded with collagen-binding human vascular endothelial growth factor accelerates healing of the injured rabbit heart. *Tissue Eng Part A*, 2011. **17**(21-22): 2739-47.
58. Miyagi, Y., L.L. Chiu, M. Cimini, R.D. Weisel, M. Radisic, and R.K. Li, Biodegradable collagen patch with covalently immobilized VEGF for myocardial repair. *Biomaterials*, 2011. **32**(5): 1280-90.
59. Cittadini, A., M.G. Monti, V. Petrillo, G. Esposito, G. Imparato, A. Luciani, F. Urciuolo, E. Bobbio, C.F. Natale, L. Sacca, and P.A. Netti, Complementary therapeutic effects of dual delivery of insulin-like growth factor-1 and vascular endothelial growth factor by gelatin microspheres in experimental heart failure. *Eur J Heart Fail*, 2011. **13**(12): 1264-74.
60. Rutanen, J., T.T. Rissanen, J.E. Markkanen, M. Gruchala, P. Silvennoinen, A. Kivela, A. Hedman, M. Hedman, T. Heikura, M.R. Orden, S.A. Stacker, M.G. Achen, J. Hartikainen, and S. Yla-Herttuala, Adenoviral catheter-mediated intramyocardial gene transfer using the mature form of vascular endothelial growth factor-D induces transmural angiogenesis in porcine heart. *Circulation*, 2004. **109**(8): 1029-35.
61. Schaper, W. and W.D. Ito, Molecular mechanisms of coronary collateral vessel growth. *Circ Res*, 1996. **79**(5): 911-9.
62. Unger, E.F., S. Banai, M. Shou, M. Jaklitsch, E. Hodge, R. Correa, M. Jaye, and S.E. Epstein, A model to assess interventions to improve collateral blood flow: continuous administration of agents into the left coronary artery in dogs. *Cardiovasc Res*, 1993. **27**(5): 785-91.

63. Iwakura, A., M. Fujita, K. Kataoka, K. Tambara, Y. Sakakibara, M. Komeda, and Y. Tabata, Intramyocardial sustained delivery of basic fibroblast growth factor improves angiogenesis and ventricular function in a rat infarct model. *Heart Vessels*, 2003. **18**(2): 93-9.
64. Nie, S.P., X. Wang, S.B. Qiao, Q.T. Zeng, J.Q. Jiang, X.Q. Liu, X.M. Zhu, G.X. Cao, and C.S. Ma, Improved myocardial perfusion and cardiac function by controlled-release basic fibroblast growth factor using fibrin glue in a canine infarct model. *J Zhejiang Univ Sci B*, 2010. **11**(12): 895-904.
65. Sakakibara, Y., K. Tambara, G. Sakaguchi, F. Lu, M. Yamamoto, K. Nishimura, Y. Tabata, and M. Komeda, Toward surgical angiogenesis using slow-released basic fibroblast growth factor. *Eur J Cardiothorac Surg*, 2003. **24**(1): 105-11; discussion 112.
66. Grines, C., G.M. Rubanyi, N.S. Kleiman, P. Marrott, and M.W. Watkins, Angiogenic gene therapy with adenovirus 5 fibroblast growth factor-4 (Ad5FGF-4): a new option for the treatment of coronary artery disease. *Am J Cardiol*, 2003. **92**(9B): 24N-31N.
67. Seiler, C., T. Pohl, K. Wustmann, D. Hutter, P.A. Nicolet, S. Windecker, F.R. Eberli, and B. Meier, Promotion of collateral growth by granulocyte-macrophage colony-stimulating factor in patients with coronary artery disease: a randomized, double-blind, placebo-controlled study. *Circulation*, 2001. **104**(17): 2012-7.
68. Zbinden, S., R. Zbinden, P. Meier, S. Windecker, and C. Seiler, Safety and efficacy of subcutaneous-only granulocyte-macrophage colony-stimulating factor for collateral growth promotion in patients with coronary artery disease. *J Am Coll Cardiol*, 2005. **46**(9): 1636-42.
69. Zohlhofer, D., I. Ott, J. Mehilli, K. Schomig, F. Michalk, T. Ibrahim, G. Meisetschlager, J. von Wedel, H. Bollwein, M. Seyfarth, J. Dirschinger, C. Schmitt, M. Schwaiger, A. Kastrati, and A. Schomig, Stem cell mobilization by granulocyte colony-stimulating factor in patients with acute myocardial infarction: a randomized controlled trial. *JAMA*, 2006. **295**(9): 1003-10.
70. Ripa, R.S., E. Jorgensen, Y. Wang, J.J. Thune, J.C. Nilsson, L. Sondergaard, H.E. Johnsen, L. Kober, P. Grande, and J. Kastrup, Stem cell mobilization induced by subcutaneous granulocyte-colony stimulating factor to improve cardiac regeneration after acute ST-elevation myocardial infarction: result of the double-blind, randomized, placebo-controlled stem cells in myocardial infarction (STEMMI) trial. *Circulation*, 2006. **113**(16): 1983-92.
71. Laham, R.J., F.W. Sellke, E.R. Edelman, J.D. Pearlman, J.A. Ware, D.L. Brown, J.P. Gold, and M. Simons, Local perivascular delivery of basic fibroblast growth factor in patients undergoing coronary bypass surgery: results of a phase I

- randomized, double-blind, placebo-controlled trial. *Circulation*, 1999. **100**(18): 1865-71.
72. Simons, M., B.H. Annex, R.J. Laham, N. Kleiman, T. Henry, H. Dauerman, J.E. Udelson, E.V. Gervino, M. Pike, M.J. Whitehouse, T. Moon, and N.A. Chronos, Pharmacological treatment of coronary artery disease with recombinant fibroblast growth factor-2: double-blind, randomized, controlled clinical trial. *Circulation*, 2002. **105**(7): 788-93.
 73. Grines, C.L., M.W. Watkins, G. Helmer, W. Penny, J. Brinker, J.D. Marmur, A. West, J.J. Rade, P. Marrott, H.K. Hammond, and R.L. Engler, Angiogenic Gene Therapy (AGENT) trial in patients with stable angina pectoris. *Circulation*, 2002. **105**(11): 1291-7.
 74. Henry, T.D., B.H. Annex, G.R. McKendall, M.A. Azrin, J.J. Lopez, F.J. Giordano, P.K. Shah, J.T. Willerson, R.L. Benza, D.S. Berman, C.M. Gibson, A. Bajamonde, A.C. Rundle, J. Fine, and E.R. McCluskey, The VIVA trial: Vascular endothelial growth factor in Ischemia for Vascular Angiogenesis. *Circulation*, 2003. **107**(10): 1359-65.
 75. Stewart, D.J., J.D. Hilton, J.M. Arnold, J. Gregoire, A. Rivard, S.L. Archer, F. Charbonneau, E. Cohen, M. Curtis, C.E. Buller, F.O. Mendelsohn, N. Dib, P. Page, J. Ducas, S. Plante, J. Sullivan, J. Macko, C. Rasmussen, P.D. Kessler, and H.S. Rasmussen, Angiogenic gene therapy in patients with nonrevascularizable ischemic heart disease: a phase 2 randomized, controlled trial of AdVEGF(121) (AdVEGF121) versus maximum medical treatment. *Gene Ther*, 2006. **13**(21): 1503-11.
 76. Stewart, D.J., M.J. Kutryk, D. Fitchett, M. Freeman, N. Camack, Y. Su, A. Della Siega, L. Bilodeau, J.R. Burton, G. Proulx, and S. Radhakrishnan, VEGF gene therapy fails to improve perfusion of ischemic myocardium in patients with advanced coronary disease: results of the NORTHERN trial. *Mol Ther*, 2009. **17**(6): 1109-15.
 77. Kastrup, J., E. Jorgensen, S. Fuchs, S. Nikol, H.E. Botker, M. Gyongyosi, D. Glogar, and R. Kornowski, A randomised, double-blind, placebo-controlled, multicentre study of the safety and efficacy of BIOBYPASS (AdGVVEGF121.10NH) gene therapy in patients with refractory advanced coronary artery disease: the NOVA trial. *EuroIntervention*, 2011. **6**(7): 813-8.
 78. von Tell, D., A. Armulik, and C. Betsholtz, Pericytes and vascular stability. *Exp Cell Res*, 2006. **312**(5): 623-9.
 79. Benjamin, L.E., D. Golijanin, A. Itin, D. Pode, and E. Keshet, Selective ablation of immature blood vessels in established human tumors follows vascular endothelial growth factor withdrawal. *J Clin Invest*, 1999. **103**(2): 159-65.

80. Stratman, A.N. and G.E. Davis, Endothelial Cell-Pericyte Interactions Stimulate Basement Membrane Matrix Assembly: Influence on Vascular Tube Remodeling, Maturation, and Stabilization. *Microsc Microanal*, 2011: 1-13.
81. Senger, D.R. and G.E. Davis, Angiogenesis. *Cold Spring Harb Perspect Biol*, 2011. **3**(8): a005090.
82. Steed, D.L., Clinical evaluation of recombinant human platelet-derived growth factor for the treatment of lower extremity ulcers. *Plast Reconstr Surg*, 2006. **117**(7 Suppl): 143S-149S; discussion 150S-151S.
83. Niklason, L.E., Building stronger microvessels. *Nat Biotechnol*, 2011. **29**(5): 405-6.
84. Valentijn, K.M., J.E. Sadler, J.A. Valentijn, J. Voorberg, and J. Eikenboom, Functional architecture of Weibel-Palade bodies. *Blood*, 2011. **117**(19): 5033-43.
85. Starke, R.D., F. Ferraro, K.E. Paschalaki, N.H. Dryden, T.A. McKinnon, R.E. Sutton, E.M. Payne, D.O. Haskard, A.D. Hughes, D.F. Cutler, M.A. Laffan, and A.M. Randi, Endothelial von Willebrand factor regulates angiogenesis. *Blood*, 2011. **117**(3): 1071-80.
86. Schepke, L., E.A. Murphy, A. Zarpellon, J.J. Hofmann, A. Merkulova, D.J. Shields, S.M. Weis, T.V. Byzova, Z.M. Ruggeri, M.L. Iruela-Arispe, and D.A. Cheresh, Notch promotes vascular maturation by inducing integrin-mediated smooth muscle cell adhesion to the endothelial basement membrane. *Blood*, 2012. **119**(9): 2149-58.
87. Greenberg, J.I., D.J. Shields, S.G. Barillas, L.M. Acevedo, E. Murphy, J. Huang, L. Schepke, C. Stockmann, R.S. Johnson, N. Angle, and D.A. Cheresh, A role for VEGF as a negative regulator of pericyte function and vessel maturation. *Nature*, 2008. **456**(7223): 809-13.
88. Murakami, M. and M. Simons, Regulation of vascular integrity. *J Mol Med (Berl)*, 2009. **87**(6): 571-82.
89. Tsigkou, O., I. Pomerantseva, J.A. Spencer, P.A. Redondo, A.R. Hart, E. O'Doherty, Y. Lin, C.C. Friedrich, L. Daheron, C.P. Lin, C.A. Sundback, J.P. Vacanti, and C. Neville, Engineered vascularized bone grafts. *Proc Natl Acad Sci U S A*, 2010. **107**(8): 3311-6.
90. Thurston, G., J.S. Rudge, E. Ioffe, H. Zhou, L. Ross, S.D. Croll, N. Glazer, J. Holash, D.M. McDonald, and G.D. Yancopoulos, Angiopoietin-1 protects the adult vasculature against plasma leakage. *Nat Med*, 2000. **6**(4): 460-3.
91. Jiang, J., N. Jiangl, W. Gao, J. Zhu, Y. Guo, D. Shen, G. Chen, and J. Tang, Augmentation of revascularization and prevention of plasma leakage by

- angiopoietin-1 and vascular endothelial growth factor co-transfection in rats with experimental limb ischaemia. *Acta Cardiol*, 2006. **61**(2): 145-53.
92. Smith, A.H., M.A. Kuliszewski, C. Liao, D. Rudenko, D.J. Stewart, and H. Leong-Poi, Sustained improvement in perfusion and flow reserve after temporally separated delivery of vascular endothelial growth factor and angiopoietin-1 plasmid deoxyribonucleic acid. *J Am Coll Cardiol*, 2012. **59**(14): 1320-8.
 93. Zhou, Y.F., E. Stabile, J. Walker, M. Shou, R. Baffour, Z. Yu, D. Rott, G.D. Yancopoulos, J.S. Rudge, and S.E. Epstein, Effects of gene delivery on collateral development in chronic hypoperfusion: diverse effects of angiopoietin-1 versus vascular endothelial growth factor. *J Am Coll Cardiol*, 2004. **44**(4): 897-903.
 94. Tao, Z., B. Chen, X. Tan, Y. Zhao, L. Wang, T. Zhu, K. Cao, Z. Yang, Y.W. Kan, and H. Su, Coexpression of VEGF and angiopoietin-1 promotes angiogenesis and cardiomyocyte proliferation reduces apoptosis in porcine myocardial infarction (MI) heart. *Proc Natl Acad Sci U S A*, 2011. **108**(5): 2064-9.
 95. Richardson, T.P., M.C. Peters, A.B. Ennett, and D.J. Mooney, Polymeric system for dual growth factor delivery. *Nat Biotechnol*, 2001. **19**(11): 1029-34.
 96. Kupatt, C., R. Hinkel, A. Pfosser, C. El-Aouni, A. Wuchrer, A. Fritz, F. Globisch, M. Thormann, J. Horstkotte, C. Leberherz, E. Thein, A. Banfi, and P. Boekstegers, Cotransfection of vascular endothelial growth factor-A and platelet-derived growth factor-B via recombinant adeno-associated virus resolves chronic ischemic malperfusion role of vessel maturation. *J Am Coll Cardiol*, 2010. **56**(5): 414-22.
 97. Levitzki, A., PDGF receptor kinase inhibitors for the treatment of restenosis. *Cardiovasc Res*, 2005. **65**(3): 581-6.
 98. Banquet, S., E. Gomez, L. Nicol, F. Edwards-Levy, J.P. Henry, R. Cao, D. Schapman, B. Dautreux, F. Lallemand, F. Bauer, Y. Cao, C. Thuillez, P. Mulder, V. Richard, and E. Brakenhielm, Arteriogenic therapy by intramyocardial sustained delivery of a novel growth factor combination prevents chronic heart failure. *Circulation*, 2011. **124**(9): 1059-69.
 99. Frontini, M.J., Z. Nong, R. Gros, M. Drangova, C. O'Neil, M.N. Rahman, O. Akawi, H. Yin, C.G. Ellis, and J.G. Pickering, Fibroblast growth factor 9 delivery during angiogenesis produces durable, vasoresponsive microvessels wrapped by smooth muscle cells. *Nat Biotechnol*, 2011. **29**(5): 421-427.
 100. Renault, M.A. and D.W. Losordo, Therapeutic myocardial angiogenesis. *Microvasc Res*, 2007. **74**(2-3): 159-71.
 101. Lee, K.Y., M.C. Peters, and D.J. Mooney, Comparison of vascular endothelial growth factor and basic fibroblast growth factor on angiogenesis in SCID mice. *J Control Release*, 2003. **87**(1-3): 49-56.

102. Freedman, S.B. and J.M. Isner, Therapeutic angiogenesis for coronary artery disease. *Ann Intern Med*, 2002. **136**(1): 54-71.
103. Simons, M. and J.A. Ware, Therapeutic angiogenesis in cardiovascular disease. *Nat Rev Drug Discov*, 2003. **2**(11): 863-71.
104. King, T.W. and C.W. Patrick, Jr., Development and in vitro characterization of vascular endothelial growth factor (VEGF)-loaded poly(DL-lactic-co-glycolic acid)/poly(ethylene glycol) microspheres using a solid encapsulation/single emulsion/solvent extraction technique. *J Biomed Mater Res*, 2000. **51**(3): 383-90.
105. Zisch, A.H., M.P. Lutolf, and J.A. Hubbell, Biopolymeric delivery matrices for angiogenic growth factors. *Cardiovasc Pathol*, 2003. **12**(6): 295-310.
106. Patel, Z.S. and A.G. Mikos, Angiogenesis with biomaterial-based drug- and cell-delivery systems. *J Biomater Sci Polym Ed*, 2004. **15**(6): 701-26.
107. Brey, E.M., S. Uriel, H.P. Greisler, and L.V. McIntire, Therapeutic neovascularization: contributions from bioengineering. *Tissue Eng*, 2005. **11**(3-4): 567-84.
108. Murphy, W.L., M.C. Peters, D.H. Kohn, and D.J. Mooney, Sustained release of vascular endothelial growth factor from mineralized poly(lactide-co-glycolide) scaffolds for tissue engineering. *Biomaterials*, 2000. **21**(24): 2521-7.
109. Cleland, J.L., E.T. Duenas, A. Park, A. Daugherty, J. Kahn, J. Kowalski, and A. Cuthbertson, Development of poly-(D,L-lactide--coglycolide) microsphere formulations containing recombinant human vascular endothelial growth factor to promote local angiogenesis. *J Control Release*, 2001. **72**(1-3): 13-24.
110. Briganti, E., D. Spiller, C. Mirtelli, S. Kull, C. Counoupas, P. Losi, S. Senesi, R. Di Stefano, and G. Soldani, A composite fibrin-based scaffold for controlled delivery of bioactive pro-angiogenic growth factors. *J Control Release*, 2010. **142**(1): 14-21.
111. Steffens, G.C., C. Yao, P. Prevel, M. Markowicz, P. Schenck, E.M. Noah, and N. Pallua, Modulation of angiogenic potential of collagen matrices by covalent incorporation of heparin and loading with vascular endothelial growth factor. *Tissue Eng*, 2004. **10**(9-10): 1502-9.
112. Silva, E.A. and D.J. Mooney, Spatiotemporal control of vascular endothelial growth factor delivery from injectable hydrogels enhances angiogenesis. *J Thromb Haemost*, 2007. **5**(3): 590-8.
113. Ishihara, M., K. Obara, S. Nakamura, M. Fujita, K. Masuoka, Y. Kanatani, B. Takase, H. Hattori, Y. Morimoto, M. Ishihara, T. Maehara, and M. Kikuchi, Chitosan hydrogel as a drug delivery carrier to control angiogenesis. *J Artif Organs*, 2006. **9**(1): 8-16.

114. Young, S., M. Wong, Y. Tabata, and A.G. Mikos, Gelatin as a delivery vehicle for the controlled release of bioactive molecules. *J Control Release*, 2005. **109**(1-3): 256-74.
115. Lee, K.Y. and D.J. Mooney, Hydrogels for tissue engineering. *Chem Rev*, 2001. **101**(7): 1869-79.
116. Chen, R.R. and D.J. Mooney, Polymeric growth factor delivery strategies for tissue engineering. *Pharm Res*, 2003. **20**(8): 1103-12.
117. Mooney, D.J., D.F. Baldwin, N.P. Suh, J.P. Vacanti, and R. Langer, Novel approach to fabricate porous sponges of poly(D,L-lactic-co-glycolic acid) without the use of organic solvents. *Biomaterials*, 1996. **17**(14): 1417-22.
118. Liao, I.C. and K.W. Leong, Efficacy of engineered FVIII-producing skeletal muscle enhanced by growth factor-releasing co-axial electrospun fibers. *Biomaterials*, 2010. **32**(6): 1669-77.
119. Sahoo, S., L.T. Ang, J.C.-H. Goh, and S.-L. Toh, Growth factor delivery through electrospun nanofibers in scaffolds for tissue engineering applications. *J Biomed Mater Res*, 2010. **93A**: 1539–1550.
120. Zou, J., Y. Yang, Y. Liu, F. Chen, and X. Li, Release kinetics and cellular profiles for bFGF-loaded electrospun fibers: Effect of the conjugation density and molecular weight of heparin. *Polymer* 2011. **52**: 3357-3367.
121. Sakiyama-Elbert, S.E. and J.A. Hubbell, Development of fibrin derivatives for controlled release of heparin-binding growth factors. *J Control Release*, 2000. **65**(3): 389-402.
122. Wong, C., E. Inman, R. Spaethe, and S. Helgerson, Fibrin-based biomaterials to deliver human growth factors. *Thromb Haemost*, 2003. **89**(3): 573-82.
123. Sahni, A. and C.W. Francis, Vascular endothelial growth factor binds to fibrinogen and fibrin and stimulates endothelial cell proliferation. *Blood*, 2000. **96**(12): 3772-8.
124. Giannoni, P. and E.B. Hunziker, Release kinetics of transforming growth factor-beta1 from fibrin clots. *Biotechnol Bioeng*, 2003. **83**(1): 121-3.
125. Jeon, O., S.H. Ryu, J.H. Chung, and B.S. Kim, Control of basic fibroblast growth factor release from fibrin gel with heparin and concentrations of fibrinogen and thrombin. *J Control Release*, 2005. **105**(3): 249-59.
126. Masuda, S., K. Doi, S. Satoh, T. Oka, and T. Matsuda, Vascular endothelial growth factor enhances vascularization in microporous small caliber polyurethane grafts. *ASAIO J*, 1997. **43**(5): M530-4.

127. Swanson, N., K. Hogrefe, Q. Javed, and A.H. Gershlick, In vitro evaluation of vascular endothelial growth factor (VEGF)-eluting stents. *Int J Cardiol*, 2003. **92**(2-3): 247-51.
128. Li, J.S., Y. Ito, J. Zheng, T. Takahashi, and Y. Imanishi, Enhancement of artificial juxtacrine stimulation of insulin by co-immobilization with adhesion factors. *J Biomed Mater Res*, 1997. **37**(2): 190-7.
129. DeLong, S.A., J.J. Moon, and J.L. West, Covalently immobilized gradients of bFGF on hydrogel scaffolds for directed cell migration. *Biomaterials*, 2005. **26**(16): 3227-34.
130. Li, L. and C.C. Chu, Nitroxyl radical incorporated electrospun biodegradable poly(ester Amide) nanofiber membranes. *J Biomater Sci Polym Ed*, 2009. **20**(3): 341-61.
131. Casper, C.L., N. Yamaguchi, K.L. Kiick, and J.F. Rabolt, Functionalizing electrospun fibers with biologically relevant macromolecules. *Biomacromolecules*, 2005. **6**(4): 1998-2007.
132. Mottaghitalaba, F., M. Farokhia, V. Mottaghitalabd, Mohammad Ziabarie, A. Divsalarf, and M.A. Shokrgozara, Enhancement of neural cell lines proliferation using nano-structured chitosan/poly(vinyl alcohol) scaffolds conjugated with nerve growth factor. *Carbohydrate Polymers* 2011. **86**: 526– 535.
133. Yang, Y., T. Xia, W. Zhi, L. Wei, J. Weng, C. Zhang, and X. Li, Promotion of skin regeneration in diabetic rats by electrospun core-sheath fibers loaded with basic fibroblast growth factor. *Biomaterials*, 2011. **32**(18): 4243-54.
134. Montero, R.B., X. Vial, D.T. Nguyen, S. Farhand, M. Reardon, S.M. Pham, G. Tsechpenakis, and F.M. Andreopoulos, bFGF-containing electrospun gelatin scaffolds with controlled nano-architectural features for directed angiogenesis. *Acta Biomater*, 2012. **8**(5): 1778-91.
135. Knight, D.K., E.R. Gillies, and K. Mequanint, Biomimetic L-aspartic acid-derived functional poly(ester amide)s for vascular tissue engineering. *Acta Biomater*, 2014. **10**(8): 3484-96.
136. Srinath, D., S. Lin, D.K. Knight, A.S. Rizkalla, and K. Mequanint, Fibrous biodegradable l-alanine-based scaffolds for vascular tissue engineering. *J Tissue Eng Regen Med*, 2012. **8**(7): 578-588.
137. Fan, Y., M. Kobayashi, and H. Kise, Synthesis and specific biodegradation of novel polyesteramides containing amino acid residues. *Journal of Polymer Science Part A: Polymer Chemistry*, 2001. **39**(9): 1318-1328.

138. Knight, D.K., E.R. Gillies, and K. Mequanint, Strategies in Functional Poly(ester amide) Syntheses to Study Human Coronary Artery Smooth Muscle Cell Interactions. *Biomacromolecules*, 2011. **12**(7): 2475-87.
139. Vert, M., S. Li, and H. Garreau, New insights on the degradation of bioresorbable polymeric devices based on lactic and glycolic acids. *Clinical materials*, 1992. **10**(1-2): 3-8.
140. Bezuidenhout, D., N. Davies, and P. Zilla, Effect of well defined dodecahedral porosity on inflammation and angiogenesis. *Asaio J*, 2002. **48**(5): 465-71.
141. Ennett, A.B., D. Kaigler, and D.J. Mooney, Temporally regulated delivery of VEGF in vitro and in vivo. *J Biomed Mater Res A*, 2006. **79**(1): 176-84.
142. Seliktar, D., A.H. Zisch, M.P. Lutolf, J.L. Wrana, and J.A. Hubbell, MMP-2 sensitive, VEGF-bearing bioactive hydrogels for promotion of vascular healing. *J Biomed Mater Res A*, 2004. **68**(4): 704-16.
143. Zisch, A.H., M.P. Lutolf, M. Ehrbar, G.P. Raeber, S.C. Rizzi, N. Davies, H. Schmokel, D. Bezuidenhout, V. Djonov, P. Zilla, and J.A. Hubbell, Cell-demanded release of VEGF from synthetic, biointeractive cell ingrowth matrices for vascularized tissue growth. *Faseb J*, 2003. **17**(15): 2260-2.
144. Lee, K.Y., M.C. Peters, K.W. Anderson, and D.J. Mooney, Controlled growth factor release from synthetic extracellular matrices. *Nature*, 2000. **408**(6815): 998-1000.
145. Peirce, S.M., R.J. Price, and T.C. Skalak, Spatial and temporal control of angiogenesis and arterialization using focal applications of VEGF164 and Ang-1. *Am J Physiol Heart Circ Physiol*, 2004. **286**(3): H918-25.
146. Chen, R.R., E.A. Silva, W.W. Yuen, and D.J. Mooney, Spatio-temporal VEGF and PDGF delivery patterns blood vessel formation and maturation. *Pharm Res*, 2007. **24**(2): 258-64.
147. Massia, S.P. and J.A. Hubbell, Human endothelial cell interactions with surface-coupled adhesion peptides on a nonadhesive glass substrate and two polymeric biomaterials. *J Biomed Mater Res*, 1991. **25**(2): 223-42.
148. Kong, H.J., T. Boontheekul, and D.J. Mooney, Quantifying the relation between adhesion ligand-receptor bond formation and cell phenotype. *Proc Natl Acad Sci U S A*, 2006. **103**(49): 18534-9.
149. Tsang, V.L. and S.N. Bhatia, Three-dimensional tissue fabrication. *Adv Drug Deliv Rev*, 2004. **56**(11): 1635-47.
150. Staples, M., K. Daniel, M.J. Cima, and R. Langer, Application of micro- and nano-electromechanical devices to drug delivery. *Pharm Res*, 2006. **23**(5): 847-63.

151. LaVan, D.A., T. McGuire, and R. Langer, Small-scale systems for in vivo drug delivery. *Nat Biotechnol*, 2003. **21**(10): 1184-91.
152. Farokhzad, O.C. and R. Langer, Nanomedicine: developing smarter therapeutic and diagnostic modalities. *Adv Drug Deliv Rev*, 2006. **58**(14): 1456-9.
153. Mitsos, S., K. Katsanos, E. Koletsis, G.C. Kagadis, N. Anastasiou, A. Diamantopoulos, D. Karnabatidis, and D. Dougenis, Therapeutic angiogenesis for myocardial ischemia revisited: basic biological concepts and focus on latest clinical trials. *Angiogenesis*, 2011.
154. Lopez, J.J., R.J. Laham, J.P. Carrozza, M. Tofukuji, F.W. Sellke, S. Bunting, and M. Simons, Hemodynamic effects of intracoronary VEGF delivery: evidence of tachyphylaxis and NO dependence of response. *Am J Physiol*, 1997. **273**(3 Pt 2): H1317-23.
155. Cuevas, P., M. Garcia-Calvo, F. Carceller, D. Reimers, M. Zazo, B. Cuevas, I. Munoz-Willery, V. Martinez-Coso, S. Lamas, and G. Gimenez-Gallego, Correction of hypertension by normalization of endothelial levels of fibroblast growth factor and nitric oxide synthase in spontaneously hypertensive rats. *Proc Natl Acad Sci U S A*, 1996. **93**(21): 11996-2001.
156. Horowitz, J.R., A. Rivard, R. van der Zee, M. Hariawala, D.D. Sheriff, D.D. Esakof, G.M. Chaudhry, J.F. Symes, and J.M. Isner, Vascular endothelial growth factor/vascular permeability factor produces nitric oxide-dependent hypotension. Evidence for a maintenance role in quiescent adult endothelium. *Arterioscler Thromb Vasc Biol*, 1997. **17**(11): 2793-800.
157. Sasaki, T., Y. Jyo, N. Tanda, Y. Kawakami, T. Nohno, H. Tamai, and G. Osawa, Changes in glomerular epithelial cells induced by FGF2 and FGF2 neutralizing antibody in puromycin aminonucleoside nephropathy. *Kidney Int*, 1997. **51**(1): 301-9.
158. Unger, E.F., L. Goncalves, S.E. Epstein, E.Y. Chew, C.B. Trapnell, R.O. Cannon, 3rd, and A.A. Quyyumi, Effects of a single intracoronary injection of basic fibroblast growth factor in stable angina pectoris. *Am J Cardiol*, 2000. **85**(12): 1414-9.
159. Mazue, G., F. Bertolero, C. Jacob, P. Sarmientos, and R. Roncucci, Preclinical and clinical studies with recombinant human basic fibroblast growth factor. *Ann N Y Acad Sci*, 1991. **638**: 329-40.
160. Baumgartner, I., G. Rauh, A. Pieczek, D. Wuensch, M. Magner, M. Kearney, R. Schainfeld, and J.M. Isner, Lower-extremity edema associated with gene transfer of naked DNA encoding vascular endothelial growth factor. *Ann Intern Med*, 2000. **132**(11): 880-4.

161. Carmeliet, P., VEGF gene therapy: stimulating angiogenesis or angioma-genesis? *Nat Med*, 2000. **6**(10): 1102-3.
162. Lee, R.J., M.L. Springer, W.E. Blanco-Bose, R. Shaw, P.C. Ursell, and H.M. Blau, VEGF gene delivery to myocardium: deleterious effects of unregulated expression. *Circulation*, 2000. **102**(8): 898-901.
163. Folkman, J., Angiogenesis in cancer, vascular, rheumatoid and other disease. *Nat Med*, 1995. **1**(1): 27-31.
164. Schumacher, B., P. Pecher, B.U. von Specht, and T. Stegmann, Induction of neoangiogenesis in ischemic myocardium by human growth factors: first clinical results of a new treatment of coronary heart disease. *Circulation*, 1998. **97**(7): 645-50.
165. Losordo, D.W., P.R. Vale, J.F. Symes, C.H. Dunnington, D.D. Esakof, M. Maysky, A.B. Ashare, K. Lathi, and J.M. Isner, Gene therapy for myocardial angiogenesis: initial clinical results with direct myocardial injection of phVEGF165 as sole therapy for myocardial ischemia. *Circulation*, 1998. **98**(25): 2800-4.

Chapter 3

3 Controlled Delivery of Fibroblast Growth Factor-9 from Biodegradable Poly(ester amide) Fibers for Building Functional Neovasculature*

Overview: This chapter discusses the fabrication and optimization of PEA electrospun fibers and loading them with a model protein (BSA) and FGF9 using either blend or emulsion electrospinning techniques and their characterization in terms of morphological properties, *in vitro* release kinetics, bioactivity of the released growth factor, and cell viability and metabolic activity.

3.1 Abstract

For building functional vasculature, controlled delivery of fibroblast growth factor-9 (FGF9) from electrospun protein-analog fibers is an appealing strategy to overcome challenges associated with its short half-life. FGF9 sustained delivery could potentially drive muscularization of angiogenic sprouts and help regenerate stable functional neovasculature in ischemic vascular disease patients. Electrospinning parameters of FGF9-loaded poly(ester amide) (PEA) fibers have been optimized, using blend and emulsion electrospinning techniques. *In vitro* PEA matrix degradation, biocompatibility, FGF9 release kinetics, and bioactivity of the released FGF9 were evaluated. qPCR was employed to evaluate platelet-derived growth factor receptor- β (PDGFR β) gene expression in NIH-3T3 fibroblasts, 10T1/2 cells, and human coronary artery smooth muscle cells cultured on PEA fibers at different FGF9 concentrations. Loaded PEA fibers exhibited controlled release of FGF9 over 28 days with limited burst effect while preserving FGF9 bioactivity.

* A version of this chapter is published as a research article “Somiraa S. Said, J. Geoffrey Pickering and Kibret Mequanint, *Pharmaceutical Research* (2014), 31(12); 3335-3347”. Adapted with permission from Springer © 2014.

FGF9-loaded and unloaded electrospun fibers were found to support the proliferation of fibroblasts for five days even in serum-depleted conditions. Cells cultured on FGF9-supplemented PEA mats resulted in upregulation of PDGFR β in concentration and cell type-dependent manner. This study supports the premise of controlled delivery of FGF9 from PEA electrospun fibers for potential therapeutic angiogenesis applications.

Keywords: Electrospinning; Fibroblast growth factor-9; Poly(ester amide)s; Therapeutic angiogenesis.

3.2 Introduction

Ischemic vascular diseases are characterized by inadequate delivery of blood and oxygen to tissues; coronary artery disease affects the heart, cerebrovascular disease affects the brain, and the peripheral arterial disease affects skeletal muscles and other internal organs [1]. The principal pathological process causing ischemic diseases is atherosclerosis, which is a progressive inflammatory condition that usually affects large arteries, in which the accumulation of lipids, inflammatory cells, and fibrous material in the inner arterial wall results in the occlusion of these arteries [2]. Some ischemic disease patients are ineligible for standard revascularization techniques due to poor overall health status or underlying comorbidities. Furthermore, a significant percentage of patients undergoing revascularization procedures do not meet the desired treatment outcome or experience restenosis, resulting in a poor prognosis and diminished quality of life, necessitating novel therapeutic alternatives for treatment of ischemic diseases [1].

Therapeutic angiogenesis, which includes the administration of growth factors for new and stable blood vessel formation, is an appealing approach to simulate angiogenesis in order to improve tissue perfusion and accelerate tissue regeneration in several pathological conditions such as ischemic heart disease, critical limb ischemia, diabetic ulcers, and delayed wound healing, leading to the functional recovery of ischemic tissues. However, the short half-life of exogenously delivered growth factors results in their rapid clearance

from the application site following their delivery in a soluble form as an injection or infusion in the systemic circulation or tissue of interest [3]. One approach to overcome such limitations is the controlled delivery of growth factors at the desired site from fibers using either blend, coaxial or emulsion electrospinning techniques [4-7]. This can boost the stability of the growth factors and enable the sustained release of angiogenic factors in a biologically active form at the site of interest [8].

Fibroblast growth factor-9 (FGF9) or glial activating factor is one of the FGF superfamily and relatively little is known regarding its physiological function [9]. It has higher specificity to fibroblast growth factor receptor-2/-3 isoforms [9-11], and was shown to demonstrate an elevated neointimal expression after arterial injury and contributes to smooth muscle cell proliferation [10]. Recently, it has been reported that even though FGF9 did not itself stimulate angiogenesis, it was found to drive muscularization of angiogenic sprouts and that its delivery imparts stability, longevity, and the ability to regulate blood flow through vasoresponsiveness of the newly formed microvessels [12]. The FGF9-induced layering of neovessels was suggested to be mediated by sonic hedgehog-PDGFR β -dependent signaling and it enhanced the ability of the neovasculature to receive flow and resist regression [12]. FGF9 delivery by means of an osmotic pump to ischemic hind limbs promoted neovascular maturation and recovery of limb function [12]. Therefore, FGF9 delivery may be required in order to drive the angiogenesis process towards completion since angiogenic growth factors by themselves cannot efficiently produce vasoreactive neovessels [13]. Controlled-release biodegradable polymeric fibers can serve as a simple, low-cost and efficient alternative for implantable mini-infusion pumps for the delivery of FGF9, without the need of delivery system removal after consumption of the growth factor.

Poly(ester amide)s (PEAs), successfully synthesized in our laboratory, are protein-analog polymers that were found to have the potential to promote vascular tissue regeneration owing to their biomimetic properties and favorable degradation profiles [14], for which bioactive molecules can be incorporated, potentially sustaining their release, enhancing their efficacy, and accelerating favorable cell-material interactions. Degradation products of PEAs derived from naturally occurring α -amino acids are nontoxic and can be well metabolized by the body. Moreover, PEA degradation is accompanied by the release of

less acidic by-products compared to polyesters, thus avoiding pH decrease in the vicinity of the scaffold, usually resulting in inflammatory responses [15]. Nevertheless, surface eroding PEA scaffolds exhibit linear drug release kinetics [16], which provides better control of the drug release profile. Although electrospinning of a small number of PEAs have been reported [17-19], these PEA fibers were either prepared from low-molecular weight PEAs resulting in large diameter-fibers (from 0.64 to 3.5 μm) [17], or a polymer blend was required for electrospinning, where polycaprolactone was added to L-alanine-based PEA as a viscosity modifier to facilitate electrospinning [18]. Moreover, *in vitro* degradation studies of other alanine-based PEA electrospun fibers showed that they were not practically degradable, where the weight loss was less than 6% after 305 days of incubation in phosphate buffered saline at 37 °C [19].

In this study, amino acid-based biodegradable protein-analog electrospun PEA fibers have been fabricated for controlled delivery of growth factors intended for therapeutic angiogenesis applications. The goal here is to prepare FGF9-loaded protein-analog fibers and characterize the fabricated fibers in terms of their morphological properties and *in vitro* degradation. The *in vitro* release kinetics were also studied together with the bioactivity of the released FGF9. The *in vitro* biocompatibility of the FGF9-loaded and unloaded electrospun fibers was tested using NIH-3T3, 10T1/2, and human coronary artery smooth muscle cells for potential therapeutic angiogenesis application

3.3 Materials and Methods

3.3.1 Materials

L-Phenylalanine, p-toluenesulfonic acid monohydrate, sebacoyl chloride, 1,4-butanediol and sodium carbonate (Alfa Aesar, Ward Hill, MA). Solvents, such as toluene, ethyl acetate, dimethyl sulfoxide (DMSO), chloroform (CHCl_3) and glass distilled dichloromethane (Caledon Laboratories, Georgetown, ON) were used without further purification. Bovine serum albumin was purchased from Sigma-Aldrich (Milwaukee, WI) and BCA protein assay kit from Thermo Scientific Pierce Inc. (IL, USA). Recombinant

human fibroblast growth factor-9 (FGF9) and human FGF9 DuoSet ELISA kit were purchased from Cedarlane (Burlington, ON).

3.3.2 Synthesis of Poly(ester amide) by Interfacial Polymerization

The poly(ester amide) was prepared as previously reported [14]. In the first step, di-p-toluenesulfonic acid salt monomer was prepared by acid-catalysed condensation. A suspension of L-phenylalanine (60.5 mM, 2.2 equivalents), p-toluenesulfonic acid monohydrate (66 mM, 2.4 equivalent), and 1,4-butanediol (27.5 mM, 1 equivalent) in toluene (100 mL) was heated to 140 °C with stirring in a flask equipped with a Dean-Stark trap. The solution was heated at reflux for 48 h, and then the solvent was removed under vacuum. The resulting material was filtered and washed with toluene. The monomer was purified by dissolving in boiling deionized water (300 mL) followed by hot filtration, and the solution was left to recrystallize overnight at 4 °C. The purification step was repeated; afterwards, the monomer crystals were filtered and dried under vacuum.

In the second step, sebacoyl chloride (5 mM, 1 equivalent) was dissolved in glass distilled anhydrous dichloromethane (15 mL) and the solution was added drop-wise to an aqueous solution (15 mL) containing di-p-toluenesulfonic acid salt monomer (5.0 mM, 1 equivalent) and sodium carbonate (10 mM, 2 equivalents), and allowed to react for 12 h. Upon completion of the reaction, the solution was rotovapped. The polymer was then washed with deionized water prior to purification via Soxhlet extraction with ethyl acetate for 48 h followed by drying under vacuum.

3.3.3 Fabrication of PEA Electrospun Fibers

The electrospinning setup was equipped with a High Voltage DC Power Supply (ES30P, Gamma high voltage, USA), a glass syringe (Becton, Dickinson and Co., 0.5 cc, NJ, USA) with a blunt-tip stainless steel needle (conducting spinneret) controlled by a syringe pump (KD101, KD scientific, USA), and a static collector covered with aluminum foil. The

process parameters including spinneret diameter (18 - 22 G) and applied voltage (15 - 20 kV), and the formulation parameters including polymer concentration (5.5 - 7 %w/w) and solvent composition (Chloroform-to-dimethyl sulfoxide ratio) were optimized, in order to obtain bead-free fibers with uniform fiber diameter distribution.

3.3.4 Characterization of PEA Electrospun Fibers

Morphological analysis of the PEA fibers was performed using scanning electron microscopy (S-3400N SEM, Hitachi, Japan). Electrospun fibrous mat samples were sputter-coated with gold/palladium (K550X sputter coater, Emitech Ltd., UK) and scanned at a working distance of 10 mm and a constant accelerating voltage of 20 kV. Three SE micrographs of the electrospun mats were analysed using computerised ImageJ software (NIH, Bethesda, MD, USA) to quantitatively determine mean fiber diameter from ten random measurements for each image. For transmission electron microscopy (Phillips CM10 TEM), the fibers were electrospun directly on the TEM grids for 30 sec, and the samples were examined at 80 kV.

3.3.5 *In vitro* Degradation Study

Samples of the fibrous mats ($1 \times 1 \text{ cm}^2$) were placed in a screw-capped glass vials filled with 10 mL of phosphate buffered saline (PBS 50 mM, pH 7.4) and removed at pre-determined time-points, rinsed with deionized water and vacuum dried for 48 h at room temperature for further analyses. Samples at the different degradation time-points were analysed morphologically using SEM. The weight loss was determined by the following equation: $\text{Mass loss} = \left[\frac{(M_i - M_t)}{M_i} \right] \times 100\%$, where, M_i is the initial dry weight of the fibrous mat at time 0 and M_t is the dry weight of the sample at the specific degradation time (after drying under vacuum). The molecular weights of the PEA fibers before and after degradation were determined using a Waters system gel permeation chromatography (GPC) equipped with two PLgel $5\mu\text{m}$ ($300 \times 1.5 \text{ mm}$) columns at 85°C and connected to

a PLgel guard column (Waters Ltd, Mississauga, ON). The eluent used was N,N-dimethylformamide (DMF) with 10 mM lithium bromide and 1% (v/v) triethylamine, and samples were injected (100 μ L) at a flow rate of 1 mL/min and calibrated against polystyrene standards. Additional degradation studies were carried out in conditioned smooth muscle cell growth medium (CSmGM); human coronary artery smooth muscle cells (HCASMCs) were cultured in SmGM for 48 h, then the media was collected and used. Samples of 1 \times 1 cm² fibrous mats were immersed in 1 mL of the degradation medium at 37 $^{\circ}$ C, and the media were refreshed every week. Samples at different degradation time-points were removed, rinsed with deionized water, vacuum dried at room temperature and analyzed morphologically using SEM. To rule out the effect of the incubation temperature, dried PEA fiber mats were kept in a vial at 37 $^{\circ}$ C as a control.

3.3.6 Loading PEA Fibers with Model Protein and Fibroblast Growth Factor-9

Bovine serum albumin (BSA) was incorporated into the PEA fibers using blend or emulsification electrospinning [5, 6]. The electrospinning parameters were adopted from the previously conducted studies for unloaded fibers. Briefly, the PEA was dissolved in chloroform and dimethyl sulfoxide (DMSO) at a ratio of (9:1). The polymer solution (0.5 ml) was electrospun using a high voltage DC power supply set to 20 kV and a syringe with a blunt-tip stainless steel spinneret (22 gauge) kept at 8 cm from the grounded collector. The flow rate was kept at 0.1 mL/h using a syringe pump. In case of the blend electrospinning, BSA was dispersed in DMSO (1 μ g/ μ L) and 100 μ L were added to the polymer solution. While, for the emulsion electrospinning, 10 μ L of stock BSA solution in PBS (10 μ g/ μ L) were dropped and ultrasonicated in the polymer solution for 30 min in an ice bath. The same protocol was adopted for FGF9 loading, except for the lower initial loading (3 μ g FGF9/ 0.5 mL polymer solution).

3.3.7 Determination of Percentage Entrapment Efficiency

Four milligrams of loaded PEA fibers were dissolved in 0.5 mL of chloroform and the tube was vortexed to dissolve the polymer. Afterwards, 2.5 mL of PBS (pH 7.4) were added to extract the protein, and the system was centrifuged at 2000 rpm for 5 min to separate the organic and aqueous phases. The aqueous phase was collected for BSA or FGF9 quantification using BCA protein assay kit (Thermo Scientific Pierce Inc., IL, USA) and ELISA assay kit (R&D systems, Inc., MN, USA), respectively. Three independent experiments on different PEA-loaded fiber batches each conducted in triplicate (n=9) were used to determine the percentage entrapment efficiency (% E.E.).

3.3.8 *In vitro* Release Study of BSA and FGF9-loaded PEA Electrospun Fibers

Samples of $1 \times 1 \text{ cm}^2$ fibrous mats were placed in a 24-well plate, and incubated with 1 ml of phosphate-buffered saline (PBS 50 mM, pH 7.4) under continuous agitation (100 strokes/min), in a thermostatically controlled micro-plate shaker (VWR, USA) at 37°C. At pre-determined time intervals, the supernatant was collected and replenished with an equal volume of fresh buffer. The supernatants were immediately frozen at -80°C until further measurements. The amount of BSA released was quantified by micro BCA protein assay kit (Thermo Scientific Pierce Inc., IL, USA), while the amount of FGF9 released was quantified by ELISA assay kit (R&D systems, Inc., MN, USA). The absorbance was measured using a micro-plate reader (UVM 340, Montreal Biotech Inc., Canada) and the unknown concentration was determined from a pre-constructed calibration curve and the % E.E. data.

3.3.9 Bioactivity Assay of the Released Growth Factor

Bioactivity of the released growth factor from the electrospun scaffolds was assayed by *in vitro* evaluation of (NIH-3T3 cell line) mouse embryonic fibroblast metabolic activity. NIH-3T3 cells were seeded in 96-well plates at a density of approximately 3000 cells/well

with 100 μL /well of advanced DMEM (GIBCO[®], Invitrogen, Burlington, ON, Canada) containing 5% FBS, 1% antibiotics and 2 mM L-glutamine, in addition to 100 μL of the released FGF9 in PBS. After an incubation time of 48 h, cell metabolic activity was determined by MTT assay following the manufacturer's protocol (Vybrant[®], Invitrogen, Burlington, ON, Canada). As a positive control, soluble FGF9 was added to the NIH-3T3 cells in amounts equivalent to those released from the FGF9-loaded scaffolds. The amount of added growth factor was calculated from the *in vitro* release data, combining release time points into: early-released FGF9 (from Day 1 to Day 14) and late-released FGF9 (from Day 15 to Day 28) for both blend and emulsion electrospinning techniques. Cells cultured without FGF9 served as a negative control.

3.3.10 Cell Viability and Confocal Microscopy

Cell viability and metabolic activity on 2D PEA films (20 μL of 1% w/v PEA in DMF solvent casted), unloaded and FGF9-loaded 3D PEA electrospun scaffolds were quantified by MTT colorimetric assay. Circular patches (4 mm in diameter) of electrospun mats on aluminium foil were punched and affixed to a 96-well cell culture plate (BD Falcon[™], Franklin Lakes, NJ) using silicone grease, sterilized by immersion in 70% ethanol (200 μL) for 30 min, and allowed to dry for one hour under germicidal UV light, before conditioning overnight in Hank's balanced salt solution (HBSS, 200 μL ; Invitrogen Canada, Burlington, ON). NIH-3T3 cells were seeded onto samples at an initial cell density of approximately 3000 cells/well and cultured for five days in advanced DMEM containing 5% FBS or serum-depleted conditions, and maintained in a humidified incubator at 37 °C and 5% CO₂. At pre-determined time points, the medium was refreshed (100 μL), followed by the addition of 10 μL of 12 mM MTT solution to each well to make the final concentration 1.10 mM and then incubated at 37°C for 4h. Yellow MTT salts are reduced to water-insoluble purple formazan by metabolically active cells. Afterwards, 100 μL 10% (w/v) SDS/HCl was added to solubilize the formazan, and further incubated at 37 °C for 18 h. Finally, the colored product was transferred to 96-well plate and the absorbance was

recorded at 570 nm by a micro-plate reader. Controls of TCPS were included in the experiments.

For confocal microscopy, NIH-3T3 fibroblasts, 10T1/2 cells, and HCASMCs were seeded, in 24-well plate at an initial cell density of approximately 2000 cells/cm², on control glass coverslips, PEA films, FGF9-loaded PEA fibers, and PEA fibers with exogenous soluble FGF9, for three days. Cells were washed with pre-warmed PBS immediately prior to fixing at ambient temperature for 15 min in 4% formaldehyde solution (1 mL; EMD Chemicals) in divalent cation-free PBS. Following three washes in PBS, HCASMCs were permeabilized with 0.1% Triton X-100 (0.5 mL; VWR International, Mississauga, ON) in PBS for 5 min and again washed three times with PBS. The cells were incubated with 1% BSA in PBS (0.5 mL; Sigma-Aldrich, Oakville, ON) for 30 min at ambient temperature prior to their incubation with AlexaTM Fluor 568-conjugated phalloidin (1:50 dilution; Invitrogen Canada, Burlington, ON) in the dark for 1 hour at ambient temperature followed by another three washes with PBS. The cells were then counterstained with 4'-6-diamidino-2-phenylindole dihydrochloride (DAPI, 300 nM in PBS, 0.5 mL; Invitrogen Canada, Burlington, ON) for 5 min to label the nuclei and again washed three times with PBS. No.1 coverslips were mounted on microscope slides with Trevigen® Fluorescence Mounting Medium (Trevigen INC., Gaithersburg, MD). Samples were analyzed with a Zeiss LSM 5 Duo confocal microscope with nine laser lines and appropriate filters (Carl Zeiss, Toronto, ON, Canada).

3.3.11 RNA Isolation and Quantitative Real-time PCR Analysis

Real-time Polymerase Chain Reaction (qPCR) combined with reverse transcription was used to quantify messenger RNA (mRNA) expression of PDGFR- β in NIH-3T3 cells grown on control (TCPS), PEA fibers, FGF9-loaded PEA fibers, and PEA fibers with exogenous soluble FGF9, at a density of 2.5×10^5 cells/sample, for 24 h. Moreover, q-PCR was employed to study the effect of FGF9 concentration gradient on PDGFR- β gene expression in different cells (NIH-3T3, 10T1/2, and HCASMCs) grown on control (TCPS) and PEA fibers with exogenous soluble FGF9 of different concentrations (0, 8, 25, and 50

ng/mL). Total RNA from the cells was extracted using Trizol® reagent (Invitrogen, Burlington, Canada) following the manufacturer's protocol. Complementary DNA (cDNA) was synthesized using 1µg of total RNA primed with oligo₁₂₋₁₈ as described in SuperScript™ (Invitrogen, Canada). Quantitative real-time PCR was conducted in 10 µl reaction volumes, using a CFX-96 Touch™ Real-time system C1000 Thermal Cycler (Bio-Rad, Mississauga, Canada) and gene expression of mouse and human PDGFR-β were then determined with iQ™ SYBR® Green Supermix (Bio-Rad) according to the recommended protocol of the manufacturer. PDGFR-β forward primer: 5'- GGAGATTCGCAGGAGGTCAC-3', reverse primer: 5'- ATAGCGTGGCTTCTTCTGCC-3', GAPDH forward primer: 5'- GTGGTCTCCTCTGACTTCAACA-3', reverse primer: 5'- TTGCTGTAGCCAAATTCGTTGT-3'. Amplification entailed 40 cycles of: denaturation 95°C (15 s), annealing 55°C (60 s), and extension 72°C (30 s). The relative mRNA expression in the cells was normalized to the housekeeping gene glyceraldehyde-3-phosphate dehydrogenase (GAPDH) with at least three repeats per experimental group and expressed as a relative ratio using the CFX Manager™ 3.0 analysis software (Bio-Rad, Mississauga, Canada).

3.3.12 Statistical Analysis

Data is presented as mean ± SEM for experiments conducted in triplicate. Statistical analysis was conducted with *t*-test or one-way ANOVA followed by Tukey's multiple comparison test using GraphPad Prism 4 software (GraphPad Software, Inc., CA, USA). Probability values less than 0.05 were considered statistically significant.

3.4 Results and Discussion

3.4.1 Synthesis of PEA by Interfacial Polymerization

In this study, the PEA was synthesized by interfacial polymerization as previously reported and the results were consistent with previous data [14]. The synthesized PEA, whose chemical structure is shown in Figure 3-1 was designated as “8-Phe-4”, whereby the 8 stands for the number of methylene groups contributed by the sebacic acid (diacid), the Phe is designated for L-phenylalanine (amino acid) and the 4 represents the number of methylene groups in the butanediol moiety (diol). The structure of 8-Phe-4 was confirmed through ^1H NMR. Interfacial polymerization is an irreversible condensation reaction occurring at the interface between two immiscible liquids; one of them is usually a water phase containing the di-functional monomer and inorganic base to activate the diol and neutralize the by-product acid, the other phase is an organic solvent containing the diacid chloride. Interfacial polymerization is preferred because it is rapid, less affected by impurities, and produces PEAs of higher molecular weights than solution polycondensation reactions [20].

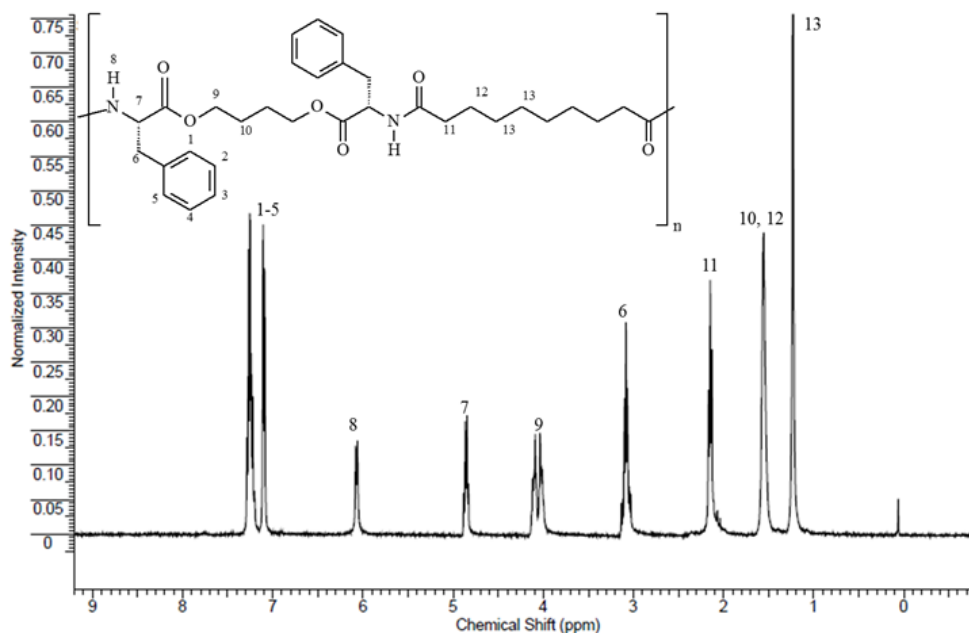


Figure 3-1: Chemical structure and corresponding ^1H -NMR of 8-Phe-4.

3.4.2 Fabrication and Optimization of PEA Electrospun Fibers

PEA fibers were prepared using a solution electrospinning technique. The goal was to develop bead-free fibers from high molecular weight-PEA and optimize the electrospinning parameters to obtain fibers of average fiber diameter between 100 - 500 nm, in order to mimic the extracellular matrix fiber diameter. It is clear from the electrospinning processes literature that the structure and morphology of the produced fibers are determined by a synergistic effect of formulation and process parameters. Formulation parameters including the effect of polymer concentration and solvent composition on fiber morphology were studied. Increasing the polymer concentration in 100% chloroform (CHCl_3) from 5.5 to 7% w/w, electrospun at 8 cm/20 kV, 22 G, and 0.1 mL/h flow rate resulted in increasing the average fiber diameter from 445 to 655 nm as illustrated in Figure 3-2 (A-C). This also led to decreased bead formation, where they transformed from spherical-shaped beads to spindle-like beads to defect-free fibers. This is consistent with previous data reporting that increasing the polymer solution viscosity by increasing its polymer concentration yielded uniform fibers with fewer beads and junctions [21]. However, at polymer concentration of 7% w/w, the polymer solution was too viscous, and chloroform evaporated too fast (B.P. = 61°C), which resulted in drying out of the polymer at the needle tip. This phenomenon was previously reported for concentrated solutions (and therefore too viscous) [22], which in this study interrupted the electrospinning process several times, demanding for an alternative solvent system.

Regarding the effect of solvent composition and conductivity on the fiber morphology, the use of a binary solvent system of chloroform and dimethylsulfoxide, $\text{CHCl}_3/\text{DMSO}$ (9:1), instead of 100% CHCl_3 resulted in eliminating the beads as illustrated in Figure 3-2 (D-F). This can be attributed to the high dielectric constant of DMSO ($\epsilon = 46.6$) contributing to the increased conductivity of the polymer solution. It has been shown that increasing the polymer solution conductivity can be used to produce more uniform fibers with fewer beads, and solvents that had sufficiently high values of dielectric constant were found to be used successfully in electrospinning [21, 23]. Further increase in the DMSO

concentration resulted in fiber fusion, due to residual DMSO that could not evaporate (B.P. = 189 °C) from the polymer solution before the fibers hit the grounded collector.

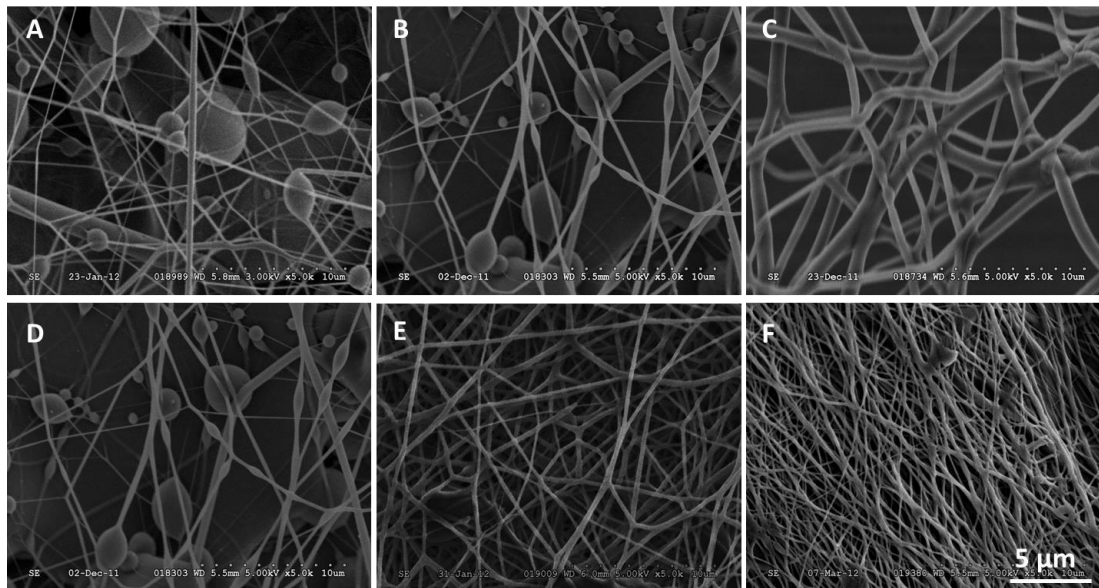


Figure 3-2: Optimization of formulation electrospinning parameters.

Effect of polymer concentration on fiber morphology and fiber diameter, 8-Phe-4 in CHCl_3 (A) 5.5% w/w, (B) 6% w/w, and (C) 7% w/w. Effect of solvent composition on fiber morphology and diameter, 6% w/w 8-Phe-4 in $\text{CHCl}_3/\text{DMSO}$ ratio of (D) (10:0), (E) (9:1), and (F) (8:2), electrospun at 8cm/20kV, 22 G, and 0.1 mL/h flow rate.

Processing parameters such as the applied voltage and spinneret diameter were also studied. Figure 3-3 (A-C) illustrates the effect of the applied voltage on fiber morphology and diameter. In the case of single solvent system of CHCl_3 , reducing the applied voltage from 20 to 15 kV resulted in decreased fiber diameter from 380 to 255 nm; however, it did not affect the fiber morphology. It has been shown that increased voltages produces jets with larger diameters and ultimately leads to the formation of several jets and the presence of beads in many polymeric systems [21]. In regards to the effect of spinneret diameter, 6% w/w PEA in $\text{CHCl}_3/\text{DMSO}$ (9:1) was electrospun at 20 kV, 8cm, and 0.1 mL/h flow

rate with increasing needle gauge from 18 to 22 gauge, which corresponds to decreasing the spinneret diameter. This resulted in a reduction in the mean fiber diameter from 345 to 250 nm Figure 3-3 (D-F) and more uniform fiber diameter distribution as shown in Figure 3-3 (G-I). Based on the optimization of PEA electrospun fibers data, the electrospinning parameters were fixed at 6% w/w PEA in CHCl₃/DMSO (9:1), electrospun at 20 kV, 8cm, 22 gauge needle, and 0.1 mL/h flow rate in all subsequent experiments.

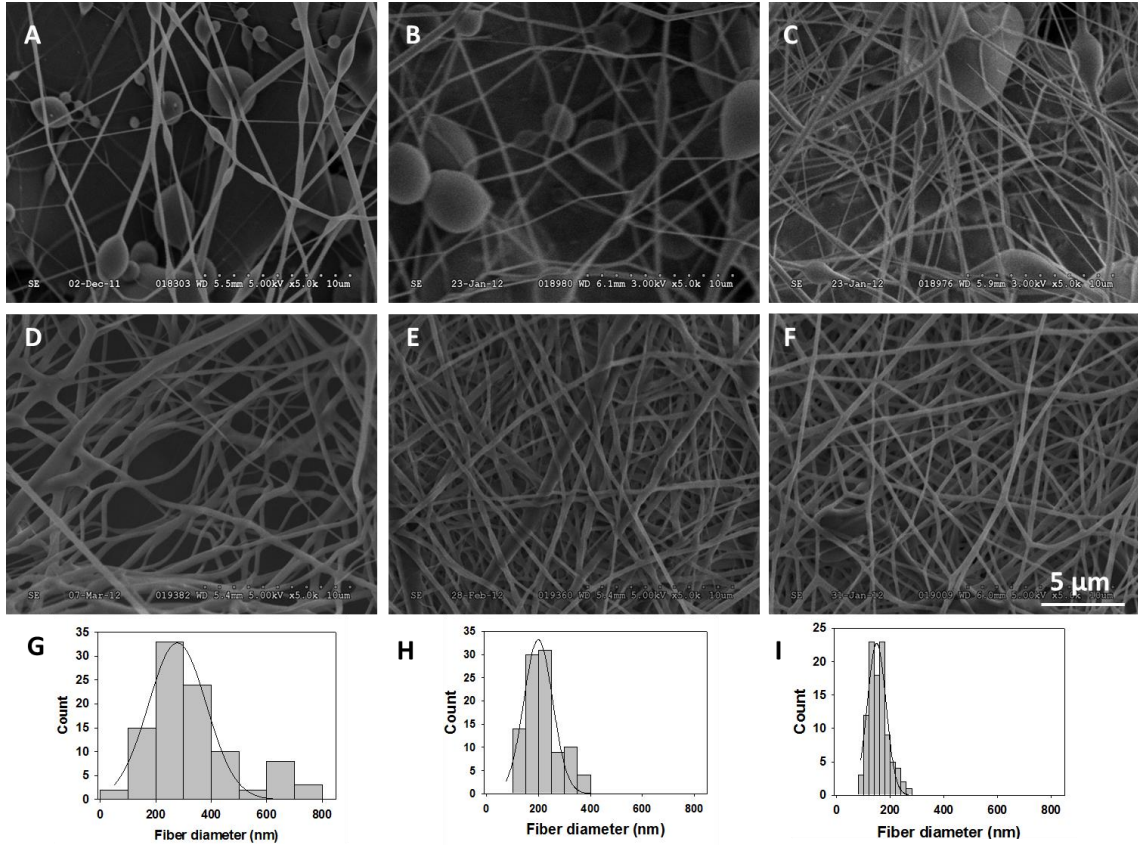


Figure 3-3: Optimization of process electrospinning parameters.

Effect of applied voltage on fiber morphology and diameter, electrospun fibers of 6% w/w 8-Phe-4 in CHCl₃ at (A) 20 kV, (B) 17 kV, and (C) 15 kV. Effect of spinneret diameter on fiber morphology and diameter, 6% w/w 8-Phe-4 in CHCl₃/DMSO (9:1) was electrospun from (D) 18 gauge, (E) 20 gauge, and (F) 22 gauge needle. Histograms of fiber diameter distribution for 8-Phe-4 fibers electrospun from (G) 18 gauge, (H) 20 gauge, and (I) 22 gauge spinneret.

3.4.3 *In vitro* Degradation Study

Scaffold degradation in phosphate buffered saline (pH 7.4) at 37 °C for a period up to four weeks was examined qualitatively using scanning electron microscopy and quantitatively by mass loss determination and molecular weight analysis using GPC. The effect of temperature alone during the degradation of the fibers was excluded by incubating control dry fiber mats at 37 °C inside a glass vial. Since the glass transition temperature of 8-Phe-4 is 41 °C, no observable changes on the fiber morphology such as fiber flattening and subsequent fusion over the 28 days was anticipated (top panel in Figure 3-4 A).

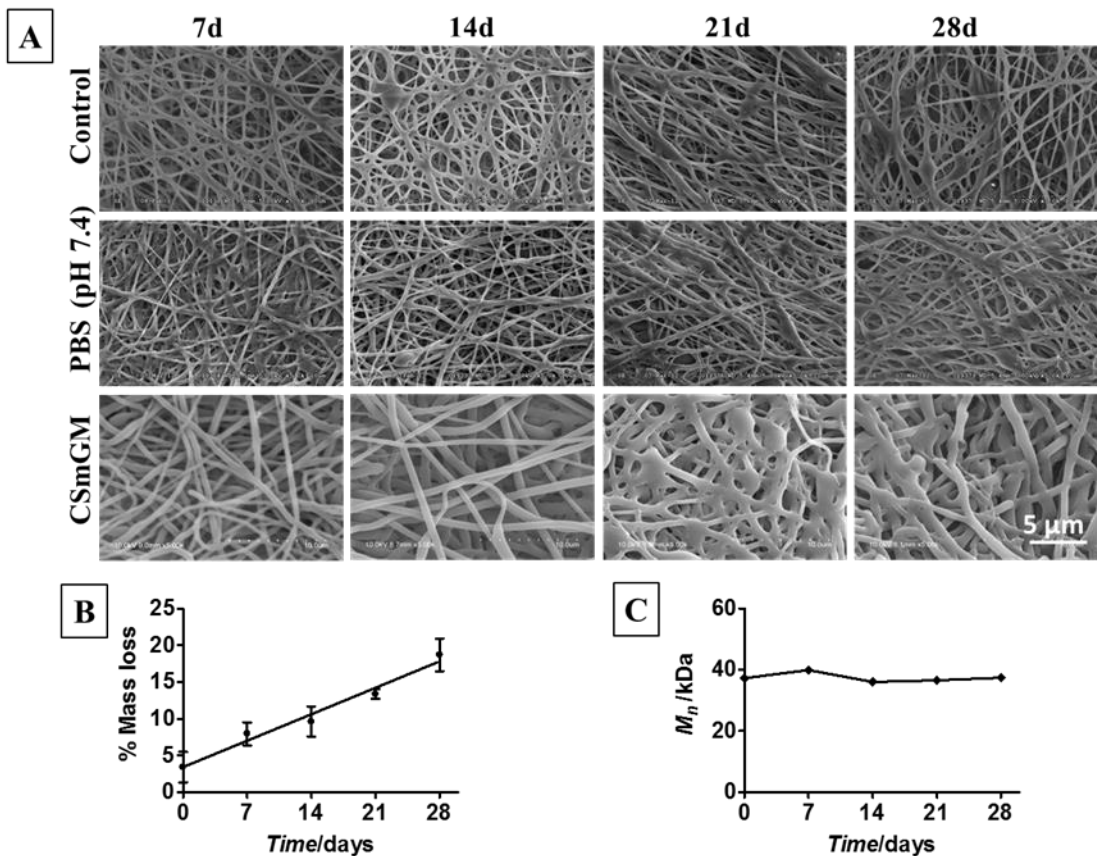


Figure 3-4: *In vitro* degradation of PEA electrospun fibers at 37 °C for 28 days.

(A) SE micrographs for fibers in PBS (pH = 7.4) and conditioned human smooth muscle cell growth medium, the control is dry PEA fibers kept at 37 °C. (B) Percentage mass loss of PEA fibers in PBS (pH = 7.4) at 37 °C at different time points (n=3) and (C) molecular weight analysis using gel permeation chromatography.

Scanning electron (SE) micrographs showed that scaffolds incubated in PBS preserved their fibrous structure over the four-week study period, with negligible morphological changes when compared to the control at 37 °C (middle panel in Figure 3-4 A). Moreover, quantitative analysis showed 21% mass loss over the 28-day study period together with insignificant change in average number molecular weight (M_n) over the four weeks (Figure 3-4 B and C). When these samples were incubated in PBS for 84 days (12 weeks), the fibers lost 48% of their mass while the molecular weight remained nearly constant. The linear decrease in mass ($r^2 = 0.99$), coupled with constant molecular weight indicate that the PEA scaffold degradation is dominated by surface erosion [18, 24]. The polydispersity indices of the samples during the incubation time in PBS for 12 weeks were 2.88 ± 0.15 , further supporting the absence of bulk degradation. Additionally, the effect of bio-relevant media on the degradation of the PEA fibers was studied, so additional degradation studies were carried out in a conditioned smooth muscle cell growth medium (CSmGM); human coronary artery smooth muscle cells (HCASMCs) were cultured in SmGM for 48 h, in which the HCASMCs would have consumed the nutrients necessary for their growth and secreted their metabolites and other products relevant to growth in culture, then the media was collected and used for the degradation study. The SE micrographs showed that the fibers did withstand this bio-relevant medium with some fiber swelling and fusion starting from Week 3 (bottom panel in Figure 3-4 A). The *in vitro* degradation data suggests that surface eroding PEA electrospun fibers can be employed for controlled delivery of bioactive molecules in biorelevant conditions.

3.4.4 *In vitro* Release Study of Loaded PEA Electrospun Fibers

The model protein, bovine serum albumin ($100 \mu\text{g BSA}/\text{cm}^2$), was successfully loaded into the PEA fibers using blend or emulsification electrospinning [5, 6]. The percentage entrapment efficiency (% E.E.) for blend and emulsion electrospun BSA-loaded fibers was $93\% \pm 3$ and $73\% \pm 4$, respectively. The lower entrapment efficiency for the emulsion electrospun fibers is related to the relatively higher viscosity of the emulsified protein/polymer mixture compared to the blend where the protein was dissolved.

Transferring a more viscous emulsion from an emulsification vial to an electrospinning syringe causes some material loss. The residual protein/polymer solution left on the inner wall of the syringe after electrospinning also accounts for some material loss.

Samples of $1 \times 1 \text{ cm}^2$ fibrous mats were placed in a 24-well plate, and incubated with 1 ml of phosphate-buffered saline (PBS 50 mM, pH 7.4) under continuous agitation (100 rpm/min) at $37 \text{ }^\circ\text{C}$. At predetermined time intervals, the amount of BSA released was quantified by BCA protein assay kit. BSA release was sustained over the 28-day study with a limited burst effect and 80% BSA liberation from the blend electrospun BSA-loaded PEA fibers (Figure 3-5 A). Given that the mass loss during the 28 days is 21%, the higher BSA release is related to its higher initial protein loading. Incorporation of higher amounts of a protein into the fibers is believed to be a driving force for protein molecules to migrate toward the surface of the fiber during electrospinning [25]. The absence of burst release highlighted BSA uniform entrapment with the polymer solution [26], resulting in perfect inclusion within the fibers [27], while the sustained release pattern confirmed the adequate structural integrity of the fibers throughout the study. For emulsion electrospun fibers, the release profile showed a decreased BSA release rate in comparison with blend electrospun fibers, reaching 37% at Day 28. This is predictable based on the notion that BSA is encapsulated in the aqueous vesicles (as demonstrated in Figure 3-5 C), which can be referred to as a “diffusion-across-a-barrier type release system” [16]; this requires the degradation of the polymeric matrix, then subsequent diffusion of BSA from the vesicles across the outer barrier layer. During an emulsion electrospinning process, the emulsion droplets move from the surface to the center to achieve their highest accumulation along the axial region [6, 28]. This inward migration of emulsion droplets is caused by rapid evaporation of the solvents during electrospinning. As the organic solvent evaporates faster than water, the viscosity of the outer layer of a fiber increases more rapidly than that of its inner layer resulting in a viscosity gradient between the aqueous droplets and the polymer matrix, which directs the emulsion droplets to settle into the fiber core rather than on the surface [16, 29].

BSA-loaded PEA fibers prepared by both electrospinning techniques followed a time-dependent power law function: $\frac{M_t}{M_\infty} = k t^n$, where, $\frac{M_t}{M_\infty}$ is the fractional release, k is a

structural/geometric constant, t is the time and n is the release exponent representing the release mechanism. The n values of blend and emulsion electrospun BSA-loaded fibers were 0.62 and 0.58, respectively. For cylindrical constructs (for which the individual fiber can be modelled), an n value between 0.45 and 0.89 indicates a coupled matrix degradation and biomolecule diffusion release mechanism [30].

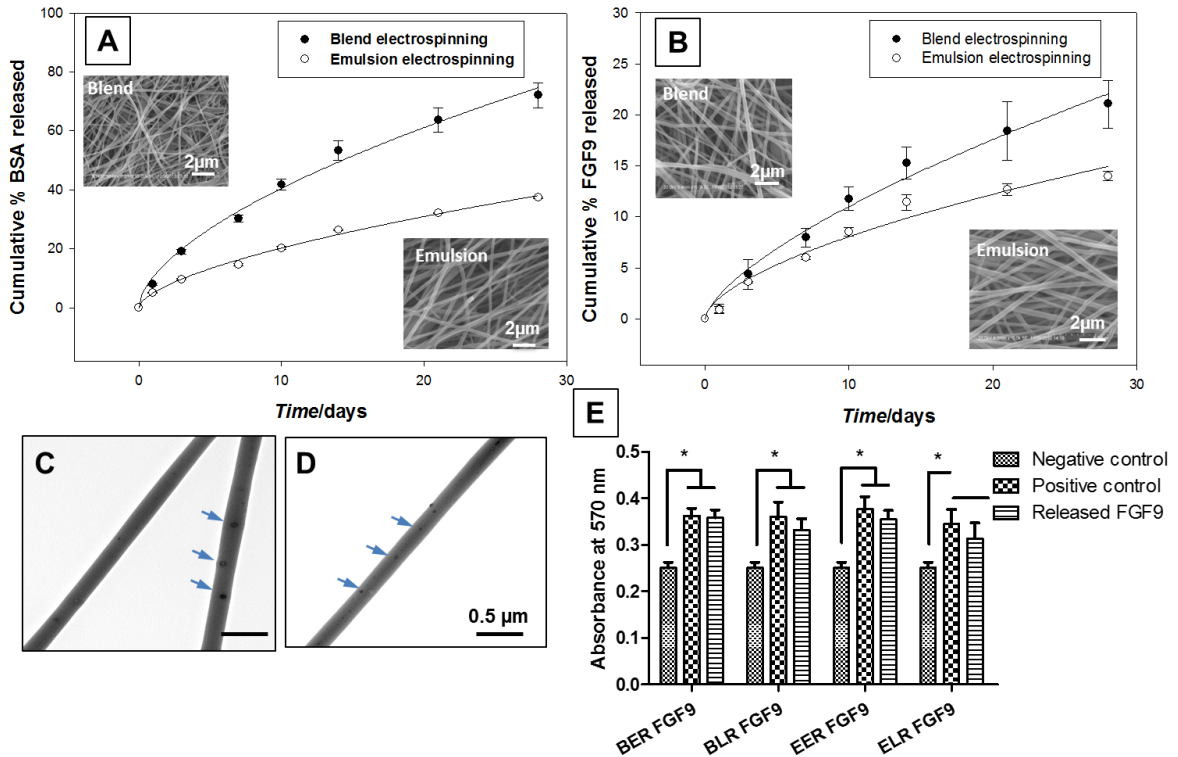


Figure 3-5: *In vitro* release study of (A) BSA-loaded PEA fibers and (B) FGF9-loaded PEA fibers, using blend and emulsion electrospinning techniques, in PBS (pH=7.4) at 37 °C (n=3).

(C) TEM of BSA-loaded PEA fibers and (D) TEM of FGF9-loaded PEA fibers, using the emulsion electrospinning technique (arrows are pointing to the aqueous vesicles). (E) Bioactivity study of FGF9 released from FGF9-loaded PEA fibers using MTT assay. Two-release time points were tested; early-released FGF9 (from Day 1 to Day 14) and late-released FGF9 (from Day 15 to Day 28) for blend and emulsion techniques. Positive controls of soluble FGF9 were included in the experiment. Data represents mean \pm SEM from three independent experiments (* $p < 0.05$).

Following the proof-of-concept of incorporating a model protein into PEA electrospun fibers, FGF9 was loaded into the PEA fibers adopting both electrospinning techniques. The % E.E. of FGF9 was $86\% \pm 3$ and $80\% \pm 3$ for blend and emulsion electrospun FGF9-loaded fibers, respectively, using ELISA kit. FGF9-loaded fibers showed a similar release profile (Figure 3-5 B) with a significant decrease in the overall release rate, due to the lower initial protein loading ($\sim 120 \text{ ng/cm}^2$). Similarly, the release exponent for blend and emulsion electrospun FGF9-loaded fibers was 0.67 and 0.59, respectively, indicating also a non-Fickian diffusion mechanism. Although the ultimate goal is to deliver FGF9 *in vivo*, BSA release studies were also conducted in this work. The rationale for using BSA was two-fold: i) it is a widely studied model protein in controlled-release studies and, ii) it is a large protein (66.5 kDa) compared with FGF-9 (23 kDa) allowing us to study the capability of PEA fibers to release proteins of different sizes in a similar mechanism. The data (Figure 3-5 A and B) showed the release mechanism for both proteins was the same suggesting that PEA electrospun fibers had shown versatility for loading different bioactive molecules (BSA and FGF9). The ability to introduce bioactive molecules into these fibrous electrospun meshes, through these aqueous pouches opens a new path to therapeutic agent delivery.

3.4.5 Bioactivity Assay of the Released Growth Factor

A metabolic activity-based assay was used to assess the bioactivity of FGF9 released at early (Day 1 - Day 14) and late (Day 15 - Day 28) collective time points from the PEA electrospun fibers using blend and emulsion techniques. The proliferating cell number was determined by a 3-(4,5-dimethylthiazol-2-yl)-2,5-diphenyltetrazolium bromide (MTT) assay on NIH-3T3 fibroblasts incubated for 48 h with media containing released FGF9 or equivalent amounts of soluble FGF9 calculated from the *in vitro* release data (positive control). There was no significant difference ($p < 0.05$) in metabolic activity between the released and control FGF9 (Figure 3-5 E). These results indicate that FGF9 released from the fibers, prepared either by blend or emulsion techniques, was bioactive up to 28 days. It is worth noting that the emulsion late-released (ELR) time point did not show a

significant difference from the untreated control (no FGF9 added), which can be attributed to the lower released amount of FGF9 in case of ELR in comparison with the other three tested conditions.

3.4.6 Cell Viability and Confocal Microscopy

For evaluation of the PEA electrospun fibers *in vitro* biocompatibility as potential drug delivery vehicle for bioactive molecules, cell viability on FGF9-loaded 3D fibers was assessed using the MTT assay and compared to 2D PEA films and unloaded 3D fibers. For this section and the following one, FGF9-loaded PEA fibers prepared by emulsion electrospinning instead of blend electrospinning were used for two reasons: (i) to provide a maximum protection for FGF9 from the organic solvent (i.e. chloroform) during electrospinning, (ii) the long-term goal is to use the fibers as a dual growth factor delivery system (the first one for inducing angiogenic sprout formation and the second one to recruit mural cells for neovessel maturation and functionality after the formation of the endothelial tubes). Since FGF9 release is needed for neovessel maturation, its delayed release is beneficial.

As shown in Figure 3-6, 2D PEA films, and both FGF9-loaded and unloaded fibers supported fibroblast viability for up to five days, in the case of 5% FBS (Serum+) conditions. In the case of serum-depleted (Serum-) conditions, the unloaded and FGF9-loaded 3D PEA fibers maintained cell viability and metabolic activity through the five-day study, whereas 2D PEA films supported only the survival of cells. Baker and Southgate [31] attempted to culture stromal cells on 3D polystyrene fibers in serum-depleted conditions, but stromal cells failed to adhere to the polystyrene fibrous scaffold in the absence of serum; in contrary to this, PEA electrospun fibers were able to support metabolically active fibroblasts in serum-depleted conditions, which could be attributed to potential peptide linkages imparted by the amino acid-based PEA fibers.

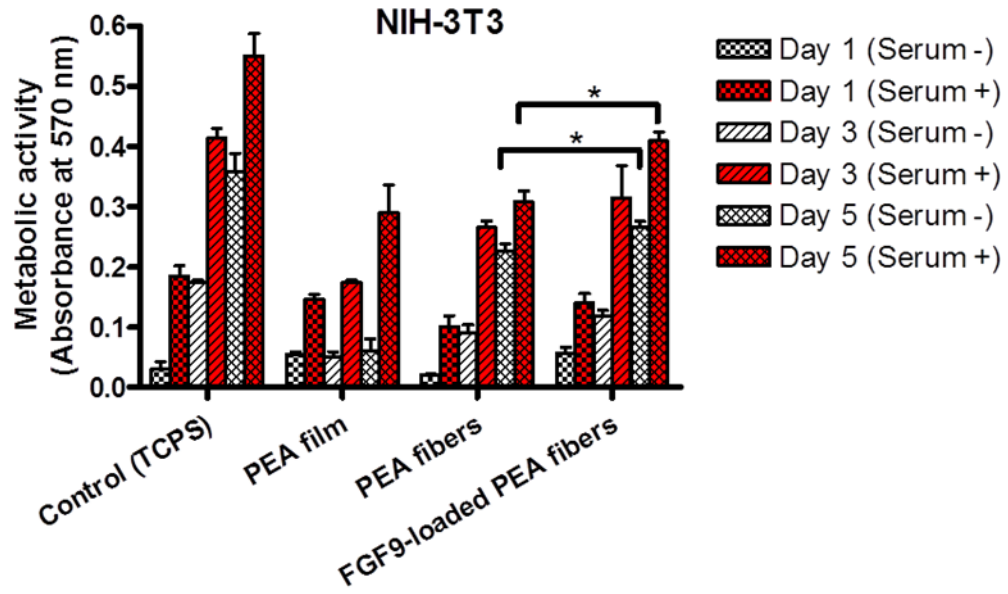


Figure 3-6: NIH-3T3 cell viability study on 2D PEA films (1% w/v), unloaded and FGF9-loaded 3D PEA emulsion electrospun fibers for 5 days, in Serum+ (5% FBS) and Serum- (serum depleted; 0.05% FBS) conditions, using MTT assay.

Data represents mean \pm SEM from three independent experiments. Student *t*-test was conducted between PEA fibers group and FGF9-loaded PEA fibers group at the same conditions and the same time point (* $p < 0.05$).

To further assess the PEA electrospun fibers as a potential sustained-delivery vehicle for FGF9, the interactions with different cell types (NIH-3T3, 10T1/2, and HCASMCs) were examined using confocal microscopy. FGF9 has reported proliferative effect on 3T3 [32, 33] and smooth muscle cells [10, 12]. As for 10T1/2 cell line, it is a smooth muscle precursor cell type that is commonly used for *in vitro* SMC phenotype studies because of its ability to maintain a stable phenotype in culture and even can be pushed toward an SMC state [34]. The cells showed good attachment and spreading on glass control and 2D PEA surfaces, and displayed interaction and infiltration in case of the 3D PEA electrospun fibers either FGF9-loaded or with exogenous supplementation of FGF9 as shown in Figure 3-7. The PEA fibers had inherent autofluorescence in the green channel, which was obscured in case of HCASMCs (Figure 3-7 K&L) due to the use of different culture medium

(Medium 231 supplemented with SMGS, GIBCO[®], Invitrogen, Burlington, ON, Canada). Biodegradable PEAs have been previously reported to support attachment, spreading, and proliferation of human coronary artery smooth muscle cells, bovine aortic endothelial cells, and fibroblasts [14, 18, 35, 36]. Together with the fact that 3D scaffolds play an important role in guiding cells to produce their own extracellular matrix and control phenotype differentiation [37, 38], by providing both mechanical and biological cues, PEA electrospun fibers were found to support cell growth even in serum-depleted conditions. This data highlights the potential expanding applications of PEA fibers in drug delivery and tissue engineering.

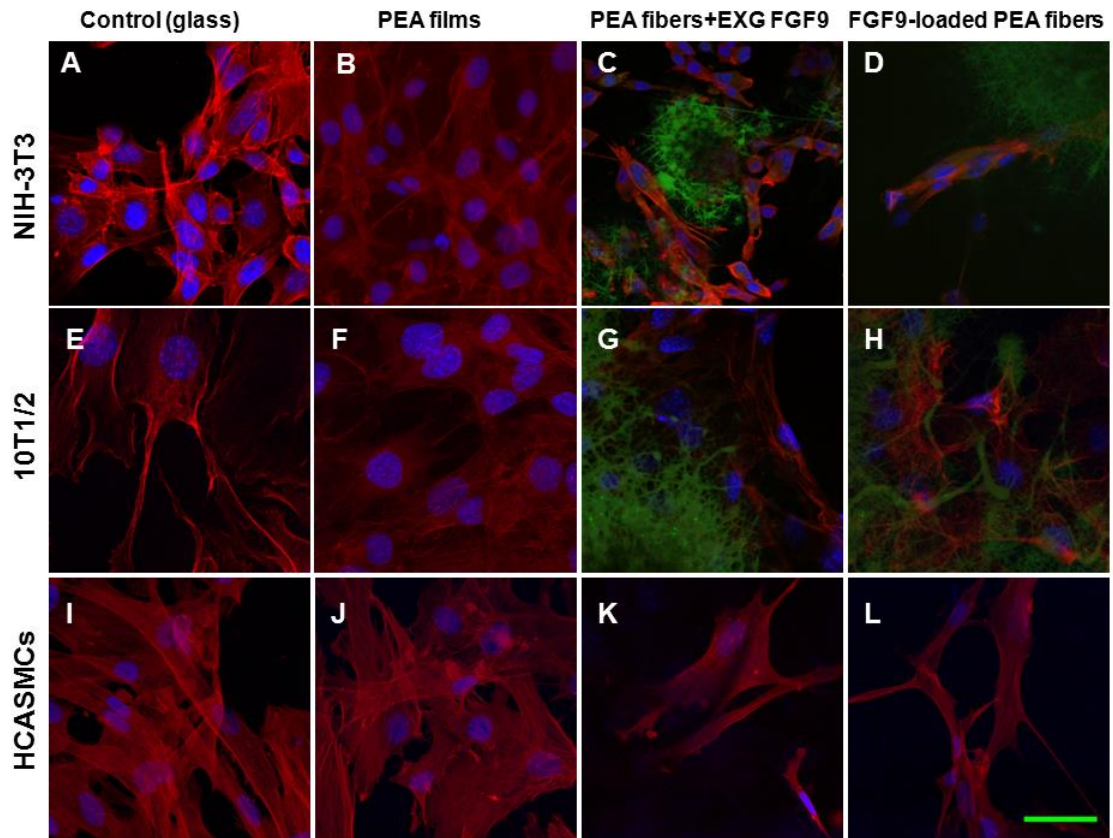


Figure 3-7: Confocal microscopy images of NIH-3T3, 10T1/2, and HCASMCs.

Cells seeded at 2000 cells/cm² for 3 days on glass coverslips (control), PEA films, PEA fibers with exogenous FGF9, and FGF9-loaded PEA fibers cultured in Serum+ media, showing F-actin (red), nuclei (blue), and PEA fibers (green). Scale bar = 40 μ m.

3.4.7 RNA Isolation and Quantitative Real-time PCR Analysis

To understand the signaling pathways underlying the reported FGF9-induced investment of neovessels by SMCs, the expression of platelet-derived growth factor receptor- β (PDGFR β), which is one of the downstream signaling molecules in FGF9-stimulated SMCs was studied. PDGFR β is a well-documented regulator of SMC migration [39] and therefore a potential mediator of FGF9-induced vessel maturation. Real-time Polymerase Chain Reaction (qPCR) preceded with reverse transcription was used to quantify messenger RNA (mRNA) expression of PDGFR β in NIH-3T3 cells grown on control (TCPS), PEA fibers, FGF9-loaded PEA fibers, and PEA fibers with exogenous soluble FGF9, at a density of 2.5×10^5 cells/sample, for 24 h. q-PCR analysis of PDGFR β expression showed insignificant difference between NIH-3T3 cells seeded on PEA fibers, FGF9-loaded fibers, or PEA fibers with exogenous FGF9 (~2.5 ng/mL, equivalent to the amount released from the FGF9-loaded PEA fibers after 24 h) as illustrated in Figure 3-8A, suggesting that the FGF9 exogenously supplemented to PEA fibers is equivalent to the released FGF9 from the loaded PEA fibers. Thus, the FGF9 exogenously supplemented PEA fibers were selected to map the effective FGF9 concentration required for PDGFR β upregulation, for future loading into the PEA fibers. Consequently, the effect of FGF9 concentration on PDGFR β gene expression was further studied in different cells (NIH-3T3, 10T1/2, and HCASMCs) seeded on control (TCPS) and PEA fibers with exogenous soluble FGF9 of different concentrations (0, 8, 25 and 50 ng/mL). The q-PCR data showed significant upregulation in the PDGFR β expression at the lowest tested FGF9 concentration (8 ng/mL) for NIH-3T3 and 10T1/2 cells (Figure 3-8 B and C). In contrast, the highest tested FGF9 concentration (50 ng/mL) was the concentration that resulted in significant upregulation in the case of HCASMCs (Figure 3-8 D). Recent studies have shown that pre-treatment of SMCs with FGF9 (100 ng/ml) for 24 h was found to increase their chemotactic response to PDGF-BB [40], which is a ligand for PDGFR β and a growth factor necessary for mural cell recruitment during development and can promote vascular stability [41]. As well, there was substantial increase in PDGFR β expression in SMC pre-exposed to increasing concentrations of FGF9 (10 - 100 ng/mL) [12]. Furthermore, when a PDGFR β blocking antibody was added to angiogenic implants, it did not affect their

vascularity after 2 weeks but reduced the number of vessels invested by mural cells expressing smooth muscle α -actin [12]. The current findings support the premise that FGF9 is a regulator of PDGFR β expression, which is the receptor necessary for FGF9-induced mural cell recruitment, and that the critical concentration of FGF9 varies between mouse fibroblasts, 10T1/2 cells, and human smooth muscle cells. This study may provide important platforms for therapeutic angiogenesis and tissue engineering applications.

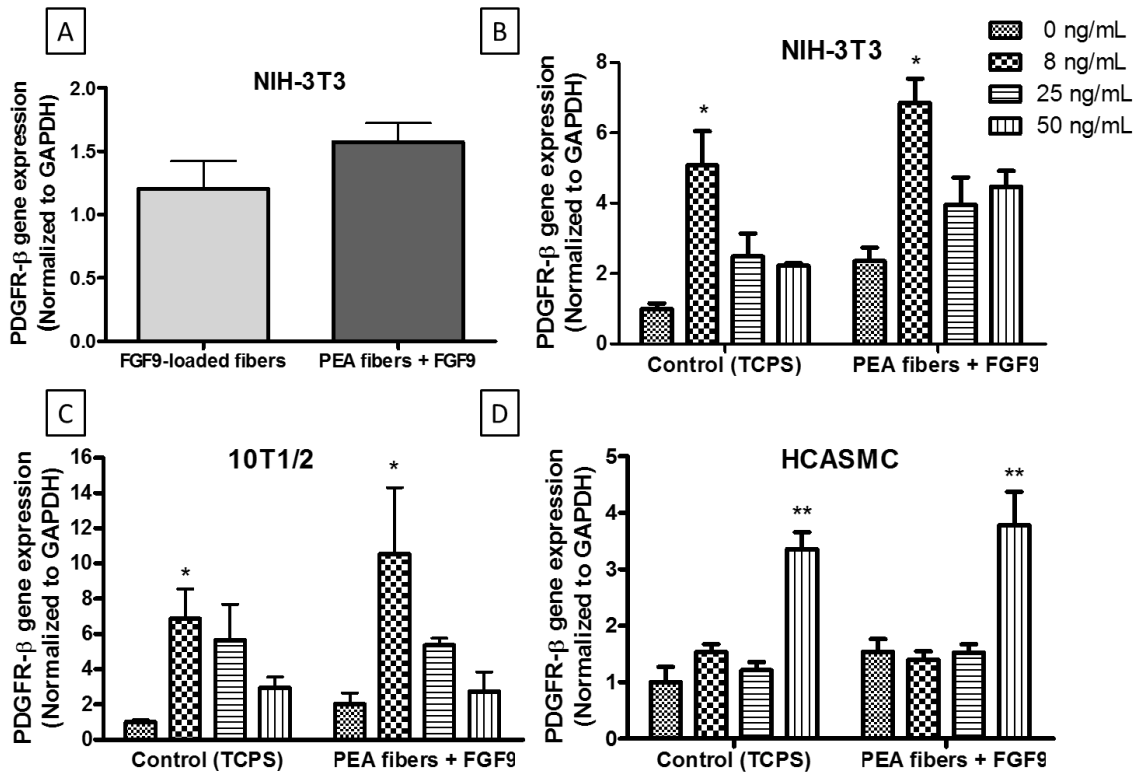


Figure 3-8: (A) Quantitative real-time PCR analysis of PDGFR- β expression for NIH-3T3 cells seeded on FGF9-loaded emulsion electrospun fibers and PEA fibers with exogenous FGF9 for 24 h.

The effect of FGF9 concentration gradient on PDGFR- β gene expression in (B) NIH-3T3 fibroblasts, (C) 10T1/2 cells, and (D) HCASMCs, seeded on TCPS (control) and PEA fibers with exogenous FGF9 for 24 h. Data represents mean \pm SEM, * indicates $p < 0.05$ and ** indicates $p < 0.01$ (n=3).

3.5 Conclusions

Biodegradable poly(ester amide) fibers were successfully fabricated using electrospinning techniques. Bead-free fibers of mean fiber diameter ~250 nm and uniform fiber diameter distribution were produced using a binary solvent system of chloroform and DMSO (9:1). PEA electrospun fibers preserved their fibrous structure over the four-week *in vitro* degradation study in PBS (pH 7.4) and conditioned smooth muscle cell growth medium at 37 °C. Loaded PEA fibers exhibited controlled-release of BSA and FGF9 over 28 days with a limited burst effect for both blend and emulsion electrospun fibers and preserved FGF9 bioactivity. Moreover, the FGF9-loaded PEA electrospun fibers were found to maintain the metabolic activity of mouse fibroblasts for up to five days. Finally, q-PCR analysis suggests that FGF9 is a stimulator of PDGFR β expression, which is the receptor necessary for FGF9-induced mural cell recruitment and vessel maturation. This data supports the premise of FGF9 sustained delivery from PEA electrospun fibers and its potential application in therapeutic angiogenesis and regenerative medicine. Future work is required to examine dual loading of angiogenic growth factors and evaluating the induced angiogenesis *in vitro* and *in vivo*.

3.6 References

1. Dragneva, G., P. Korpiälö, and S. Ylä-Herttuala, Promoting blood vessel growth in ischemic diseases: challenges in translating preclinical potential into clinical success. *Dis Model Mech*, 2013. **6**(2): 312-22.
2. Lusis, A.J., Atherosclerosis. *Nature*, 2000. **407**(6801): 233-41.
3. Lee, K.Y., M.C. Peters, and D.J. Mooney, Comparison of vascular endothelial growth factor and basic fibroblast growth factor on angiogenesis in SCID mice. *J Control Release*, 2003. **87**(1-3): 49-56.
4. Said, S.S., J.G. Pickering, and K. Mequanint, Advances in growth factor delivery for therapeutic angiogenesis. *J Vasc Res*, 2013. **50**(1): 35-51.
5. Sahoo, S., L.T. Ang, J.C.-H. Goh, and S.-L. Toh, Growth factor delivery through electrospun nanofibers in scaffolds for tissue engineering applications. *J Biomed Mater Res*, 2010. **93A**: 1539–1550.

6. Yang, Y., T. Xia, W. Zhi, L. Wei, J. Weng, C. Zhang, and X. Li, Promotion of skin regeneration in diabetic rats by electrospun core-sheath fibers loaded with basic fibroblast growth factor. *Biomaterials*, 2011. **32**(18): 4243-54.
7. Seyednejad, H., W. Ji, F. Yang, C.F. van Nostrum, T. Vermonden, J.J. van den Beucken, W.J. Dhert, W.E. Hennink, and J.A. Jansen, Coaxially electrospun scaffolds based on hydroxyl-functionalized poly(epsilon-caprolactone) and loaded with VEGF for tissue engineering applications. *Biomacromolecules*, 2012. **13**(11): 3650-60.
8. Roy, R.S., B. Roy, and S. Sengupta, Emerging technologies for enabling proangiogenic therapy. *Nanotechnology*, 2011. **22**(49): 494004.
9. Rubanyi, G.M., *Angiogenesis in health and disease: Basic mechanisms and clinical applications*. 2000, New york: Marcel Dekker Inc.
10. Agrotis, A., P. Kanellakis, G. Kostolias, G. Di Vitto, C. Wei, R. Hannan, G. Jennings, and A. Bobik, Proliferation of neointimal smooth muscle cells after arterial injury. Dependence on interactions between fibroblast growth factor receptor-2 and fibroblast growth factor-9. *J Biol Chem*, 2004. **279**(40): 42221-9.
11. Spicer, D., FGF9 on the move. *Nat Genet*, 2009. **41**(3): 272-3.
12. Frontini, M.J., Z. Nong, R. Gros, M. Drangova, C. O'Neil, M.N. Rahman, O. Akawi, H. Yin, C.G. Ellis, and J.G. Pickering, Fibroblast growth factor 9 delivery during angiogenesis produces durable, vasoresponsive microvessels wrapped by smooth muscle cells. *Nat Biotechnol*, 2011. **29**(5): 421-427.
13. Richardson, T.P., M.C. Peters, A.B. Ennett, and D.J. Mooney, Polymeric system for dual growth factor delivery. *Nat Biotechnol*, 2001. **19**(11): 1029-34.
14. Knight, D.K., E.R. Gillies, and K. Mequanint, Strategies in Functional Poly(ester amide) Syntheses to Study Human Coronary Artery Smooth Muscle Cell Interactions. *Biomacromolecules*, 2011. **12**(7): 2475-87.
15. Vert, M., S. Li, and H. Garreau, New insights on the degradation of bioresorbable polymeric devices based on lactic and glycolic acids. *Clinical materials*, 1992. **10**(1-2): 3-8.
16. Szentivanyi, A., T. Chakradeo, H. Zernetsch, and B. Glasmacher, Electrospun cellular microenvironments: Understanding controlled release and scaffold structure. *Adv Drug Deliv Rev*, 2011. **63**(4-5): 209-20.
17. Li, L. and C.C. Chu, Nitroxyl radical incorporated electrospun biodegradable poly(ester Amide) nanofiber membranes. *J Biomater Sci Polym Ed*, 2009. **20**(3): 341-61.

18. Srinath, D., S. Lin, D.K. Knight, A.S. Rizkalla, and K. Mequanint, Fibrous biodegradable l-alanine-based scaffolds for vascular tissue engineering. *J Tissue Eng Regen Med*, 2012. **8**(7): 578-588.
19. del Valle, L.J., M. Roa, A. Díaz, M.T. Casas, J. Puiggalí, and A. Rodríguez-Galán, Electrospun nanofibers of a degradable poly(ester amide). Scaffolds loaded with antimicrobial agents. *Journal of Polymer Research*, 2012. **19**(2): 1-13.
20. Morgan, P.W., Interfacial Polymerization, in *Encyclopedia of Polymer Science and Technology*. 2002, John Wiley & Sons, Inc.
21. Pham, Q.P., U. Sharma, and A.G. Mikos, Electrospinning of polymeric nanofibers for tissue engineering applications: a review. *Tissue Eng*, 2006. **12**(5): 1197-211.
22. Zong, X., K. Kim, D. Fang, S. Ran, B.S. Hsiao, and B. Chu, Structure and process relationship of electrospun bioabsorbable nanofiber membranes. *Polymer*, 2002. **43**(16): 4403-4412.
23. Jarusuwannapoom, T., W. Hongrojjanawiwat, S. Jitjaicham, L. Wannatong, M. Nithitanakul, C. Pattamaprom, P. Koombhongse, R. Rangkupan, and P. Supaphol, Effect of solvents on electro-spinnability of polystyrene solutions and morphological appearance of resulting electrospun polystyrene fibers. *European Polymer Journal*, 2005. **41**(3): 409-421.
24. Tsitlanadze, G., M. Machaidze, T. Kviria, N. Djavakhishvili, C.C. Chu, and R. Katsarava, Biodegradation of amino-acid-based poly(ester amide)s: in vitro weight loss and preliminary in vivo studies. *J Biomater Sci Polym Ed*, 2004. **15**(1): 1-24.
25. Zamani, M., M. Morshed, J. Varshosaz, and M. Jannesari, Controlled release of metronidazole benzoate from poly epsilon-caprolactone electrospun nanofibers for periodontal diseases. *Eur J Pharm Biopharm*, 2010. **75**(2): 179-85.
26. Zeng, J., L. Yang, Q. Liang, X. Zhang, H. Guan, X. Xu, X. Chen, and X. Jing, Influence of the drug compatibility with polymer solution on the release kinetics of electrospun fiber formulation. *J Control Release*, 2005. **105**(1-2): 43-51.
27. Maretschek, S., A. Greiner, and T. Kissel, Electrospun biodegradable nanofiber nonwovens for controlled release of proteins. *J Control Release*, 2008. **127**(2): 180-7.
28. Sy, J.C., A.S. Klemm, and V.P. Shastri, Emulsion as a Means of Controlling Electrospinning of Polymers. *Advanced Materials*, 2009. **21**(18): 1814-1819.
29. Yang, Y., X. Li, S. He, L. Cheng, F. Chen, S. Zhou, and J. Weng, Biodegradable ultrafine fibers with core–sheath structures for protein delivery and its optimization. *Polym Adv Technol*, 2011. **22**(12): 1842-1850.

30. Ritger, P.L. and N.A. Peppas, A simple equation for description of solute release I. Fickian and non-fickian release from non-swellable devices in the form of slabs, spheres, cylinders or discs. *J Control Release*, 1986. **5**(1): 23-36.
31. Baker, S.C. and J. Southgate, Towards control of smooth muscle cell differentiation in synthetic 3D scaffolds. *Biomaterials*, 2008. **29**(23): 3357-66.
32. Naruo, K., C. Seko, K. Kuroshima, E. Matsutani, R. Sasada, T. Kondo, and T. Kurokawa, Novel secretory heparin-binding factors from human glioma cells (glia-activating factors) involved in glial cell growth. Purification and biological properties. *J Biol Chem*, 1993. **268**(4): 2857-64.
33. Rubin, J.S., A.M. Chan, D.P. Bottaro, W.H. Burgess, W.G. Taylor, A.C. Cech, D.W. Hirschfield, J. Wong, T. Miki, and P.W. Finch, A broad-spectrum human lung fibroblast-derived mitogen is a variant of hepatocyte growth factor. *Proceedings of the National Academy of Sciences*, 1991. **88**(2): 415-419.
34. Richardson, W.J., E. Wilson, and J.E. Moore, Jr., Altered phenotypic gene expression of 10T1/2 mesenchymal cells in nonuniformly stretched PEGDA hydrogels. *Am J Physiol Cell Physiol*, 2013. **305**(1): C100-10.
35. Horwitz, J.A., K.M. Shum, J.C. Bodle, M. Deng, C.C. Chu, and C.A. Reinhart-King, Biological performance of biodegradable amino acid-based poly(ester amide)s: Endothelial cell adhesion and inflammation in vitro. *J Biomed Mater Res A*, 2010. **95**(2): 371-80.
36. Deng, M., J. Wu, C.A. Reinhart-King, and C.C. Chu, Biodegradable functional poly(ester amide)s with pendant hydroxyl functional groups: synthesis, characterization, fabrication and in vitro cellular response. *Acta Biomater*, 2011. **7**(4): 1504-15.
37. Lin, S., M. Sandig, and K. Mequanint, Three-dimensional topography of synthetic scaffolds induces elastin synthesis by human coronary artery smooth muscle cells. *Tissue Eng Part A*, 2011. **17**(11-12): 1561-71.
38. Carlson, A.L., C.A. Florek, J.J. Kim, T. Neubauer, J.C. Moore, R.I. Cohen, J. Kohn, M. Grumet, and P.V. Moghe, Microfibrous substrate geometry as a critical trigger for organization, self-renewal, and differentiation of human embryonic stem cells within synthetic 3-dimensional microenvironments. *Faseb J*, 2012. **26**(8): 3240-51.
39. Zhou, L., Y. Takayama, P. Boucher, M.D. Tallquist, and J. Herz, LRP1 Regulates Architecture of the Vascular Wall by Controlling PDGFR β -Dependent Phosphatidylinositol 3-Kinase Activation. *PLoS ONE*, 2009. **4**(9): e6922.
40. Hellstrom, M., M. Kalen, P. Lindahl, A. Abramsson, and C. Betsholtz, Role of PDGF-B and PDGFR-beta in recruitment of vascular smooth muscle cells and pericytes during embryonic blood vessel formation in the mouse. *Development*, 1999. **126**(14): 3047-55.

41. Zhang, H., X. Jia, F. Han, J. Zhao, Y. Zhao, Y. Fan, and X. Yuan, Dual-delivery of VEGF and PDGF by double-layered electrospun membranes for blood vessel regeneration. *Biomaterials*, 2012. **34**(9): 2202-12.

Chapter 4

4 Concurrent and Sustained Delivery of FGF2 and FGF9 from Electrospun Poly(ester amide) Fibrous Mats for Therapeutic Angiogenesis*

Overview: This chapter discusses the dual loading of the PEA electrospun fibers with FGF2 and FGF9 using a mixed blend and emulsion electrospinning technique, and studies the effect of the dual-loaded PEA electrospun fibrous scaffolds on endothelial cell tube formation and directed smooth muscle cell migration. Moreover, it investigates the inflammatory host response *in vitro* using THP-1 human monocytes and *in vivo* by subcutaneous implantation into B6 mice.

4.1 Abstract

Therapeutic angiogenesis has emerged as a potential strategy to treat ischemic vascular diseases. However, systemic or local administration of growth factors is usually inefficient for maintaining the effective concentration at the site of interest due to their rapid clearance or degradation. In this study, a differential and sustained release of an angiogenic factor; fibroblast growth factor-2 (FGF2), and an arteriogenic factor; fibroblast growth factor-9 (FGF9), from α -amino acid-derived biodegradable poly(ester amide) (PEA) fibers was reported towards targeting neovessel formation and maturation. FGF2 and FGF9 were dual-loaded using a mixed blend and emulsion electrospinning technique, and exhibited differential and sustained-release from PEA fibers over 70 days with preserved bioactivity. *In vitro* angiogenesis assays showed enhanced endothelial cell (EC) tube formation and

* A version of this chapter is published as a research article “Somiraa S. Said, Caroline O’Neil, Hao Yin, Zengxuan Nong, J. Geoffrey Pickering and Kibret Mequanint, *Tissue Engineering Part A* (2016)”. Adapted with permission from **Mary Ann Liebert © 2016**.

directed-migration of smooth muscle cells (SMCs) to PDGF-BB, and stabilized EC/SMC tube formation. FGF2/FGF9-loaded PEA fibers did not induce inflammatory responses *in vitro* using human monocytes or *in vivo* after their subcutaneous implantation into mice. Histological examination showed that FGF2/FGF9-loaded fibers induced cell niche recruitment around the site of implantation. Furthermore, controlled *in vivo* delivery of FGF9 to mouse tibialis anterior muscle resulted in a dose-dependent expansion of mesenchymal progenitor cell-like layers and ECM deposition. The data suggests that the release of FGF2 and FGF9 from PEA fibers offers an efficient differential and sustained growth factor-delivery strategy with relevance to therapeutic angiogenesis.

Keywords: Electrospinning; Fibroblast growth factor-2; Fibroblast growth factor-9; Poly(ester amide)s; Therapeutic angiogenesis.

4.2 Introduction

Therapeutic angiogenesis, the induction of new blood vessel formation, has emerged as a potential approach to treat ischemia caused by coronary and peripheral arterial diseases [1]. A fundamental component of regenerative medicine is neovascularisation, which can be induced by promoting expression of angiogenic genes or targeted delivery of angiogenic growth factors and progenitor cells via engineered materials [2]. Although angiogenic protein therapy is the simplest and most straightforward approach for therapeutic angiogenesis, systemic administration of angiogenic factors is usually inefficient for reaching and/or maintaining the desired effective concentration at the site of interest due to rapid clearance or degradation of the delivered protein [3, 4]. Local administration (*e.g.* intracoronary, intramyocardial, or intracerebral injection) can better confine the distribution of the growth factors at the desired site; however, it requires expensive pumps or invasive surgeries [5]. Recently, biomimetic nanofibers have become auspicious candidates for delivering bioactive molecules, promoting a viable approach for local and controlled delivery of angiogenic factors to overcome the aforementioned challenges [6-9].

Neovessel formation and maturation requires the precise spatiotemporal presentation of both angiogenic and arteriogenic growth factors, so that endothelial tubes can form and recruit mural cells for subsequent investment of these nascent vessels with perivascular cell coverage, which is essential for stable blood vessel formation [10, 11]. FGF2 is one of the most extensively studied angiogenic factors in therapeutic angiogenesis [12-15]. However, clinical studies of FGF2 showed short-term induced angiogenesis as the new microvessels regressed over time and therefore did not confer long-term improvements in tissue perfusion [16, 17]. This is probably due to quick inactivation of FGF2 with bolus delivery, issues with patient selection and clinical trial end points [18], and the generation of immature and unstable blood vessels that regressed over time [9, 19]. Unlike FGF2, FGF9 is not angiogenic but it is known to target the mesenchyme [20], and to elevate neointimal smooth muscle cell proliferation after arterial injury [21]. Previously, the combination of FGF2 and FGF9 was shown to stimulate the formation of robust microvessels in Matrigel plugs that are more likely to persist compared with using only FGF2, and had the ability to respond to vasoactive agents [22]. In an ischemic hind limb mouse model, vessels formed in the presence of FGF9, delivered by means of an osmotic pump, were physiologically mature due to smooth muscle migration that wrapped the nascent microvessels resulting in their stabilization [22]. Notwithstanding this encouraging data, the use of an osmotic/infusion pump was accompanied by induced inflammation and is not clinically practical. Therefore, differential delivery of these growth factors in a pump-free controlled and sustained manner remains to be an immediate need.

In order to protect the growth factors from rapid clearance and to target neovessel maturation, the proposed strategy is to differentially deliver angiogenic (FGF2) and arteriogenic (FGF9) growth factors from a single electrospun biomaterial system. The differential delivery of this new combination of growth factors is promising; since FGF2 will be released at a higher rate in the early stage inducing vessel formation, while FGF9 will be released at a lower rate recruiting mural cells at a later stage prompting vessel stabilization. Different laboratories reported the release of two or more growth factors from composite biomaterial delivery systems where growth factors were loaded in different polymers and then combined to form a composite system [23-26]. It would be more

practical if differential release is attained from only one biomaterial; but this is challenging owing to the bulk degradation properties of most biomaterials. Vascular endothelial growth factor (VEGF) and platelet derived-growth factor (PDGF) has been a very popular combination and their dual delivery was widely investigated for blood vessel regeneration [8, 23, 27]; however, it has been reported that VEGF can act as a negative regulator for pericyte coverage of vascular sprouts through VEGFR-2 and consequently hinder vessel maturation under the conditions of PDGF-mediated angiogenesis [28].

In the current study, α -amino acid derived poly(ester amide) (PEA) electrospun fibers were proposed as a versatile controlled delivery vehicle for FGF2 and FGF9 to target neovascular maturation. PEAs derived from α -amino acids were previously shown to degrade by surface erosion mechanism and were biocompatible for tissue engineering applications [29-31]. Following a proof of principle study on the feasibility of biodegradable α -amino acid derived PEA nanofibers to deliver FGF9 [32], the objectives of the current study were three-fold: (i) to dual load FGF2 and FGF9 into PEA fibers using a mixed blend and emulsion electrospinning technique and study the morphological properties and the *in vitro* dual release kinetics, (ii) to examine the *in vitro* angiogenesis capacities of the co-released FGF2 and FGF9 using endothelial tube formation and directed smooth muscle cell migration assays and, (iii) to evaluate the *in vitro* and *in vivo* inflammatory responses and potential cell niche recruitment.

4.3 Materials and Methods

4.3.1 Materials

The poly(ester amide) 8-Phe-4 was synthesized from L-phenylalanine, sebacoyl chloride, and 1,4-butanediol *via* interfacial polymerization and characterized as described in previous publications [29, 32]. Bovine serum albumin (BSA) and Fibronectin were purchased from Sigma-Aldrich Canada Co. (Oakville, ON). Micro BCA protein assay kit from Thermo Scientific Pierce Inc. (Rockford, IL). Recombinant human fibroblast growth factor-9 (FGF9), fibroblast growth factor-2 (FGF2), Platelet-derived growth factor BB (PDGF-BB), and human FGF9 and FGF2 DuoSet[®] ELISA kit were purchased from R&D

Systems Inc. (Minneapolis, MN). Vybrant[®] DiI and Hoechst 33342 dyes were from Life technologies (Burlington, ON).

4.3.2 Cell Culture and Maintenance

Primary human coronary artery smooth muscle cells (HCASMCs) were purchased from Lonza (Walkersville, MD) and cultured according to the supplier's instructions in Medium 231 and Smooth muscle growth supplement, complemented with 100 units/ml penicillin G sodium, 100 µg/ml streptomycin sulphate, and 2 mM L-glutamine (Invitrogen, Burlington, ON). Primary human coronary artery endothelial cells (HCAECs) were purchased from Lonza (Walkersville, MD) and cultured according to supplier's instructions in EGM–MV Bullet Kit (Lonza, Walkersville, MD). THP-1 human monocytes (ATCC[®] TIB202[™]) were cultured in RPMI 1640 medium supplemented with 2 mM L-glutamine, 10% FBS, and 1% penicillin/streptomycin (Invitrogen, Burlington, ON). All cultures were maintained in a humidified chamber at 37°C containing 5% CO₂. Cells were passaged every 7 days at a split ratio of 1:3 and used between passages 6 to 8.

4.3.3 Dual-loading of PEA Fibers

Dual loading of model protein BSA or FGF2, and FGF9 into the PEA fibers was carried out using a mixed technique of blend and emulsion electrospinning. The electrospinning parameters were established in previous studies [32]. Briefly, the PEA (8-Phe-4, average number MW between 30-40 kDa) was dissolved in chloroform and dimethyl sulfoxide (DMSO) at a ratio of (9:1). The polymer solution (0.5 mL) at 7.5% w/w concentration was electrospun using a high voltage DC power supply (ES30P, Gamma high voltage, USA) set to 20 kV and a 0.5 cc glass syringe (Becton, Dickinson and Co., Franklin Lakes, NJ) with a blunt–tip stainless steel spinneret (22 gauge) kept at 8 cm from the grounded collector (a rotating mandrel covered with aluminum foil rotating at 1000 rpm). The flow rate was kept at 0.1 mL/h using a syringe pump (KD101, KD scientific, Holliston, MA). BSA was dissolved in DMSO (1 µg/µL) and 100 µL were blended in the polymer solution. The same protocol was adopted for FGF2 loading, except for the lower initial loading (3.6

μg FGF2 per 100 μL of DMSO). Whereas, 30 μL of stock FGF9 solution in PBS (120 ng/ μL) were emulsified in the polymer solution by ultrasonication for 30 min in an ice bath. Similarly, Vybrant[®] DiI and Hoechst 33342 dyes were dual-loaded into the PEA fibers following the same procedure as FGF2 and FGF9, respectively.

4.3.4 Characterization of PEA Electrospun Fibers

Morphological analysis of the PEA fibers was performed using scanning electron microscopy and confocal laser scanning microscopy. For SEM, electrospun fibrous mat samples were sputter-coated with gold/palladium (K550X sputter coater, Emitech Ltd., UK) and scanned at a working distance of 10 mm and a constant accelerating voltage of 20 kV, using S-3400N SEM (Hitachi, Japan). Vybrat[®] DiI and Hoechst dual loaded-PEA fibers were electrospun on No.1 coverslips for 30 s. Another No.1 coverslip was mounted over the coverslip containing the fibers and Trevigen[®] Fluorescence Mounting Medium (Trevigen INC., Gaithersburg, MD), and confocal images of Vybrat[®] DiI and Hoechst dual loaded-PEA fibers were captured with a Zeiss LSM 5 Duo confocal microscope equipped with nine laser lines and appropriate filters (Carl Zeiss, Toronto, ON).

4.3.5 *In vitro* Release Study of Dual-loaded PEA Electrospun Fibers

In vitro release studies of dual loaded PEA fibers were conducted as described previously for FGF9-loaded fibers [32]. Samples of 1 cm \times 1 cm fibrous mats (with total amount of 4 μg of BSA or 120 ng FGF2, and 120 ng FGF9/mat) were placed in a 24-well plate, and incubated with 1 mL of phosphate-buffered saline (PBS 50 mM, pH 7.4) under continuous agitation (100 strokes/min), in a thermostatically controlled micro-plate shaker (VWR International, Mississauga, ON) at 37°C. At pre-determined time intervals (Day 1, 3, 7, 10, 14, and weekly thereafter), the supernatant was collected and replenished with an equal volume of fresh buffer. The supernatants were immediately frozen at -80°C until further measurements. The amount of BSA released was quantified by micro BCA protein assay kit, while the amount of FGF2 and FGF9 released was quantified by DuoSet[®] ELISA assay kit. The absorbance was measured using a micro-plate reader (UVM 340, Montreal

Biotech Inc., QC) and the unknown concentration was determined from a pre-constructed calibration curve and the percentage entrapment efficiency data. In order to correlate the *in vitro* release of the growth factors to the degradation rate of the PEA fibers; *in vitro* degradation of (1 cm × 1 cm) dual-loaded PEA mats was studied in PBS (50 mM, pH 7.4) at 37 °C for 3 months and evaluated by % mass loss and molecular weight analysis as previously described [32].

4.3.6 *In vitro* Angiogenesis Assays: Matrigel Tube Formation Assay

Cell viability and metabolic activity of HCAECs on the 3D FGF2/FGF9-loaded PEA fibers was determined for 5 days by MTT assay following the manufacturer's protocol (Vybrant®, Invitrogen, Burlington, ON, Canada). Unloaded fibers supplemented with soluble FGF2 and FGF9 was included as a positive control, and TCPS as a negative control. The experiments were conducted in triplicate as previously described [32]. Evaluation of *in vitro* tube formation using Matrigel assay was conducted by means of digital time-lapse video microscopy [33]. FGF2/FGF9-loaded fibers were allowed to release the growth factors in 35 mm culture dishes containing EC culture media (EGM-MV BulletKit, Lonza) for 7 days, in an incubator at 37°C and 5% CO₂; 1 cm × 1 cm mats were utilized with total amount of 120 ng FGF2 and 120 ng FGF9/mat. 200-μL aliquots of the growth factor-reduced Matrigel (VWR International, Mississauga, ON) were added per well to a 24-well plate and allowed to polymerize at 37°C for 30 min. HCAECs were trypsinized then suspended in a 250 μL media containing the released FGF2 and FGF9, and seeded at a density of 75,000 cells/well on Matrigel for 4 days. Images were acquired on an Olympus IX51 inverted microscope, using a 10× objective. The numbers of tube branch points were counted for two fields of view per well for different time points. Culture media incubated with unloaded PEA fibers served as a negative control, whereas media supplemented with FGF2 and FGF9, equivalent to that released at 7 days from the loaded fibers calculated from the *in vitro* release data, served as a positive control. Each treatment was performed in duplicate and three independent experiments were conducted.

A modified tube formation assay was adopted in order to evaluate the interaction between endothelial cells and smooth muscle cells. To do this, HCAECs were infected with 30 μL

of Red Fluorescent Protein-Adenovirus (RFP-Adenovirus)/10 mm dish, while HCASMCs were infected with 100 μ L of Green Fluorescent Protein-Adenovirus (GFP-Adenovirus)/10 mm dish for 48 h. Tube formation assay protocol was followed as mentioned above and after 5 h incubation of RFP-expressing HCAECs on the Matrigel, GFP-expressing HCASMCs were added at 75,000 cells/well and incubated for further 24 h to evaluate SMC-interaction with the endothelial tubes using digital time-lapse video microscopy. Images were acquired, using a 10 \times objective, every 30 min for 24 h on Leica DMI8 inverted fluorescent microscope integrated with LAS-AF lite 2.6 software (Leica Microsystems Inc., Concord, ON).

4.3.7 Directed Human Coronary Artery Smooth Muscle Cell Migration Assay

Directed vascular smooth muscle cell migration was assessed by the transwell migration assay [34], using a Boyden-type microchemotaxis chamber (Neuro Probe, Inc., Gaithersburg, MD). HCASMCs were treated with FGF2/FGF9-loaded fibers for 7 days. HCASMCs were seeded onto 35 mm tissue culture dishes at cell density of 100,000 cells/dish. The cells were allowed to attach for 1 h in the incubator, and then the 1 cm \times 1 cm FGF2/FGF9-loaded mat was suspended in the dish. The dual-loaded mats were allowed to release both FGF2 and FGF9 over 6 days (the SMC culture media containing 10% FBS was refreshed every other day). On Day 6, HCASMCs were starved for 24h by refreshing with serum-depleted media (containing 2% FBS). Polycarbonate membranes (Neuro Probe, Inc., Gaithersburg, MD) with 10 μ m pores were pre-coated with 10 μ g/mL fibronectin and kept at 4 $^{\circ}$ C overnight. Untreated or FGF2/FGF9-treated SMCs were washed in HBSS, trypsinized, and 25,000 cells re-suspended in 50 μ L of serum-depleted media were added to the upper well of the Boyden chamber. The lower well of the chamber was filled with 28 μ L of serum-depleted media with or without the chemotactic agent PDGF-BB. Migration was allowed to proceed for 6 h at 37 $^{\circ}$ C under 5% CO₂. SMCs remaining on the upper surface of the membrane (non-migrated cells) were mechanically removed using a wiper blade after dipping in PBS, and then the membrane was fixed in methanol (for 5 min) and stained with Harris's hematoxylin (for 10 min). The number of cells that had migrated to the lower surface was determined by counting under high-power

microscopy (40× objective) in eight fields of view per well using an Olympus BX51 inverted microscope. The experiments were performed in triplicate, and positive controls of soluble FGF2/FGF9–treated SMCs were included in the experiment. Moreover, this assay was used to test the bioactivity of the early released (cumulative released FGF2 and FGF9 between Day 1 and Day 13) and late released (cumulative released FGF2 and FGF9 between Day 14 and Day 28) growth factors from the dual loaded PEA fibers, collected during the *in vitro* release study.

4.3.8 *In vitro* Gene Expression of the Inflammatory Marker (Interleukin 8)

Unloaded and FGF9/FGF2–loaded PEA fibers were affixed to the bottom of 12–well plate, sterilized by immersion in 70% ethanol (200 µL) for 30 min, and allowed to dry for one hour under germicidal UV light, before conditioning overnight in Hank’s balanced salt solution (HBSS, 200 µL; Invitrogen, Burlington, ON). THP-1 human monocytes were seeded onto the samples at an initial cell density of approximately 2×10^5 cells/well and cultured for three days in RPMI 1640 media containing 10% FBS, 1% penicillin/styptomycin and 2 mM L–glutamine, and maintained in a humidified incubator at 37 °C and 5% CO₂. Negative controls (TCPS), and positive controls of cells incubated with *Escherichia coli* lipopolysaccharide (*E. coli* LPS) at concentration of 5 µg/mL, were included in the experiment. After 72 h, the cells were collected and total RNA was extracted following TRIzol® reagent manufacturer’s protocol for suspended cells, and quantitative real-time Polymerase Chain Reaction (RT-qPCR) assay was employed to evaluate the RNA expression of the inflammatory marker interleukin 8 (IL-8) [35].

4.3.9 RNA Isolation and Quantitative Real–time PCR Analysis

qPCR combined with reverse transcription was used to quantify messenger RNA (mRNA) expression of IL–8 in THP–1 cells seeded on control (TCPS), incubated with a positive control of *E. coli* lipopolysaccharide (*E. coli* LPS), unloaded PEA fibers, and FGF2/ FGF9–loaded PEA fibers. Total RNA from the cells was extracted using TRIzol® reagent (Invitrogen, Burlington, ON) following the manufacturer’s protocol. Complementary DNA

(cDNA) was synthesized using 1 µg of total RNA primed with oligo₁₂₋₁₈ as described in SuperScript™ (Invitrogen, Burlington, ON). qPCR was conducted in 10 µl reaction volumes, using a CFX-96 Touch™ Real-time system C1000 Thermal Cycler (Bio-Rad, Mississauga, ON) and gene expressions of human IL-8 was then determined with SsoAdvanced™ SYBR® Green Supermix (Bio-Rad) according to the recommended protocol of the manufacturer. IL-8 forward primer: 5'-CTTCCTGATTTCTGCAGCTCT-3', reverse primer: 5'-GTGGTCCACTCTCAATCACTC-3', GAPDH forward primer: 5'-GGTGGTCTCCTCTGACTTCAACA-3', reverse primer: 5'-GTTGCTGTAGCCAAATTCGTTGT-3'. Amplification entailed 40 cycles of: denaturation 95°C (15 s), annealing 55°C (30 s), and extension 65°C (30 s). The relative mRNA expression in the cells was normalized to the housekeeping gene glyceraldehyde-3-phosphate dehydrogenase (GAPDH) with at least three repeats per experimental group and expressed as a relative ratio using the CFX Manager™ 3.0 analysis software (Bio-Rad, Mississauga, ON).

4.3.10 Implantation into Subcutaneous and Tibialis Anterior Muscle Tissues

The host response was evaluated by subcutaneously implanting unloaded and FGF2/FGF9-loaded PEA fibrous mats in 8-week old male C57BL/6J mice (The Jackson Laboratory, Bar Harbor, Maine). Experiments were conducted in accordance with the University of Western Ontario Animal Use Subcommittee. Briefly, samples of (4 mm × 4 mm) PEA fibrous mats, unloaded or dual-loaded with FGF2 and FGF9 with total amount of 20 ng FGF2 and 20 ng FGF9/mat (n = 4), were surgically implanted into the dorsal subcutaneous tissue just superficial to the skeletal muscle and were harvested after 6 days. Prior to implantation, all the mats were sterilized under ultraviolet radiation for 4 h/each side. The mice were anaesthetized with Forane® (Baxter, Deerfield, IL) and their backs were shaved and wiped with alcohol. Two 6 mm horizontal full thickness skin incisions were made and the unloaded PEA mat was inserted in the left incision while the growth factor-loaded was implanted in the right incision and the incision was sutured using 6-0 silk sutures to retain the mat in place. Sham surgery was included in the experiment to

serve as a control (n=2), where the incisions were made and sutured without the insertion of the PEA mats. The mice were sacrificed after 6 days, and the mats with the attached subcutaneous tissue were excised for histological examination. The tissue sections collected from the mice were fixed in 4% paraformaldehyde and dehydrated in 70% ethanol, then embedded in paraffin wax. Five micrometer-thick sections were cut with a rotary microtome (Leica 5 micron microtome) and Hematoxylin and Eosin (H&E) stained. H&E stained sections were examined with a Leica inverted light microscope (Leica Microsystems Inc., Concord, ON) and investigated for the infiltration of inflammatory cells. Follow-up experiments were carried out to evaluate the effect of FGF9 controlled delivery from the PEA fibers, at different initial loading concentrations (0, 20, 40, and 80 ng/mat), on cell and tissue reaction upon implantation on the tibialis anterior muscle in the hind limb of B6 mice. Seven days after implantation of the FGF9-loaded PEA fibers onto the TA muscle, the mice were sacrificed and perfusion-fixed with 4% paraformaldehyde. The anterior calf muscle bundle was dehydrated in 70% ethanol, paraffin-embedded, and 5 μ m sections were subjected to H&E staining and investigated for cell niche recruitment.

4.3.11 Statistical Analysis

Data is presented as mean \pm SEM for experiments conducted in triplicate. Statistical analysis was conducted with one-way ANOVA followed by Tukey's multiple comparison test using GraphPad Prism 4 software (GraphPad Software, Inc., San Diego, CA). Probability values less than 0.05 were considered statistically significant, unless otherwise stated.

4.4 Results

4.4.1 Differential Release of FGF2 and FGF9 from Dual-loaded PEA Fibers

In previous work, successful loading of FGF9 into PEA fibers was reported using blend and emulsion electrospinning techniques [32]. In the current study, a mixed blend and

emulsion electrospinning technique was proposed for dual loading of FGF2 and FGF9 into PEA fibers for therapeutic angiogenesis application. Confocal microscopy was employed to examine the dual loading strategy using two model fluorescent dyes. Red Vybrant[®] DiI was loaded using blend electrospinning, while blue Hoechst 33342 was loaded using emulsion electrospinning. The presence of blue vesicles along the red PEA fiber matrix (Figure 4-1 A) confirms the success of the dual loading strategy for the two model dyes using the mixed electrospinning technique.

To demonstrate the controlled and differential release of bioactive molecules, a model protein (BSA, 4 $\mu\text{g}/\text{cm}^2$) was dual-loaded with FGF9 (120 ng/cm^2) into the PEA fibers. The morphology of the fibers was investigated using SEM, showing bead-free fibers with uniform fiber diameter distribution (Figure 4-1 B inset). The *in vitro* release of BSA and FGF9 was sustained over the 4 weeks study, in PBS (pH 7.4) at 37 °C, reaching approximately 76.9% and 25.3% for BSA and FGF9, respectively after 28 days (Figure 4-1 B). In the same way, FGF2 (120 ng/cm^2) and FGF9 (120 ng/cm^2) were dual loaded into the PEA fibers. Similar sustained and differential release profiles were attained, which were fitted to a time-dependent power-law function [36]. The amount of FGF2 and FGF9 released from the PEA fibers at the end of the 4-week study was approximately 28.5% and 19.4%, respectively (Figure 4-1 C). Release studies for longer time periods (70 days), also showed a continuous controlled release of the growth factors reaching about 54.2% for FGF2 and 40.7% for FGF9 (Figure 4-1 C). *In vitro* degradation of the PEA fibers was previously investigated in PBS (pH 7.4) at 37°C for 4 weeks [32], and the fibrous mats maintained their structural integrity with total percentage mass loss of 21% after 28 days and without significant change in molecular weight. Longer degradation time-points showed 48% mass loss after 84 days while the molecular weight did not change appreciably indicating surface erosion degradation mechanism, which matches the *in vitro* release data (Figure 4-1 D-E). This supports the idea that biodegradable PEA fibers could be utilized in sustained co-delivery of FGF2 and FGF9 while attaining a differential release of the dual-loaded growth factors.

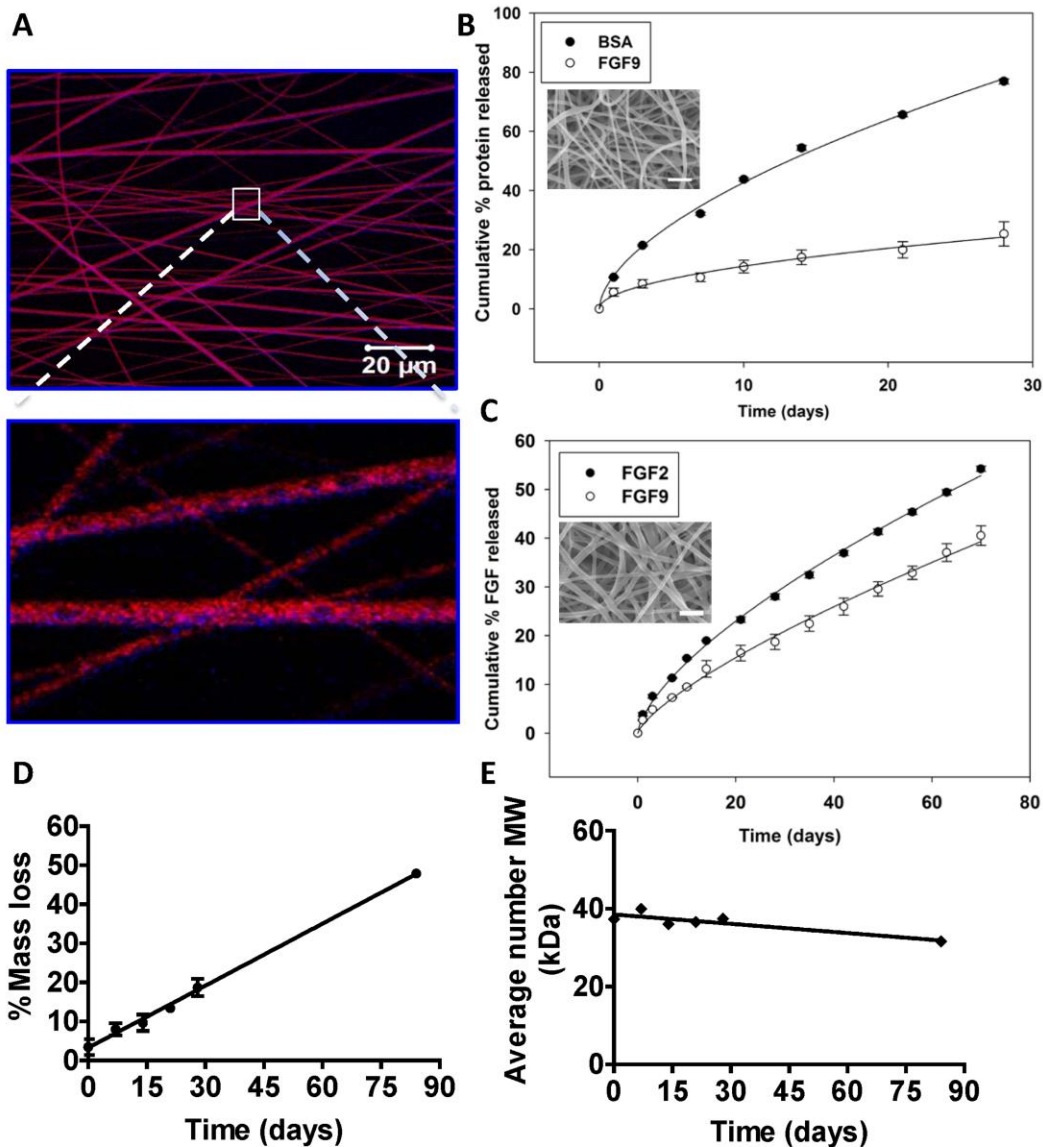


Figure 4-1: Combined blend and emulsion electrospinning of growth factors facilitate differential release of the loaded proteins.

(A) Confocal microscopy images of DiI and Hoechst dyes dual-loaded PEA fibers following the same mixed electrospinning protocol for growth factor loading. *In vitro* release study of (B) BSA and FGF9, (C) FGF2 and FGF9 dual-loaded PEA fibers, in PBS pH 7.4 at 37 °C for 4 weeks (n=3), with corresponding SEM insets, scale bar = 2 μm. *In vitro* degradation of PEA electrospun fibers in PBS (pH=7.4) at 37°C for 84 days. (D) Percentage mass loss of PEA fibers at different time points (n=3) and (E) molecular weight analysis using gel permeation chromatography.

4.4.2 Co-released FGF2 and FGF9 from PEA Fibers Enhanced Tube Formation and Directed SMC Migration

The MTT metabolic activity assay showed that the number of attached human coronary artery endothelial cells (HCAECs) at Day 1 on both dual-loaded and unloaded fibres supplemented with FGF2 and FGF9 were fewer than those on the TCPS control (Figure 4-2). However, those attached cells were viable for up to 5 days. Since visualization of tube formation on the 3D fibers/Matrigel *via* microscopy is not feasible due to the non-transparency of the fibers, tube formation was investigated using a Matrigel tube formation assay employing HCAECs treated with media containing the co-released FGF2 and FGF9.

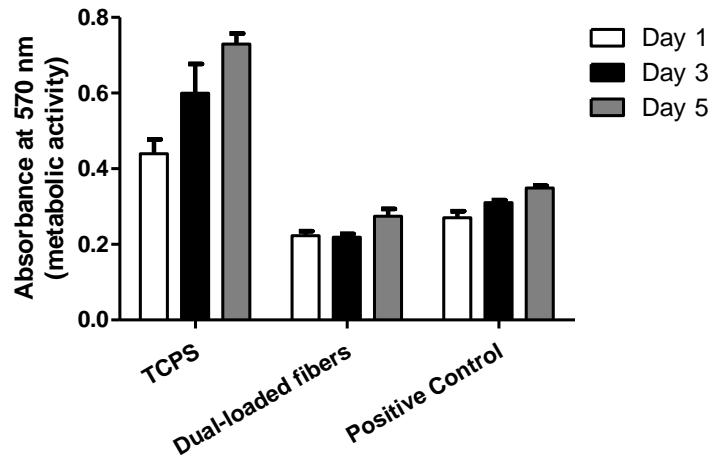


Figure 4-2: Human coronary artery endothelial metabolic activity study on 3D FGF2/FGF9-loaded PEA fibers, unloaded fibers supplemented with soluble FGF2 and FGF9 as a positive control, and TCPS as a negative control, for 5 days using MTT assay. Data represents mean \pm SEM from three independent experiments.

Endothelial tubes formed after 24 h of incubation were visualized by optical microscopy using a 10 \times objective (Figure 4-3). Quantitative representation of the data showed significant increase in the number of tubule branch points at 24 h in the case of co-released FGFs from the dual loaded PEA fibers compared to the negative control of culture media, whereas there was no significant difference from the positive control of soluble FGF2 and FGF9 ($p < 0.05$) as illustrated in Figure 4-3. Although the endothelial tubes would

eventually regress, the endothelial tubes treated with the co-released FGFs were holding better than the negative control after 4 days. This data supports that FGF2, being an angiogenic growth factor, stimulates tube formation and proposes potential benefits of strategically pairing it with FGF9.

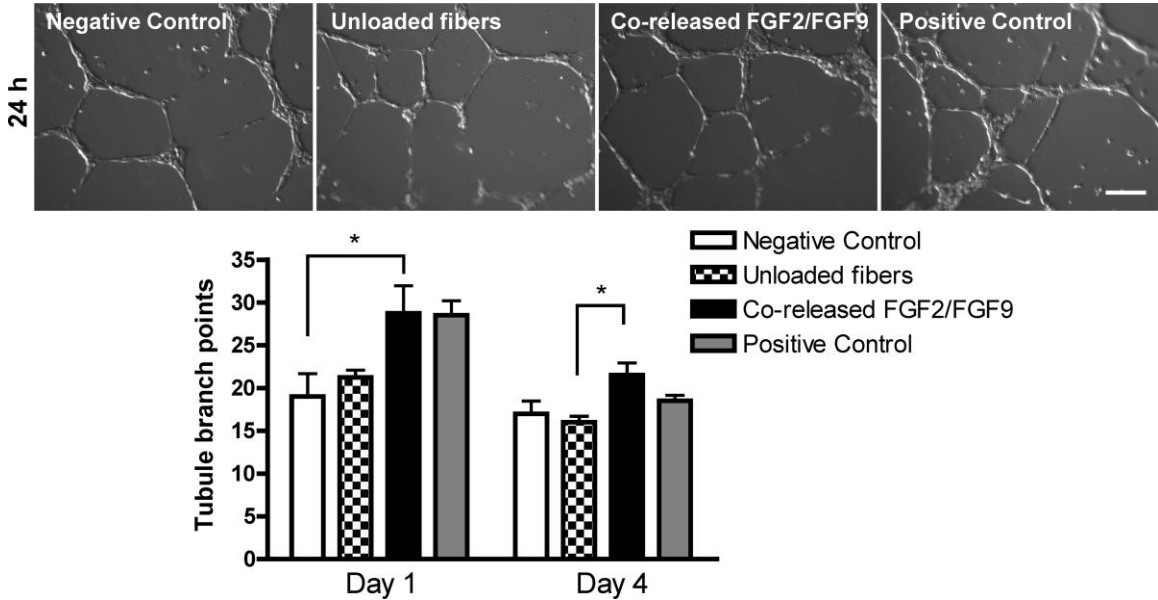


Figure 4-3: Co-released FGF2 and FGF9 from PEA fibers increased endothelial cell tube formation. Endothelial cells were treated with co-released FGFs or soluble FGF and cultured on growth factor–reduced Matrigel for 24 h.

The tubule branch points were counted using an inverted microscope at 10× objective at different time points (n=3). Fresh culture media and growth factor-supplemented media were used as negative and positive controls, respectively. Scale bar = 200 μm, * indicates $p < 0.05$.

A Boyden chamber transwell migration assay was employed to evaluate the directed migration of FGF2/FGF9 treated–human coronary artery smooth muscle cells (HCASMCs) to the chemotactic agent PDGF-BB. As illustrated in Figure 4-4 A-B, there was a significant increase in the number of migrated SMCs in the presence of PDGF-BB as a chemotactic agent compared to the group without PDGF-BB. This suggested that the

migration of FGF2/FGF9-treated SMCs was dominated by active directed migration to PDGF-BB instead of random migration. Also, the HCASMCs treated with the FGF2/FGF9 dual-loaded fibers for 7 days showed a significant increase in directed migration compared to the negative control of untreated SMCs ($p < 0.05$). This indicated that FGF2/FG9 treated-SMCs were more attracted to PDGF-BB.

Ongoing research has shown the need of prolonged exposure of ischemic tissues to angiogenic and arteriogenic growth factors for the development of robust and sustained neovascularization [1, 18]. Since the ultimate goal is to use electrospun PEA fibers as a depot for FGF2 and FGF9 for ischemic tissue repair, the bioactivity of the co-released growth factors was evaluated over a period of 4 weeks. The data revealed that both early (released between Day 1 and Day 14) and late released (released between Day 15 and Day 28) growth factor-treated SMCs showed significant increase in the number of migrated cells compared to that of the negative control ($p < 0.01$); while the difference with their respective positive controls was not significant ($p > 0.05$; Figure 4-4 C-D). This observation suggests that the released growth factors from the PEA fibers will be available in a bioactive form for the period required to secure the stabilization and survival of the newly formed vessels.

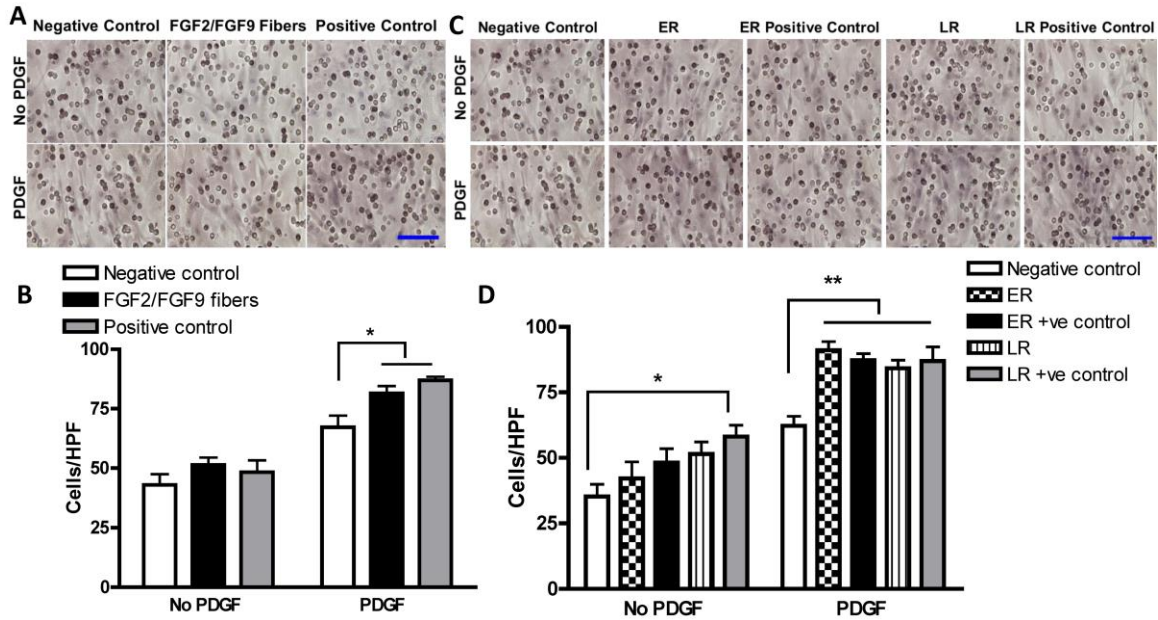


Figure 4-4: Co-released FGF2 and FGF9 enhanced directed smooth muscle cell migration.

(A and B) SMCs were incubated with FGF2/FGF9 dual loaded PEA fibers for 7 days and the treated SMCs that had migrated to PDGF-BB, after 6 h of incubation in Boyden chamber, were fixed, stained with Haematoxylin, and counted under high-power microscopy (40× objective) (n=3). Darker dots represent the membrane pores and lighter ones represent the nuclei. (C and D) Early co-released (Day 1 - Day 14; *ER*) and late co-released (Day 15 - Day 28; *LR*) FGF2 and FGF9 from the PEA fibers from *in vitro* release study. Negative control of untreated SMCs and positive control of FGF2/FGF9-treated SMCs were included in the experiment. Scale bar = 100 μm, * indicates $p < 0.05$, ** indicates $p < 0.01$.

Neovessel maturation requires the recruitment of mural cells and the subsequent wrapping of the nascent endothelial tubes with smooth muscle cells, which is essential for stable blood vessel formation. Tube formation assay protocol was used to evaluate SMC interaction with the endothelial tubes using digital time-lapse video fluorescent microscopy. GFP-expressing HCASMCs were attracted to the RFP-expressing HCAEC tubes. After 24 h of incubation, SMCs invested the tube network of GFP-expressing

endothelial cells on Matrigel; the SMCs were wrapping the EC tubes resulting in thicker EC/SMC tubes when treated with the co-released FGF2 and FGF9 or soluble FGFs compared to the negative control (Figure 4-5). This demonstrates that co-released FGF2 and FGF9 from the dual loaded PEA fibers can enhance the SMC-EC interaction and stabilize tube formation *in vitro*.

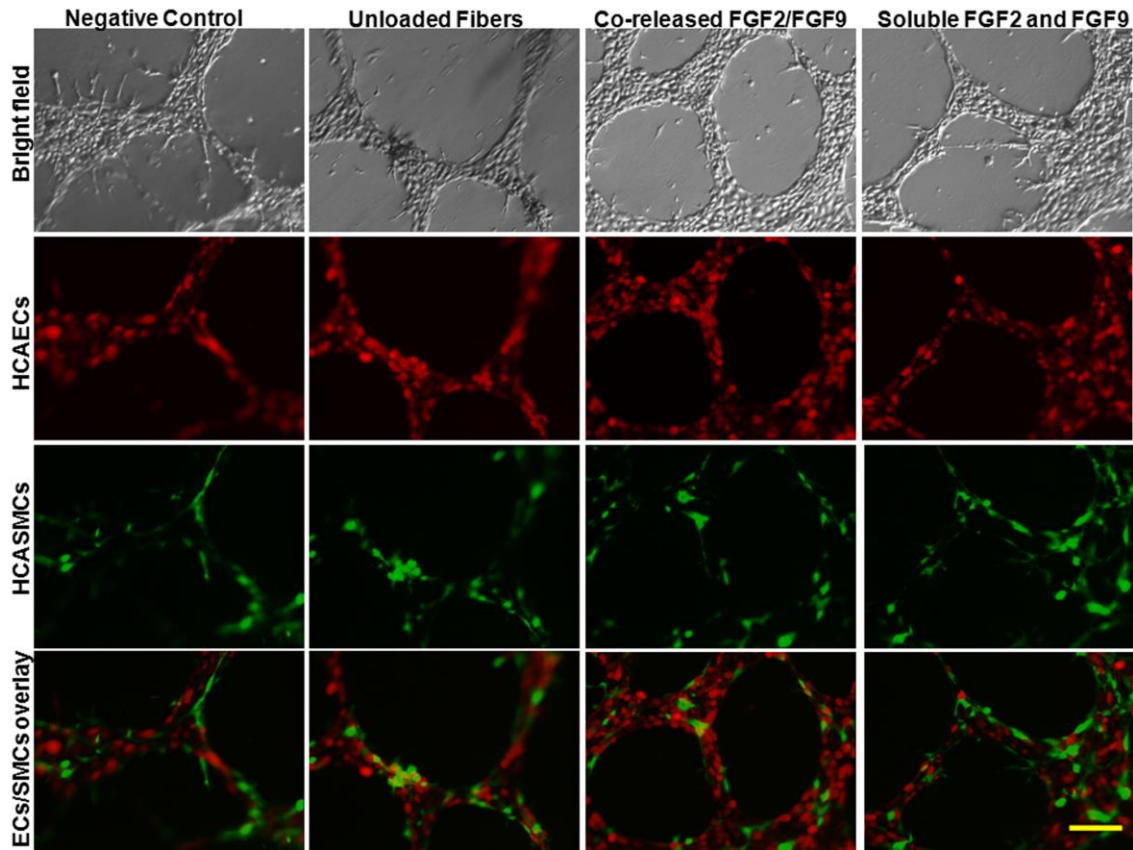


Figure 4-5: Co-released FGF2 and FGF9 from dual-loaded PEA fibers stabilize tube formation.

RFP-expressing endothelial cells were treated with co-released FGFs or soluble FGFs and cultured on growth factor–reduced Matrigel and incubated for 5 h, followed by culturing GFP-expressing smooth muscle cells at same cell density (75,000 cells/well) and further incubation for 24 h. Images were acquired, using a 10× objective, every 30 min for 24 h on Leica DMI8 inverted fluorescent microscope (n = 3). Negative control of fresh culture media and positive control of soluble growth factor-supplemented media were included in the experiment. Scale bar = 100 μm.

4.4.3 FGF2 and FGF9 Dual-loaded PEA Fibers did not Induce Inflammatory Responses

The utility of FGF2/FGF9-dual loaded PEA fibers for therapeutic angiogenic application necessitates evaluating the induced inflammatory responses. For *in vitro* studies, human monocytes (THP-1) were incubated with unloaded and FGF2/FGF9 dual-loaded PEA fibers for 72 h, followed by evaluation of the RNA expression of a selected inflammatory marker (IL-8) using quantitative real time PCR assay. Figure 4-6 shows that both unloaded and dual-loaded PEA fibers did not show a significant difference in IL-8 gene expression compared with the negative control tissue culture polystyrene (TCPS). On the other hand, the *E. coli* LPS-treated human THP-1 monocytes (positive control) showed significant fold increase in gene expression of IL-8 ($p < 0.01$). Therefore the lower RNA expression of IL-8, a cytokine known for its leukocyte chemotactic activity,[37] may lead to a lesser leukocyte chemotaxis at the site of the PEA fibers implantation and this will lead to a reduced host immune response [35].

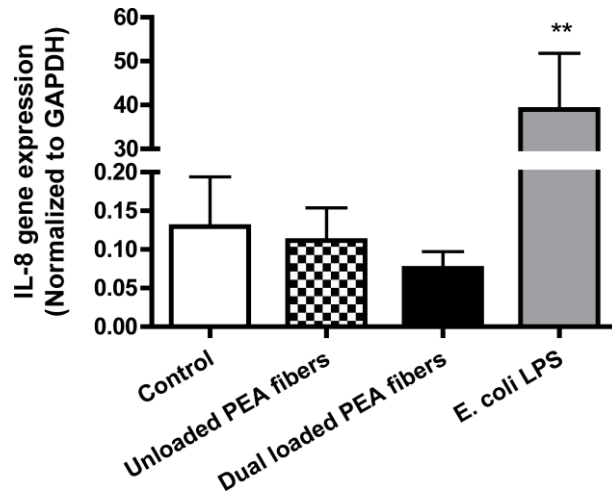


Figure 4-6: FGF2/FGF9-loaded PEA electrospun fibers did not induce an inflammatory response *in vitro*.

The gene expression of the inflammatory marker IL-8 was evaluated using quantitative real-time PCR assay after incubation of the PEA fibrous mats with THP-1 monocytes for 72 h ($n = 3$). Positive control of *E. coli* lipopolysaccharide was included in the experiment, ** ($p < 0.01$).

The *in vivo* tissue response was evaluated by implanting unloaded and growth factor-loaded PEA fibrous mat subcutaneously at the back of 8-week male B6 mice for 6 days, followed by the excision of the tissue and H&E staining for histological examination. H&E histological sections of the unloaded and the FGF2/FGF9-dual loaded PEA fibers demonstrated that the fibers did not fully degrade after 6 days of subcutaneous implantation and did not stimulate inflammatory cell infiltration or induce scar formation (Figure 4-7). Interestingly, in the case of the FGF2/FGF9-loaded PEA fibers; robust cell niche recruitment was observed around the mat. Furthermore, the damaged connective tissue started to regenerate around the fibers and there was higher population of cells resembling mesenchymal progenitor cells with increased ECM secretion around the FGF2/FGF9-dual loaded PEA fibrous mat.

FGF9-loaded PEA fibers were implanted onto the tibialis anterior muscle of B6 mice for 7 days in order to evaluate the effect of FGF9 controlled delivery from the PEA fibers, at different initial loading concentration (0, 120, 240, 480 ng/cm²), on cell niche recruitment in the context of hind limb muscles. Histological examination of the H&E sections demonstrated that the unloaded PEA fibrous mat implantation resulted in the encapsulation of inflammatory cells (Figure 4-8 A inset, red arrows). The induced inflammation was diffusive, but limited to the area surrounding the hypodermis and muscle surface. On the other hand, FGF9-loaded PEA fibrous mat implantation resulted in the amelioration of the inflammatory reaction (Figure 4-8 B-D). More importantly, FGF9 loading resulted in a dose-dependent expansion of mesenchymal progenitor-like cells that were organized in layers and deposited extracellular matrix surrounding the fibrous mat, but did not invade into the skin or the muscle. The highest tested initial FGF9-loading (480 ng/cm²) showed the most distinct expansion of the matrix-depositing cells and their higher level organization into layers (Figure 4-8 D inset, green brackets).

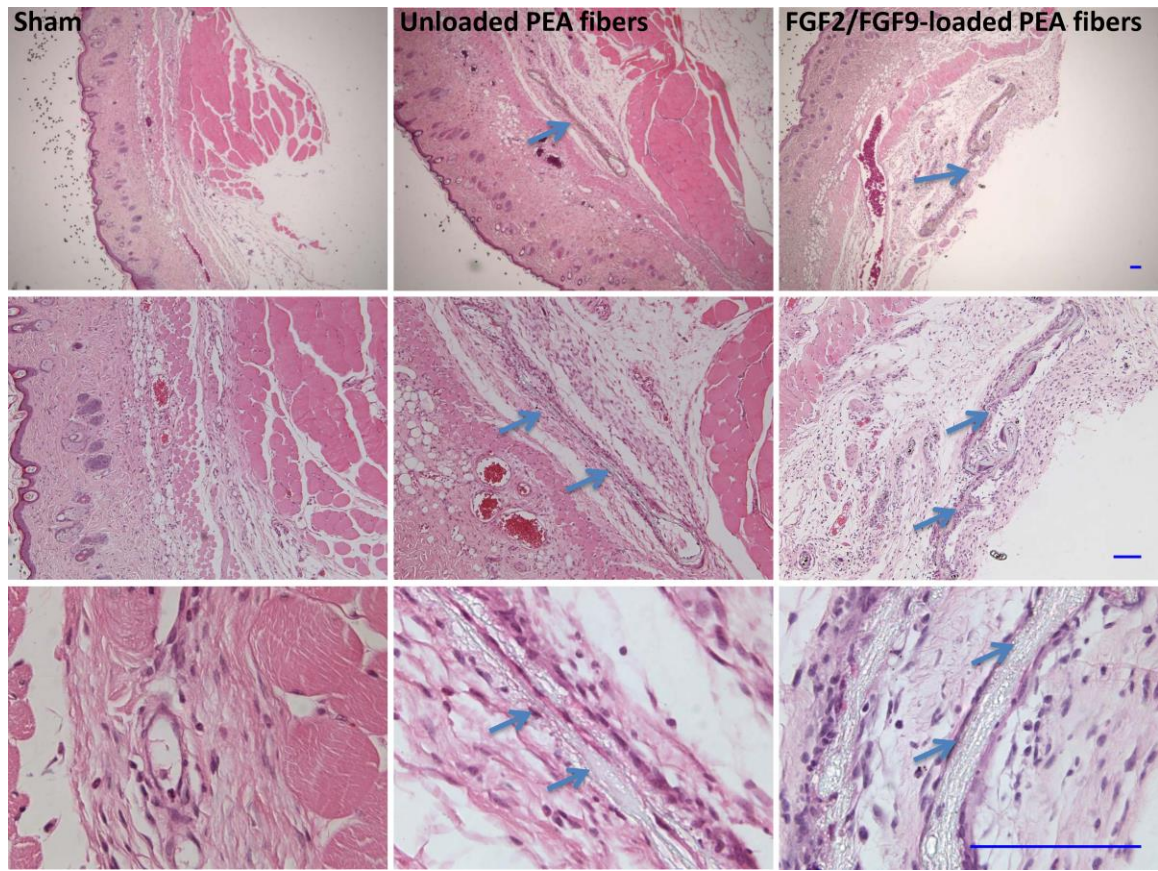


Figure 4-7: Subcutaneous implantation of FGF2/FGF9-loaded PEA electrospun fibers in B6 mice did not induce inflammatory cell infiltration.

Sham surgery and negative control of unloaded PEA fibers were included in the experiment (n = 4). H&E histological sections were examined with a Leica inverted light microscope for inflammatory cell infiltration. Blue arrows are pointing to the PEA fibers and scale bar = 100 μ m.

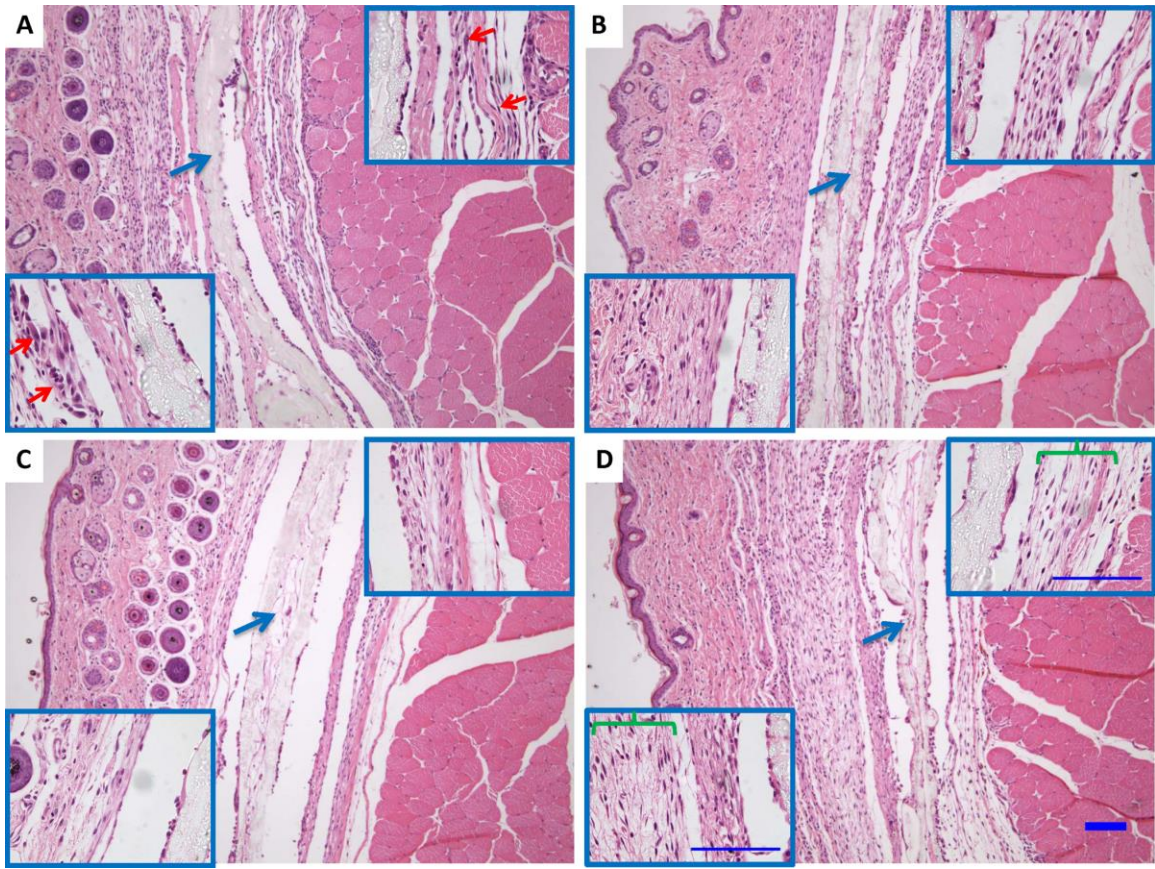


Figure 4-8: Controlled delivery of FGF9 from PEA fibrous mats resulted in a dose-dependent expansion of mesenchymal progenitor-like cell layers and ECM deposition.

FGF9-loaded PEA fibrous mats were implanted onto the TA muscle of B6 mice ($n = 3$), for 7 days to evaluate the effect of FGF9 controlled delivery (0, 120, 240, 480 ng/cm^2) from the PEA fibers on cell niche recruitment (A-D), respectively. Blue arrows are pointing to the PEA fibrous mats with insets of higher magnification for the skin and muscle sides, red arrows point to the encapsulated inflammatory cells, and green bracket indicate the organized mesenchymal progenitor-like cell layers. Scale bar = 100 μm .

4.5 Discussion

The differential delivery of more than one growth factor from a single electrospun biomaterial has not been achieved as yet. The strategy developed in previous studies is to use a polymer blend, or multiple polymers each of which is loaded with one growth factor, and electrospun to form composite delivery systems [8, 38-40]. As an example, nanocomposite bone scaffolds, where FGF18-preloaded mesoporous bioactive glass nanospheres were incorporated within the FGF2-loaded core-shell electrospun polycaprolactone and poly(ethyleneoxide) fibers for bone regeneration were reported [39]. In another study, collagen-gelatin-hyaluronic acid composite delivery system incorporating three growth factors for wound healing was also reported [38]. In our study, a single α -amino acid-derived biomaterial that degrades by surface erosion [32, 41], was utilized for dual loading and differential release of FGF2 and FGF9 for therapeutic angiogenesis application. The *in vitro* release data showed sustained and differential delivery of FGF2 and FGF9 from the PEA electrospun fibers (Figure 4-1 C), which can positively influence the natural angiogenesis process; where the angiogenic growth factor (FGF2) plays an early role in the nascent tube formation stage, while the arteriogenic growth factor (FGF9) is needed later on in the process of vessel maturation and stabilization [42-44]. FGF2 was previously loaded into electrospun fibers using blend, emulsion and coaxial electrospinning [45-47], or through heparin immobilization onto polycaprolactone electrospun scaffolds [48]. However, the complexity of the angiogenesis process and the need for more than one growth factor for functional vascular tissue formation suggest the use of a differential and sustained delivery approach in order to pattern neovascular maturation.

Angiogenesis is a multifaceted process that starts with the migration and proliferation of endothelial cells in response to angiogenic factors, followed by their remodeling into tubes. Subsequently, the maturation of the newly formed vessels requires the recruitment of mural cells [49]. The *in vitro* angiogenesis assays data demonstrated that HCAECs treated with the co-released FGF2 and FGF9 from the FGF2/FGF9-dual loaded PEA fibers showed enhanced tube formation (Figure 4-2). Moreover, HCASMCs treated with FGF2/FGF9-dual loaded fibers exhibited enhanced migration to PDGF-BB (Figure 4-3 A-B), which was

expected due to FGF2-induced increase in surface expression of $\alpha_2\beta_1$ integrin [34] and FGF9-induced upregulation of platelet derived-growth factor receptor β (PDGFR β) in human vascular SMCs, reported in previous work [22, 32, 50]. Furthermore, previously the upregulation of PDGFR β have been shown to be mediated by sonic hedgehog-PDGFR β -dependent signaling [22]. Although the angiogenic synergism between FGF2 and PDGF-BB has been reported [51], upregulating the receptor (PDGFR β) *via* FGF9 is a more valid approach than delivering the PDGFR β ligand. PDGF-BB delivery has been implicated to abolish the natural gradients of PDGF-BB required for SMC recruitment [52], whereas FGF9 delivery would not. Also, in the case of treating HCASMC/HCAEC co-culture with the co-released FGF2 and FGF9, enhanced SMC-EC interaction was observed further stabilizing *in vitro* tube formation (Figure 4-4). In view of all this, dual delivery of FGF2 and FGF9 additively enhanced directed SMC migration and vessel stability.

Biomaterials are implanted into a host either as delivery vehicles for delivering drugs and growth factors or as a tissue replacement. In either case, inflammatory response is inevitable. Although inflammation is associated with negative outcomes (e.g. fibrosis and implant rejection), some inflammatory reactions can promote biomaterial-tissue integration [53-55]. This is particularly beneficial if the implant is a tissue-engineered construct since the presence of macrophages could potentially yield a positive influence on stem cell recruitment and differentiation, allowing tissue integration, regeneration, and healing. Emerging data [53, 56] demonstrated that the positive influence of macrophages to be the result of a transition from a pro-inflammatory (M1) phenotype to a regulatory or anti-inflammatory M2 phenotype, thus promoting functional outcomes instead of scar tissue formation [56]. Scaffold surface topography appeared to be partially responsible for this phenotype transition since it affects monocyte/macrophage activation [57]. In addition to topography effects, implant integration to the host is facilitated by monocyte chemoattractant protein-1 (MCP-1). For instance, when vascular scaffolds fabricated from polyglycolic acid were seeded with bone marrow mononuclear cells (BMC) and implanted in mice, MCP-1 was secreted by BMC enhancing monocyte recruitment, which in turn recruited vascular progenitor cells [58]. Notwithstanding the above, inflammatory reaction to scaffolds loaded with growth factors/drugs is not generally desirable [24, 26, 59]. The

reason for this requirement is that inflammatory reaction often accelerates degradation of the scaffold implying rapid release of the payload instead of sustained release. Conversely, inflammatory reaction could also form a layer of fibrous capsule on the scaffold, which could potentially delay the release of the loaded growth factors. Induced inflammation and host response often preclude many synthetic biomaterials from growth factor-delivery applications [60]. This new class of α -amino acid-derived biodegradable PEAs, which are susceptible to either hydrolytic or enzymatic degradation [30, 61, 62], showed minimal induced inflammatory response *in vitro* (Figure 4-5). Moreover, subcutaneous implantation of the unloaded and the FGF2/FGF9-dual loaded PEA fibers in B6 mice did not induce significant inflammatory cell infiltration or scar formation (Figure 4-6). This was attributed to the naturally occurring degradation by-products that can be metabolized physiologically, limiting their potential inflammatory response and systemic toxicity [29]. Moreover, the degradation mechanism is governed by surface erosion [32], which limits the localized accumulation of acidic degradation by-products, thus avoiding significant pH decrease in the vicinity of the fibrous mat that usually results in inflammatory responses [63].

In this study robust cell niche recruitment was observed around the FGF2/FGF9-loaded PEA fibers when implanted subcutaneously in mice. Cell niche recruitment is most likely attributed to FGF9 [22], and the H&E sections of the FGF9-loaded PEA fibers implanted onto the tibialis anterior muscle of B6 mice for 7 days confirmed that controlled delivery of FGF9 resulted in a dose-dependent recruitment of mesenchymal progenitor-like cells that were organized in layers and deposited extracellular matrix (Figure 4-7 A-D). FGF9 has been reported to amplify mesenchymal progenitors in developing tissues [20, 64], and to maintain SMC progenitor cells in embryonic microvascular development [65]. FGF9 is expected to stimulate vascular maturation *via* recruitment of SMC progenitors to the nascent endothelial tubes and differentiation of some of this cell niche into contractile SMCs [22]. This highlights the role of the mesenchyme-targeting growth factor (FGF9) and its controlled delivery in the process of vascular maturation. In future studies, ischemic hindlimb mouse model will be utilized to examine the potential of FGF2/FGF9 dual-loaded PEA fibers to regenerate competent vasculature and to identify the recruited cell niche. Taken together, this data suggests the versatility of electrospun α -amino acid-derived PEA

fibers as promising candidates for the controlled delivery of angiogenic and arteriogenic growth factors with relevance to therapeutic angiogenesis and vascularization of *in vitro* tissue-engineered constructs.

4.6 Conclusions

Differential presentation of angiogenic and arteriogenic growth factors is beneficial to induce stable neovascularization. In this study, it has been shown that FGF2/FGF9 dual-loaded PEA fibers can be potential candidates for sustained and localized co-delivery of growth factors. The differentially released FGFs enhanced the directed SMC migration to PDGF-BB and stabilized tube formation *in vitro*. Particularly controlled delivery of FGF9 *in vivo* resulted in a dose-dependent recruitment of mesenchymal progenitor-like cells that were organized in layers and deposited ECM. Altogether, with the absence of any induced inflammatory response *in vitro* or *in vivo*, FGF2/FGF9 dual-loaded PEA fibers can have a promising therapeutic angiogenesis application for treatment of ischemic vascular diseases.

4.7 References

1. Chu, H. and Y. Wang, Therapeutic angiogenesis: controlled delivery of angiogenic factors. *Ther Deliv*, 2012. **3**(6): 693-714.
2. Park, K.M. and S. Gerecht, Harnessing developmental processes for vascular engineering and regeneration. *Development*, 2014. **141**(14): 2760-2769.
3. Lazarous, D.F., M. Shou, J.A. Stiber, D.M. Dadhania, V. Thirumurti, E. Hodge, and E.F. Unger, Pharmacodynamics of basic fibroblast growth factor: route of administration determines myocardial and systemic distribution. *Cardiovasc Res*, 1997. **36**(1): 78-85.
4. Sommer, A. and D.B. Rifkin, Interaction of heparin with human basic fibroblast growth factor: protection of the angiogenic protein from proteolytic degradation by a glycosaminoglycan. *J Cell Physiol*, 1989. **138**(1): 215-20.
5. Laham, R.J., M. Rezaee, M. Post, F.W. Sellke, R.A. Braeckman, D. Hung, and M. Simons, Intracoronary and intravenous administration of basic fibroblast growth

- factor: myocardial and tissue distribution. *Drug Metab Dispos*, 1999. **27**(7): 821-826.
6. Roy, R.S., B. Roy, and S. Sengupta, Emerging technologies for enabling proangiogenic therapy. *Nanotechnology*, 2011. **22**(49): 494004.
 7. Yang, Y., X. Li, S. He, L. Cheng, F. Chen, S. Zhou, and J. Weng, Biodegradable ultrafine fibers with core–sheath structures for protein delivery and its optimization. *Polym Adv Technol*, 2011. **22**(12): 1842-1850.
 8. Zhang, H., X. Jia, F. Han, J. Zhao, Y. Zhao, Y. Fan, and X. Yuan, Dual-delivery of VEGF and PDGF by double-layered electrospun membranes for blood vessel regeneration. *Biomaterials*, 2012. **34**(9): 2202-12.
 9. Said, S.S., J.G. Pickering, and K. Mequanint, Advances in growth factor delivery for therapeutic angiogenesis. *J Vasc Res*, 2013. **50**(1): 35-51.
 10. Rubanyi, G.M., Mechanistic, technical, and clinical perspectives in therapeutic stimulation of coronary collateral development by angiogenic growth factors. *Mol Ther*, 2013. **21**(4): 725-38.
 11. Cao, L. and D.J. Mooney, Spatiotemporal control over growth factor signaling for therapeutic neovascularization. *Adv Drug Delivery Rev*, 2007. **59**(13): 1340-50.
 12. Hosaka, A., H. Koyama, T. Kushibiki, Y. Tabata, N. Nishiyama, T. Miyata, H. Shigematsu, T. Takato, and H. Nagawa, Gelatin hydrogel microspheres enable pinpoint delivery of basic fibroblast growth factor for the development of functional collateral vessels. *Circulation*, 2004. **110**(21): 3322-8.
 13. Takehara, N., Y. Tsutsumi, K. Tateishi, T. Ogata, H. Tanaka, T. Ueyama, T. Takahashi, T. Takamatsu, M. Fukushima, M. Komeda, M. Yamagishi, H. Yaku, Y. Tabata, H. Matsubara, and H. Oh, Controlled delivery of basic fibroblast growth factor promotes human cardiosphere-derived cell engraftment to enhance cardiac repair for chronic myocardial infarction. *J Am Coll Cardiol*, 2008. **52**(23): 1858-65.
 14. Iwakura, A., M. Fujita, K. Kataoka, K. Tambara, Y. Sakakibara, M. Komeda, and Y. Tabata, Intramyocardial sustained delivery of basic fibroblast growth factor improves angiogenesis and ventricular function in a rat infarct model. *Heart Vessels*, 2003. **18**(2): 93-99.
 15. Sakakibara, Y., K. Tambara, G. Sakaguchi, F. Lu, M. Yamamoto, K. Nishimura, Y. Tabata, and M. Komeda, Toward surgical angiogenesis using slow-released basic fibroblast growth factor. *Eur J Cardiothorac Surg*, 2003. **24**(1): 105-112.
 16. Laham, R.J., F.W. Sellke, E.R. Edelman, J.D. Pearlman, J.A. Ware, D.L. Brown, J.P. Gold, and M. Simons, Local perivascular delivery of basic fibroblast growth factor in patients undergoing coronary bypass surgery: results of a phase I

- randomized, double-blind, placebo-controlled trial. *Circulation*, 1999. **100**(18): 1865-71.
17. Simons, M., B.H. Annex, R.J. Laham, N. Kleiman, T. Henry, H. Dauerman, J.E. Udelson, E.V. Gervino, M. Pike, M.J. Whitehouse, T. Moon, and N.A. Chronos, Pharmacological treatment of coronary artery disease with recombinant fibroblast growth factor-2: double-blind, randomized, controlled clinical trial. *Circulation*, 2002. **105**(7): 788-93.
 18. Simons, M. and J.A. Ware, Therapeutic angiogenesis in cardiovascular disease. *Nat Rev Drug Discov*, 2003. **2**(11): 863-71.
 19. Aviles, R.J., B.H. Annex, and R.J. Lederman, Testing clinical therapeutic angiogenesis using basic fibroblast growth factor (FGF-2). *Br J Pharmacol*, 2003. **140**(4): 637-646.
 20. White, A.C., K.J. Lavine, and D.M. Ornitz, FGF9 and SHH regulate mesenchymal Vegfa expression and development of the pulmonary capillary network. *Development*, 2007. **134**(20): 3743-52.
 21. Agrotis, A., P. Kanellakis, G. Kostolias, G. Di Vitto, C. Wei, R. Hannan, G. Jennings, and A. Bobik, Proliferation of neointimal smooth muscle cells after arterial injury. Dependence on interactions between fibroblast growth factor receptor-2 and fibroblast growth factor-9. *J Biol Chem*, 2004. **279**(40): 42221-9.
 22. Frontini, M.J., Z. Nong, R. Gros, M. Drangova, C. O'Neil, M.N. Rahman, O. Akawi, H. Yin, C.G. Ellis, and J.G. Pickering, Fibroblast growth factor 9 delivery during angiogenesis produces durable, vasoresponsive microvessels wrapped by smooth muscle cells. *Nat Biotechnol*, 2011. **29**(5): 421-427.
 23. Chen, R.R., E.A. Silva, W.W. Yuen, and D.J. Mooney, Spatio-temporal VEGF and PDGF delivery patterns blood vessel formation and maturation. *Pharm Res*, 2007. **24**(2): 258-64.
 24. Richardson, T.P., M.C. Peters, A.B. Ennett, and D.J. Mooney, Polymeric system for dual growth factor delivery. *Nat Biotechnol*, 2001. **19**(11): 1029-34.
 25. Lu, S., J. Lam, J.E. Trachtenberg, E.J. Lee, H. Seyednejad, J.J. van den Beucken, Y. Tabata, M.E. Wong, J.A. Jansen, A.G. Mikos, and F.K. Kasper, Dual growth factor delivery from bilayered, biodegradable hydrogel composites for spatially-guided osteochondral tissue repair. *Biomaterials*, 2014. **35**(31): 8829-39.
 26. Elia, R., P.W. Fuegy, A. VanDelden, M.A. Firpo, G.D. Prestwich, and R.A. Peattie, Stimulation of in vivo angiogenesis by in situ crosslinked, dual growth factor-loaded, glycosaminoglycan hydrogels. *Biomaterials*, 2010. **31**(17): 4630-8.

27. Awada, H.K., N.R. Johnson, and Y. Wang, Sequential delivery of angiogenic growth factors improves revascularization and heart function after myocardial infarction. *J Control Release*, 2015. **207**: 7-17.
28. Greenberg, J.I., D.J. Shields, S.G. Barillas, L.M. Acevedo, E. Murphy, J. Huang, L. Schepke, C. Stockmann, R.S. Johnson, N. Angle, and D.A. Cheresh, A role for VEGF as a negative regulator of pericyte function and vessel maturation. *Nature*, 2008. **456**(7223): 809-13.
29. Knight, D.K., E.R. Gillies, and K. Mequanint, Strategies in Functional Poly(ester amide) Syntheses to Study Human Coronary Artery Smooth Muscle Cell Interactions. *Biomacromolecules*, 2011. **12**(7): 2475-87.
30. Srinath, D., S. Lin, D.K. Knight, A.S. Rizkalla, and K. Mequanint, Fibrous biodegradable l-alanine-based scaffolds for vascular tissue engineering. *J Tissue Eng Regen Med*, 2012. **8**(7): 578-588.
31. Knight, D.K., E.R. Gillies, and K. Mequanint, Biomimetic L-aspartic acid-derived functional poly(ester amide)s for vascular tissue engineering. *Acta Biomater*, 2014. **10**(8): 3484-96.
32. Said, S.S., J.G. Pickering, and K. Mequanint, Controlled Delivery of Fibroblast Growth Factor-9 from Biodegradable Poly(ester amide) Fibers for Building Functional Neovasculature. *Pharm Res*, 2014. **31**: 3335–3347.
33. Borradaile, N.M. and J.G. Pickering, Nicotinamide phosphoribosyltransferase imparts human endothelial cells with extended replicative lifespan and enhanced angiogenic capacity in a high glucose environment. *Aging Cell*, 2009. **8**(2): 100-12.
34. Pickering, J.G., S. Uniyal, C.M. Ford, T. Chau, M.A. Laurin, L.H. Chow, C.G. Ellis, J. Fish, and B.M. Chan, Fibroblast growth factor-2 potentiates vascular smooth muscle cell migration to platelet-derived growth factor: upregulation of alpha2beta1 integrin and disassembly of actin filaments. *Circ Res*, 1997. **80**(5): 627-37.
35. Briganti, E., D. Spiller, C. Mirtelli, S. Kull, C. Counoupas, P. Losi, S. Senesi, R. Di Stefano, and G. Soldani, A composite fibrin-based scaffold for controlled delivery of bioactive pro-angiogenic growth factors. *J Control Release*, 2010. **142**(1): 14-21.
36. Ritger, P.L. and N.A. Peppas, A simple equation for description of solute release I. Fickian and non-fickian release from non-swellable devices in the form of slabs, spheres, cylinders or discs. *J Control Release*, 1986. **5**(1): 23-36.
37. Mukaida, N., A. Harada, and K. Matsushima, Interleukin-8 (IL-8) and monocyte chemotactic and activating factor (MCAF/MCP-1), chemokines essentially

- involved in inflammatory and immune reactions. *Cytokine Growth Factor Rev*, 1998. **9**(1): 9-23.
38. Lai, H.J., C.H. Kuan, H.C. Wu, J.C. Tsai, T.M. Chen, D.J. Hsieh, and T.W. Wang, Tailored design of electrospun composite nanofibers with staged release of multiple angiogenic growth factors for chronic wound healing. *Acta Biomater*, 2014. **10**(10): 4156-66.
 39. Kang, M.S., J.H. Kim, R.K. Singh, J.H. Jang, and H.W. Kim, Therapeutic-designed electrospun bone scaffolds: Mesoporous bioactive nanocarriers in hollow fiber composites to sequentially deliver dual growth factors. *Acta Biomater*, 2015. **16**: 103-16.
 40. Xie, Z., C.B. Paras, H. Weng, P. Punnakitikashem, L.C. Su, K. Vu, L. Tang, J. Yang, and K.T. Nguyen, Dual growth factor releasing multi-functional nanofibers for wound healing. *Acta Biomater*, 2013. **9**(12): 9351-9.
 41. Srinath, D., S. Lin, D.K. Knight, A.S. Rizkalla, and K. Mequanint, Fibrous biodegradable l-alanine-based scaffolds for vascular tissue engineering. *J Tissue Eng Regen Med*, 2014. **8**(7): 578-88.
 42. Carmeliet, P., Angiogenesis in health and disease. *Nat Med*, 2003. **9**(6): 653-60.
 43. Adams, R.H. and K. Alitalo, Molecular regulation of angiogenesis and lymphangiogenesis. *Nat Rev Mol Cell Biol*, 2007. **8**(6): 464-78.
 44. Potente, M., H. Gerhardt, and P. Carmeliet, Basic and therapeutic aspects of angiogenesis. *Cell*, 2011. **146**(6): 873-87.
 45. Sahoo, S., L.T. Ang, J.C.-H. Goh, and S.-L. Toh, Growth factor delivery through electrospun nanofibers in scaffolds for tissue engineering applications. *J Biomed Mater Res*, 2010. **93A**: 1539–1550.
 46. Yang, Y., T. Xia, W. Zhi, L. Wei, J. Weng, C. Zhang, and X. Li, Promotion of skin regeneration in diabetic rats by electrospun core-sheath fibers loaded with basic fibroblast growth factor. *Biomaterials*, 2011. **32**(18): 4243-54.
 47. Rubert, M., J. Dehli, Y.-F. Li, M.B. Taskin, R. Xu, F. Besenbacher, and M. Chen, Electrospun PCL/PEO coaxial fibers for basic fibroblast growth factor delivery. *J Mater Chem B*, 2012. **2**(48): 8538-8546.
 48. Leong, N.L., A. Arshi, N. Kabir, A. Nazemi, F.A. Petrigliano, B.M. Wu, and D.R. McAllister, In vitro and in vivo evaluation of heparin mediated growth factor release from tissue-engineered constructs for anterior cruciate ligament reconstruction. *J Orthop Res*, 2015. **33**(2): 229-236.

49. Reginato, S., R. Gianni-Barrera, and A. Banfi, Taming of the wild vessel: promoting vessel stabilization for safe therapeutic angiogenesis. *Biochem Soc Trans*, 2011. **39**(6): 1654-8.
50. Yin, H., M.J. Frontini, J.M. Arpino, Z. Nong, C. O'Neil, Y. Xu, B. Balint, A.D. Ward, S. Chakrabarti, C.G. Ellis, R. Gros, and J.G. Pickering, Fibroblast Growth Factor 9 Imparts Hierarchy and Vasoreactivity to the Microcirculation of Renal Tumors and Suppresses Metastases. *J Biol Chem*, 2015. **290**(36): 22127-42.
51. Cao, R., E. Brakenhielm, R. Pawliuk, D. Wariaro, M.J. Post, E. Wahlberg, P. Leboulch, and Y. Cao, Angiogenic synergism, vascular stability and improvement of hind-limb ischemia by a combination of PDGF-BB and FGF-2. *Nat Med*, 2003. **9**(5): 604-13.
52. Nissen, L.J., R. Cao, E.M. Hedlund, Z. Wang, X. Zhao, D. Wetterskog, K. Funa, E. Brakenhielm, and Y. Cao, Angiogenic factors FGF2 and PDGF-BB synergistically promote murine tumor neovascularization and metastasis. *J Clin Invest*, 2007. **117**(10): 2766-77.
53. Brown, B.N., B.M. Sicari, and S.F. Badylak, Rethinking regenerative medicine: a macrophage-centered approach. *Front Immunol*, 2014. **5**: 510.
54. Crupi, A., A. Costa, A. Tarnok, S. Melzer, and L. Teodori, Inflammation in tissue engineering: The Janus between engraftment and rejection. *European Journal of Immunology*, 2015. **45**(12): 3222-3236.
55. Padmanabhan, J. and T.R. Kyriakides, *Nanomaterials, Inflammation, and Tissue Engineering. Wiley Interdisciplinary Reviews-Nanomedicine and Nanobiotechnology*, 2015. **7**(3): 355-370.
56. Brown, B.N., R. Londono, S. Tottey, L. Zhang, K.A. Kukla, M.T. Wolf, K.A. Daly, J.E. Reing, and S.F. Badylak, Macrophage phenotype as a predictor of constructive remodeling following the implantation of biologically derived surgical mesh materials. *Acta Biomaterialia*, 2012. **8**(3): 978-987.
57. Bota, P.C., A.M. Collie, P. Puolakkainen, R.B. Vernon, E.H. Sage, B.D. Ratner, and P.S. Stayton, Biomaterial topography alters healing in vivo and monocyte/macrophage activation in vitro. *J Biomed Mater Res A*, 2010. **95**(2): 649-57.
58. Roh, J.D., R. Sawh-Martinez, M.P. Brennan, S.M. Jay, L. Devine, D.A. Rao, T. Yi, T.L. Mirensky, A. Nalbandian, B. Udelsman, N. Hibino, T. Shinoka, W.M. Saltzman, E. Snyder, T.R. Kyriakides, J.S. Pober, and C.K. Breuer, Tissue-engineered vascular grafts transform into mature blood vessels via an inflammation-mediated process of vascular remodeling. *Proceedings of the National Academy of Sciences of the United States of America*, 2010. **107**(10): 4669-4674.

59. Patel, Z.S., S. Young, Y. Tabata, J.A. Jansen, M.E. Wong, and A.G. Mikos, Dual delivery of an angiogenic and an osteogenic growth factor for bone regeneration in a critical size defect model. *Bone*, 2008. **43**(5): 931-40.
60. Anderson, J.M., A. Rodriguez, and D.T. Chang, Foreign body reaction to biomaterials. *Semin Immunol*, 2008. **20**(2): 86-100.
61. Karimi, P., A.S. Rizkalla, and K. Mequanint, Versatile Biodegradable Poly(ester amide)s Derived from α -Amino Acids for Vascular Tissue Engineering. *Materials*, 2010. **3**(4): 2346-2368.
62. Pang, X. and C.C. Chu, Synthesis, characterization and biodegradation of functionalized amino acid-based poly(ester amide)s. *Biomaterials*, 2010. **31**(14): 3745-54.
63. Nair, L.S. and C.T. Laurencin, Biodegradable polymers as biomaterials. *Prog Polym Sci*, 2007. **32**(8-9): 762-798.
64. Geske, M.J., X. Zhang, K.K. Patel, D.M. Ornitz, and T.S. Stappenbeck, Fgf9 signaling regulates small intestinal elongation and mesenchymal development. *Development*, 2008. **135**(17): 2959-68.
65. Yi, L., E.T. Domyan, M. Lewandoski, and X. Sun, Fibroblast growth factor 9 signaling inhibits airway smooth muscle differentiation in mouse lung. *Dev Dyn*, 2009. **238**(1): 123-37.

Chapter 5

5 *In vivo* Evaluation of FGF-loaded Electrospun Poly(ester amide) Fibers for Therapeutic Angiogenesis*

Overview: This chapter focuses on the in vivo angiogenesis evaluation of the FGF-loaded PEA fibers using the ex ovo chick chorioallantoic membrane model coupled with power Doppler ultrasound imaging and the ischemic hindlimb mouse model followed by CatWalk assay and histological analysis.

5.1 Abstract

Angiogenic protein therapies have shown great promise in preclinical studies; however, limited positive results have been achieved from clinical angiogenesis trials, in part, due to neovessel regression. A major limitation of angiogenic protein therapy is the rapid degradation and clearance from the site of delivery due to the short half-life of these exogenous angiogenic factors, resulting in a temporary therapeutic effect at the tissue of interest. Controlled delivery of angiogenic growth factors from polymeric-delivery system could overcome the aforementioned challenge. In this study, electrospun poly(ester amide) (PEA) fibers have been loaded with either fibroblast growth factor-9 (FGF9) alone or with FGF9 and fibroblast growth factor-2 (FGF2) to maintain a controlled release of these growth factors in a bioactive form over a period of months in an attempt to achieve vessel maturation and stabilization. FGF-loaded PEA fibers were evaluated using two *in vivo* models, the chick chorioallantoic membrane (CAM) model as a screening platform and the ischemic hindlimb mouse model as a pathological pre-clinical model. The CAM assay coupled with 3D power Doppler vascular quantification showed localized angiogenic effects at regions beneath the FGF-loaded fibrous mats. Moreover, the implantation of the FGF9-loaded PEA fibrous mats on the surface of infarcted tibialis anterior muscle resulted

* A version of this chapter is currently in preparation to be submitted for publication as “Somiraa S. Said, Hao Yin, Mai Elfarnawany, Zengxuan Nong, Caroline O’Neil, Hon Leong, James Lacefield, Kibret Mequanint and Geoffrey Pickering”.

in an enhanced skeletal muscle regeneration and increased abundance of mural-wrapped microvessels compared with the unloaded fibers control group as demonstrated by histological analysis. This supports the hypothesis that controlled delivery of FGF9 from electrospun PEA fibers enhances the assembly of functional and stable microvessels.

Key words: Angiogenic protein therapy; Poly(ester amide) electrospun fibers; Fibroblast growth factor-2; Fibroblast growth factor-9; CAM angiogenesis assay; Ischemic hindlimb mouse model.

5.2 Introduction

In vitro angiogenesis assays are quantitative and efficient but their findings should be confirmed by *in vivo* models. *In vivo* assays are more laborious and challenging to quantitate; however, the formation of functional blood vessels involves complex interactions between multiple cell types, which necessitates preclinical testing. Simple animal models such as the chick chorioallantoic membrane (CAM) [1, 2], zebra fish embryo [3, 4] and rabbit corneal pocket [5] have been widely used to assess angiogenesis *in vivo*. Clinically-relevant animal models have also been used to demonstrate the potential of angiogenic therapies for myocardial and peripheral ischemia [6]. Myocardial ischemia is most commonly induced by ligation of the anterior descending branch of the left coronary artery [7] or by placing ameroid constrictors around the coronary artery [8]. Hindlimb ischemia is typically induced by ligation and/or excision of the common femoral artery or iliac artery [9, 10], with or without accompanying ligation of collateral vessels. In animal models, histological demonstration of enhanced angiogenesis and tissue healing or perfusion after an acute arterial occlusion is a common preclinical endpoint [6]; however, the functionality of the newly formed vessels and the restoration of the ischemic muscle function should also be considered in animal models. The most studied growth factors in animal models for therapeutic angiogenesis are vascular endothelial growth

factor (VEGF), fibroblast growth factor-2 (FGF2) and platelet-derived growth factor (PDGF)-BB [6].

In this chapter, the chick CAM model is proposed as an *in vivo* angiogenesis assay to evaluate the developed FGF2/FGF9 dual loaded PEA fibrous mats. Since the chick embryo is a living system, this model provides a simplistic physiological system for *in vivo* analysis than the *in vitro* assays. The CAM is the extraembryonic membrane that lies directly under the egg shell of all avian species allowing for gas and nutrient exchange [11, 12]. It is highly vascular, readily accessible, relatively immunotolerant and inexpensive [13]. Large numbers of eggs can be prepared for the CAM assay in a relatively short time and the results can be quantified rapidly with minimal equipment allowing for large-scale screening. This system has been used for the study of vascular development and angiogenesis [14]. Because of its rapid vascular growth, many pro- and anti-angiogenic agents have been tested by quantifying the morphological responses of the CAM vasculature [15]. Moreover, it is possible to test controlled release delivery systems *via* local application on the CAM surface [1], and the lack of excretion allows to preserve the concentration of bioactive reagents in the circulation for extended period of time [13]. Power Doppler ultrasound imaging of the CAM allows for better interpretation of vascular remodeling in the local microenvironment of the angiogenic therapy.

Since a single *in vivo* model is usually inadequate to fully investigate the process of angiogenesis, a more clinically relevant model, the ischemic hindlimb mouse model, was considered to further investigate the potential of FGF9-loaded electrospun PEA fibers to induce the formation of mature vasculature in ischemic conditions. Ischemic conditions usually creates high FGF2 gradient in the affected tissue [16], which minimizes the need for FGF2 controlled delivery. If a sufficient amount of FGF9 is delivered to the ischemic tissue, it may act in the local microenvironment where most of the growth factors, their receptors and signaling pathways necessary for the vascular remodeling are already present [17-19]; therefore, it will not need to initiate and maintain the whole complicated process of angiogenesis. Hence, the study focused on the local and controlled delivery of FGF9 and testing the effects of FGF9-loaded PEA fibrous mats on tissue regeneration and new microvessel stabilization using the ischemic hindlimb mouse model.

In the current study, FGF-loaded PEA fibrous mats were studied using two *in vivo* models; the CAM model coupled with power Doppler ultrasound imaging to study localized angiogenesis, and the ischemic hindlimb model followed by quantitative CatWalk gait assay and histological analysis including H&E and double immunofluorescent staining to study tissue regeneration and mature neovessel formation.

5.3 Material and Methods

5.3.1 Materials

The poly(ester amide) 8-Phe-4 was synthesized from L-phenylalanine, sebacoyl chloride, and 1,4-butanediol through interfacial polymerization and characterized as described in previous publications [20, 21]. Recombinant human FGF9 and FGF2 were purchased from R&D Systems, Inc. (Minneapolis, MN). Hank's balanced salt solution was purchased from Invitrogen Canada (Burlington, ON). The FGF-loaded PEA fibers were fabricated by the electrospinning technique and characterized as previously reported [21, 22].

5.3.2 Chick Chorioallantoic Membrane (CAM) as an Angiogenesis Screening Platform for FGF2/FGF9 Dual-loaded PEA Fibrous Mats

Fertilized White Leghorn chicken eggs were obtained from McKinley Hatchery (St Mary's, ON, Canada). Eggs were incubated for three days at 38 °C and 80% relative humidity (RH) in a rotating hatcher (Sportsman hatcher, Berry Hill, ON). On Day 4 post-fertilization, the eggs were removed from the hatcher and were cracked gently using a blade. The embryos were transferred into weighing boats with a plastic cover, an *ex ovo* culture system, to expose the CAM and make it accessible for imaging (Figure 5-1). The *ex ovo* culture protocol is previously described [23]. The shell-less chick embryos were returned to the incubator (38 °C, ~80% RH) till Day 10.

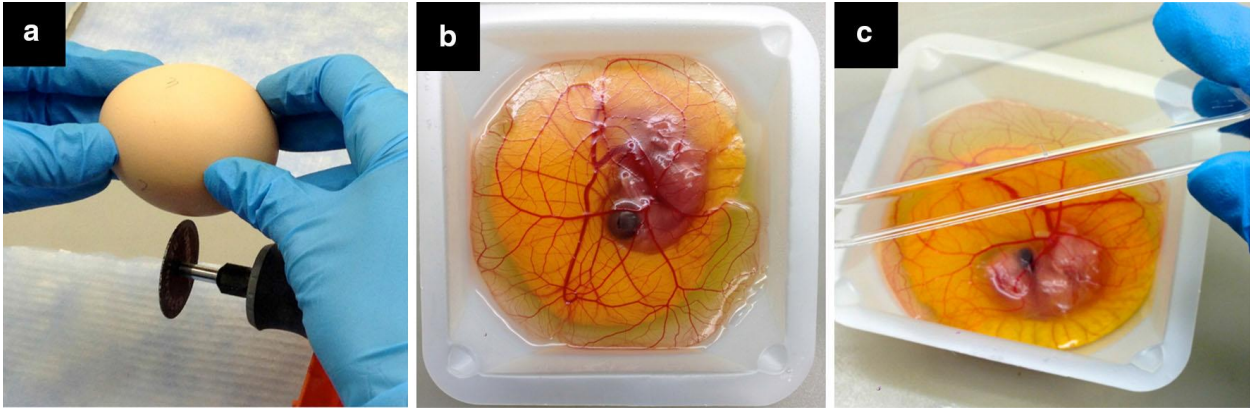


Figure 5-1: The *ex ovo* CAM cultivation protocol steps.

(a) Gentle cracking of the egg using a blade, (b) transferring the contents into weighing boats and (c) covering with a plastic cover. Adapted from [15].

5.3.2.1 Experimental Design

On Day 10, the CAMs were retrieved from the incubator to start the study. Four test conditions were examined to study the vascular density increase of the full CAM surface: soluble growth factors on Kimwipe™ (1 cm × 1 cm) (10 μL FGF2 solution and 10 μL FGF9 solution in PBS at a concentration of 1 ng/μL), unloaded PEA fibers (1 cm × 1 cm), FGF2/FGF9 dual-loaded PEA fibers (1 cm × 1 cm), and control (no fibers). The samples were conditioned overnight in Hank's balanced salt solution (HBSS) before placing on the CAM. To maintain the temperature during the experiment, the chick embryos were placed over a warming pad (Gaymar Industries, Inc., Orchard Park, NY) set to 40 °C. A total of 3 CAMs were used for each condition and the experiment was repeated three times. The CAMs were supplemented with 50 μL of HBSS at pre-determined time intervals to keep the mats moist, which could assist in the process of growth factor diffusion. Each CAM was digitally photographed at Day 0, 2, 5, and 8, and then imaged using power Doppler ultrasound at Day 8 when the vascular network of the CAM fully matures as previously reported [12]. The embryos were allowed to stabilize for 2-5 minutes prior to image acquisition. All procedures complied with the guidelines of the Canadian Council on Animal Care.

5.3.2.2 Image Acquisition

Digital photographs (2448×2448 pixels) of the full CAM surface were captured using a Samsung Galaxy S6 camera (16 MP, Samsung Electronics Canada Inc., Mississauga, ON). The phone was placed on a custom made stage designed to keep the phone parallel to and at a fixed height from the CAM surface. Three dimensional (3D) power Doppler images of the CAM vasculature were acquired using a 40 MHz linear array transducer (MS550D, FUJIFILM VisualSonics, Inc., Toronto, Canada) and Vevo 2100 high-frequency imaging system (FUJIFILM VisualSonics, Inc) setup to the digital RF mode. The settings were fixed throughout the study (frequency, 40 MHz; power, 100%; B-mode gain, 22 dB; power Doppler gain, 12 dB; dynamic range, 65 dB; pulse repetition frequency, 1 kHz; wall-filter, low). Warmed Aquasonic 100 ultrasound transducer gel (Parker Laboratories, Inc., NJ, USA) was applied to the transducer face and used for coupling between the transducer and the CAM surface. Few drops of warmed saline were applied to the CAM surface at the CAM-transducer contact area as a lubricant to prevent sticking of the CAM surface to the transducer gel. Imaged regions of interest (ROI) were set to (lateral \times axial \times elevation = $13.88 \times 10.00 \times 14.10$ mm with an elevation spacing between B-mode planes of 0.0762 mm) and were selected to include clear arterial and venular branching patterns far enough from the embryo body to reduce reflection and motion artifacts. The 3D power Doppler images were exported in the quadrature demodulated (IQ).

5.3.2.3 Digital Image Pre-processing

Using the full view of the CAM surface, the scale was calibrated using the reference dimensions of the plastic weighing boats carrying the embryos ($89 \text{ mm} \times 89 \text{ mm}$). Images were then cropped keeping only the region showing the vascular network of the CAM using the polygon selection tool in Fiji software (NIH, Maryland, USA) [24]. The percentage vascular density, the number of pixels representing vessels (white pixels) divided by the total number of pixels in the ROI $\times 100$, was automatically calculated from the cropped images using *Vessel Analysis* plugin for Fiji software developed by Nivetha Govindaraju and Mai Elfarnawany [URL link to the page: http://imagej.net/Vessel_Analysis]. The

plugin applies a series of filters, noise reduction, thresholding and binarization functions to the ROIs prior to estimating the vascular density. The pre-processing steps and a sample of the final binary image are shown in Figure 5-2.

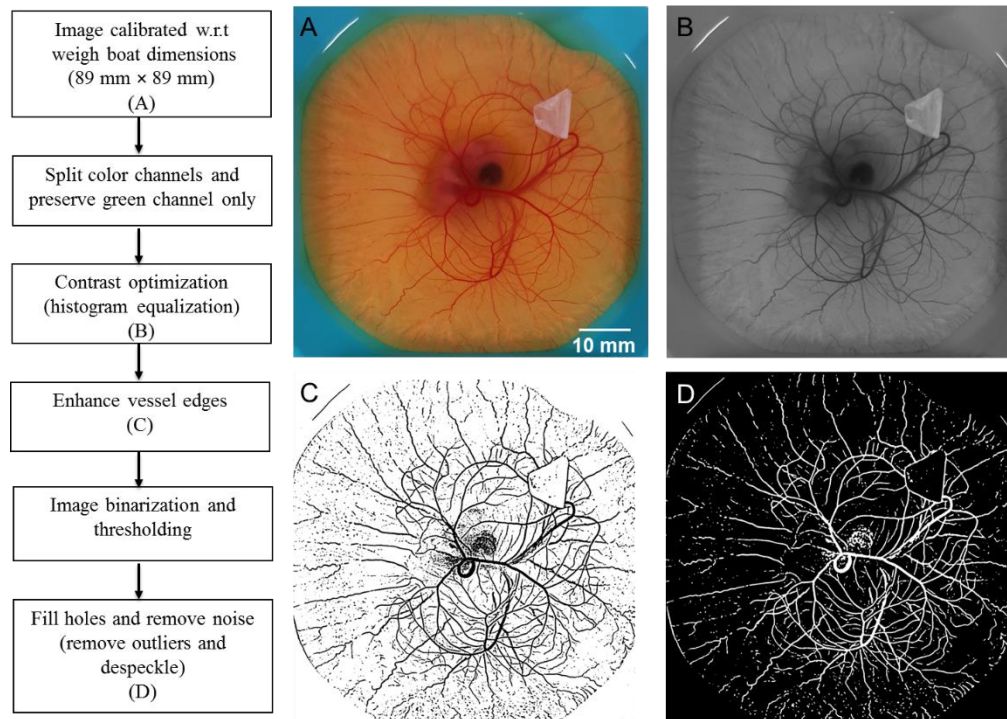


Figure 5-2: Steps of digital image pre-processing to produce the final binary CAM image used in percentage vascular density analysis.

5.3.2.4 Power Doppler Processing and Vascular Quantification

Power Doppler quadrature demodulated (IQ) data was processed using software implemented in MATLAB R2013a (The MathWorks, Inc., MA, USA) to apply the two-stage method for power Doppler microvascular angiography developed by Elfarnawany *et al.* [25, 26]. In the first stage, the wall filter cut-off frequency is spatially tuned for local variations in the processed image using the wall filter selection curve (WFSC) method [27]. The 3D power Doppler volume of the vascular network is reconstructed from the spatially

tuned images. In the second stage, a 3D vessel tree is extracted from the power Doppler volume by applying a 3D skeletonization algorithm followed by reconstruction of the full diameters of the vessels along the skeletons. To retain the intensity values of the power Doppler signal in the final image, the original 3D power Doppler volume is masked using the 3D vessel tree resulting in a power-weighted 3D vessel tree with reduced color voxel artifacts.

The resulting 3D power Doppler vessel tree was quantified using the three standard power Doppler angiography metrics [28]:

$$\text{Vascularization index (VI)} = \frac{\text{color voxels}}{\text{total voxels in ROI}}$$

$$\text{Flow index (FI)} = \frac{\text{weighted color voxels}}{\text{volume of colored voxels (mm}^3\text{)}}$$

$$\text{Vascularization flow index (VFI)} = \frac{\text{weighted color voxels}}{\text{volume of total voxels in ROI (mm}^3\text{)}}$$

where, VI measures the proportion of color voxels in the ROI, representing the amount of moving blood in the tissue, FI, the mean power signal of blood flow, represents the intensity of flow at the time of acquisition and VFI is a combination of vascularization and flow indices representing both blood flow and vascularization. The denominators of the FI and VFI metrics were modified by Elfarnawany *et al.* [26] from their original definition by replacing the number of voxels by the total volume occupied by these voxels in mm³ to compensate for longitudinal variations in the voxel size when using differently sized Doppler ROIs at different time points. These three vascularization measurements were calculated from the 3D power Doppler volumes for the four test conditions and compared to give an idea about the quality of the induced vasculature in the localized volume of the CAM underneath the fibrous mats.

5.3.3 Ischemic Hindlimb Mouse Model: *In vivo* Angiogenesis Assay for FGF9-loaded PEA Fibers

5.3.3.1 Experimental Design

Male C57BL6/J mice 3 month of age were anesthetized by Isoflurane inhalation (Forane[®], Baxter, Deerfield, IL) and hindlimb ischemia was induced as described in Figure 5-3 [9]. Briefly, the right femoral artery was exposed through an incision in the skin overlying the middle portion of the hind limb. The femoral artery was ligated above and below the profunda femoris branch using 6-0 silk sutures. The artery and vein with all side-branches were dissected, avoiding the femoral nerve, and the intervening 5–6 mm portion of artery was excised. Nine mice were used per group (FGF9-loaded vs unloaded fibers group). FGF9-loaded fibrous mats (~2 ng release per cm² per day) and control of unloaded fibrous mats were implanted subcutaneously on the calf region, as a layer of 5 mm × 7 mm sheet, at the interface between the skin and tibialis anterior (TA) muscle. The fibrous mat covered the lower 2/3 of the TA muscle surface. The fibers were pre-implanted 3 days before hindlimb ischemia was induced. Seven days post-ischemia induction, mice were subjected to CatWalk gait analysis and then sacrificed and the calf tissues were harvested for histological analysis. All animal procedures were approved by the Council on Animal Care of the University of Western Ontario and were in accordance with the guidelines of the Canadian Council on Animal Care.

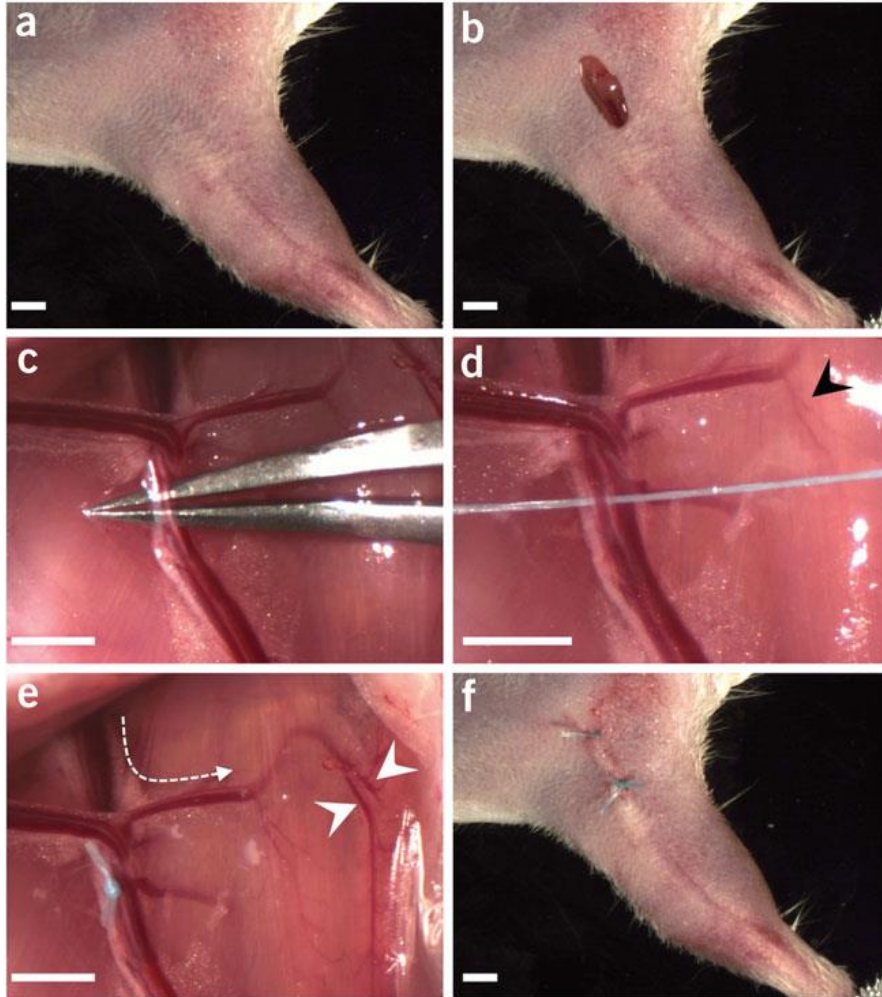


Figure 5-3: Surgical procedure for induction of hindlimb ischemia by femoral artery ligation in C57BL6/J male mice.

Ventral aspect of right mouse thigh and upper hind limb after hair removal (a). Surgical skin incision (5 mm) beginning from the groin skinfold following and immediately lateral to the vascular contours visible through the skin (b). Blunt dissection and separation of the femoral artery and vein (c). Insertion of surgical thread underneath the femoral artery (d). Faint appearance of collaterals from the deep branch (arrowhead). Ligation of the femoral artery distal to the origin of the deep branch by a triple surgical knot (e). Blood flow is diverted to collaterals (dashed white arrow) and collateral arteries now appear prominent (compare arrowheads from d and e). Over-and-over skin suture (f). Scale bars = 2 mm. Used with permission from Macmillan Publishers Limited [9] © 2009.

5.3.3.2 CatWalk Automated Quantitative Gait Analysis

CatWalk assay is a highly sensitive tool to assess gait and locomotion. The mouse traverses a glass plate voluntarily, and its footprints are captured. It visualizes the prints and calculates statistics related to print dimensions and the time and distance relationships between paw falls. CatWalk assay usually used in neurological research, but it has been used in this study to assess functional recovery of the ischemic hindlimb by determining the extent to which the injured limb was used for walking [29]. The mice were subjected to the CatWalk assay at Day 7, and the average of at least 3 runs across the glass plate of an enclosed walkway was used for further analysis by the Noldus 7.1 software (Noldus Information Technology Inc., Leesburg, VA). In the CatWalk system, LED light from a fluorescent lamp illuminates the inside of the glass floor plate of the walkway. Light is reflected downward at sites of paw contact with the upper surface of the glass plate, the intensity of which is proportional to the relative force being exerted by the paw. Light reflection was recorded with a video camera and analyzed to determine the print intensity, print area and duty cycle for comparison between the FGF9-loaded fibers and the unloaded fibers-treated mice groups. Print intensity is expressed as the mean brightness of all pixels of the print at maximum contact, the print area (mm^2) is the surface area (in pixels) of the complete print, while the duty cycle (%) expresses the stance duration as a percentage of the duration step cycle including stands and swings. All values were normalized to the contralateral healthy (left) hindlimb and expressed as mean percentage.

5.3.3.3 Histological Analysis

The mice were sacrificed at Day 7 and perfusion-fixed with 4% paraformaldehyde (PFA). The whole hindlimbs were immersed in 4% PFA overnight. The anterior calf muscle bundle was isolated and fixed with 4% PFA for another 24 h before paraffin embedding. Muscle tissues, including TA, extensor digitorum longus (EDL) and palmaris longus (PL) muscles, were cross-sectioned at 5 μm thickness and subjected to hematoxylin and eosin (H&E) staining, or double-immunostained using biotinylated rat anti-mouse CD31 antibody (Clone MEC13.3, BD Biosciences) and mouse anti-smooth muscle α -actin (SM

α -actin) antibody conjugated with alkaline phosphatase (Clone 1A4, Sigma), or rat anti-mouse endomucin antibody (V.7C7, Santa Cruz) and rabbit anti-NG2 Chondroitin sulfate proteoglycan antibody (AB5320, EMD Millipore). Images were acquired on an Olympus IX51 inverted microscope equipped with North Eclipse software, using 20 \times and 40 \times objective. Due to inter-individual variation in muscle regeneration at Day 7, the histological comparison was limited to regions with similar degree of myofiber regeneration in the TA muscle. Five ROIs per section were analyzed qualitatively for H&E stained sections in terms of induced inflammation and the degree of regeneration of the infarcted TA muscle, and quantitatively for double-immunofluorescent stained sections by counting mural-covered microvessels (SM α -actin or NG2 positive microvessels) using ImageJ software.

5.3.4 Statistical Analysis

Data is presented as mean \pm SEM for experiments conducted in triplicate. Statistical analysis was conducted with t-test or one-way ANOVA followed by Tukey's multiple comparison test using GraphPad Prism 4 software (GraphPad Software, Inc., CA, USA). Probability values less than 0.05 were considered statistically significant, unless otherwise was specified.

5.4 Results and Discussion

5.4.1 FGF2/FGF9 Dual-loaded PEA Fibers Induced Localized Angiogenesis in CAM Model

5.4.1.1 Analysis of Vascular Density of the Full CAM Surface

Figure 5-4 A shows the digital photographs (2448 \times 2448 pixels) of the full CAM surface, captured using a Samsung Galaxy S6 camera and the images were processed using ImageJ software, following the previously described scheme (Figure 5-2). The percentage increase in vascular density of the CAM at each time-point was calculated by subtracting the initial

vascular density at Day 0 for each chick embryo from the vascular density at Day 2, 5, and 8. The digital images showed a qualitative increase in vascular density of the CAMs treated with the 4 test conditions with time; however, there was no significant difference in the vascular density of the CAM between the 4 test conditions at Day 2, 5, and 8 (Figure 5-4 B). The *ex ovo* CAM model had some limitations in detecting a significant increase in vascular density of the full CAM vasculature due to its rapid vascular growth that outpaced the controlled and relatively slow release of FGF2 and FGF9 from the PEA fibers. Furthermore, the released amount of growth factors from the fibers might not have reached the effective therapeutic dose to induce significant angiogenesis in the full CAM surface.

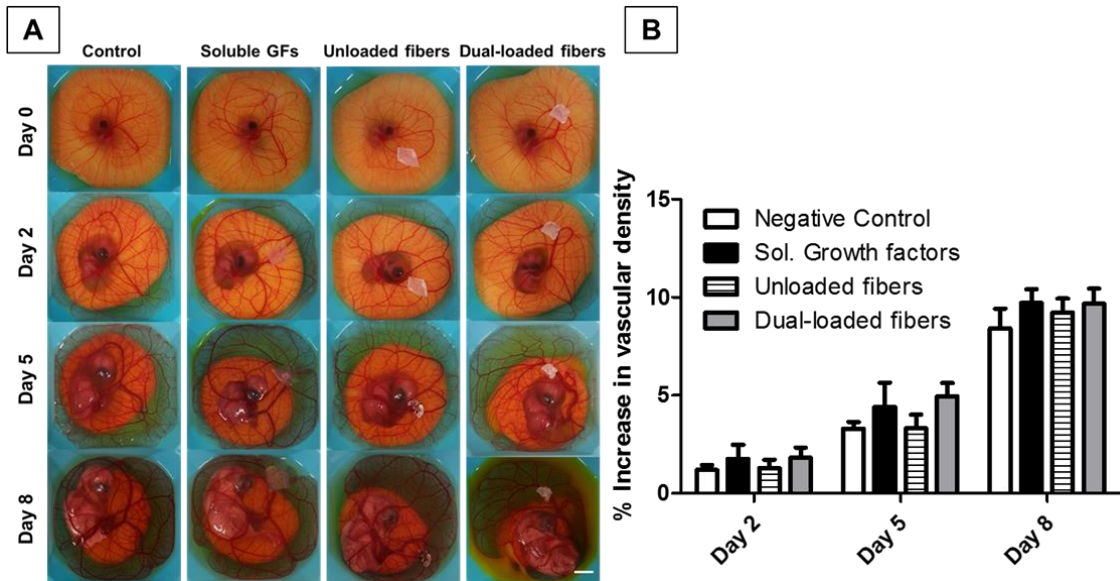


Figure 5-4: The effect of FGF2/FGF9 dual-loaded PEA fibers on CAM vasculature.

(A) Digital photographs of the full CAM surface, (B) Percentage increase in vascular density of the full CAM vascular density calculated at pre-determined time intervals (Day 2, 5, and 8) for the control (no fibers), CAMs treated with soluble growth factor, unloaded PEA fibers, and FGF2/FGF9 dual-loaded PEA fibers with respect to Day 0. Scale bar = 10 mm, (n=3).

5.4.1.2 Vascular Quantification Using 3D Power Doppler Volumes of the CAM

The 2D power Doppler images showed an increase in the CAM thickness in case of the soluble GFs on Kimwipe™ group with the soluble growth factors, unloaded PEA fibers, and the FGF2/FGF9 dual-loaded PEA fibers compared to the control (no fibers), which might be due to induced inflammation of the CAM surface, as indicated by the increased thickness of the CAM tissue (Figure 5-5). Nevertheless, it is worth noting that the induced inflammation due to the PEA fibers was much less than that induced in the soluble GFs on Kimwipe™ group (Kimwipe was used in the study to confine the GF solution and provide comparable conditions to the PEA fibrous mat). Furthermore, the PEA fibers were more flexible and adapting with the increased vascularity of the CAM surface with time.

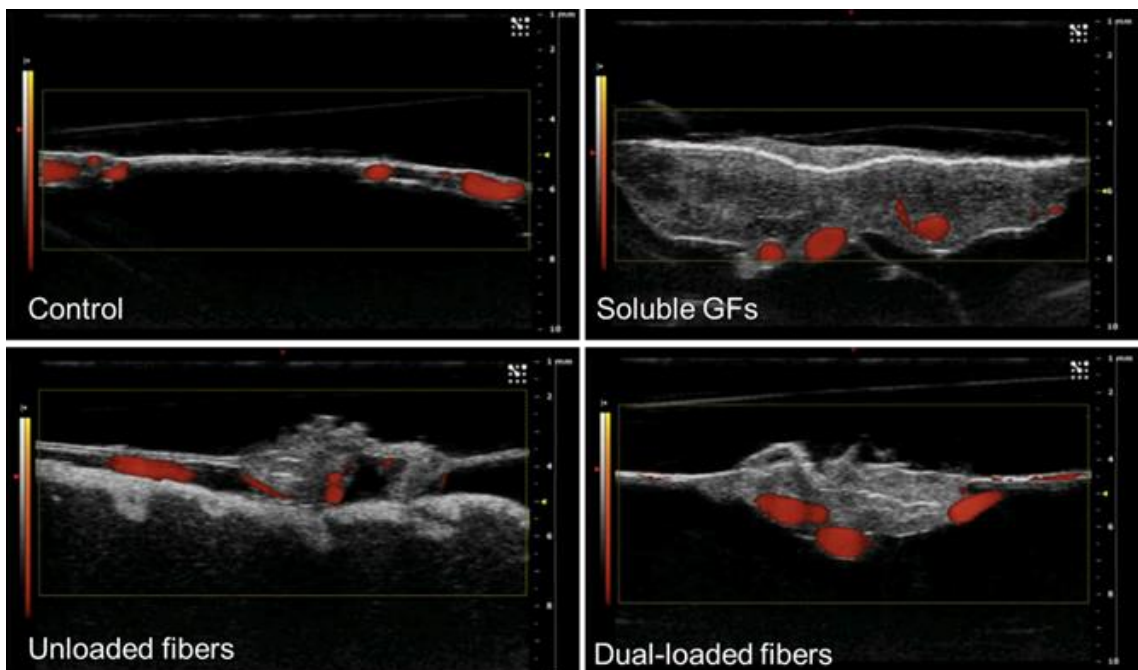


Figure 5-5: The power Doppler 2D images of the control (no fibers), CAMs treated with soluble growth factor, unloaded PEA fibers, and FGF2/FGF9 dual-loaded PEA fibers, acquired at Day 8.

The power Doppler 2D images show transverse sections of the CAM tissue represented in gray scale and the vessels represented in red.

Moreover, the fibers did not interrupt the vascular network of the CAM underneath, which resulted in slight bending of the horizontal vessel network when compared to the control as shown in the power Doppler 3D volumes (Figure 5-6). In addition, the 3D volumes showed the formation of smaller vessels near the CAM surface in case of the dual-loaded PEA fibers and soluble GFs on Kimwipe™ treated CAMs, which were not observed in case of the unloaded PEA fibers treated and the control CAMs (Figure 5-6). This suggests a localized angiogenic effect at the interface between the fibrous mat and the CAM surface.

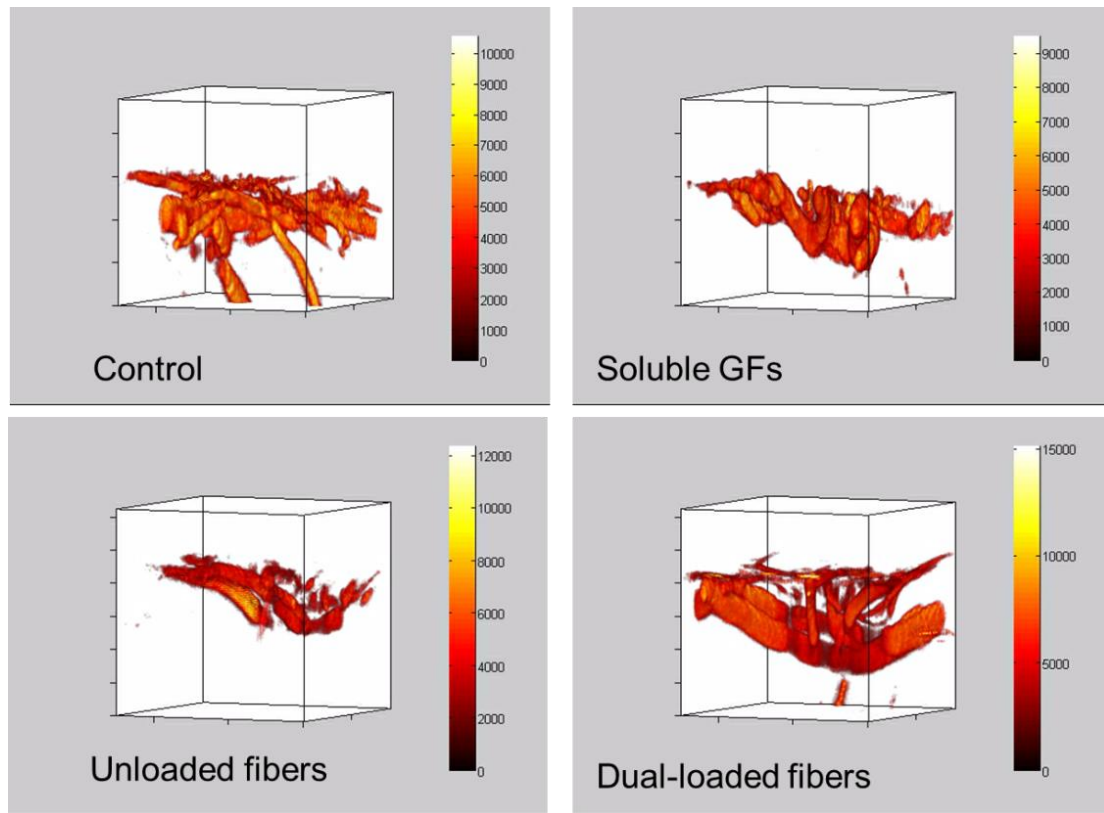


Figure 5-6: The power Doppler 3D vessel trees resulting from applying the two-stage signal processing method for power Doppler angiography [26].

3D volumes for ROIs (lateral × axial × elevation= 13.88 × 10.00 × 14.10 mm with elevation spacing between B-mode planes of 0.0762 mm) of the control, and CAMs treated with soluble growth factor, unloaded PEA fibers, and FGF2/FGF9 dual-loaded PEA fibers, acquired at Day 8.

Furthermore, vascular quantification of the 3D power Doppler volumes was carried out using modified Pairleitner *et al.* equations [28]. Vascularization and flow metrics for VI, VFI, and FI (Figure 5-7) indicated a statistically significant increase in vascularization and vascularization flow indices (VI and VFI) for the dual-loaded PEA fibers group versus the unloaded PEA fibers group, which might indicate the assembly of a better quality microvessels and increased amount of moving blood in the CAM underneath the fibrous mat owing to the controlled release of FGF2 and FGF9.

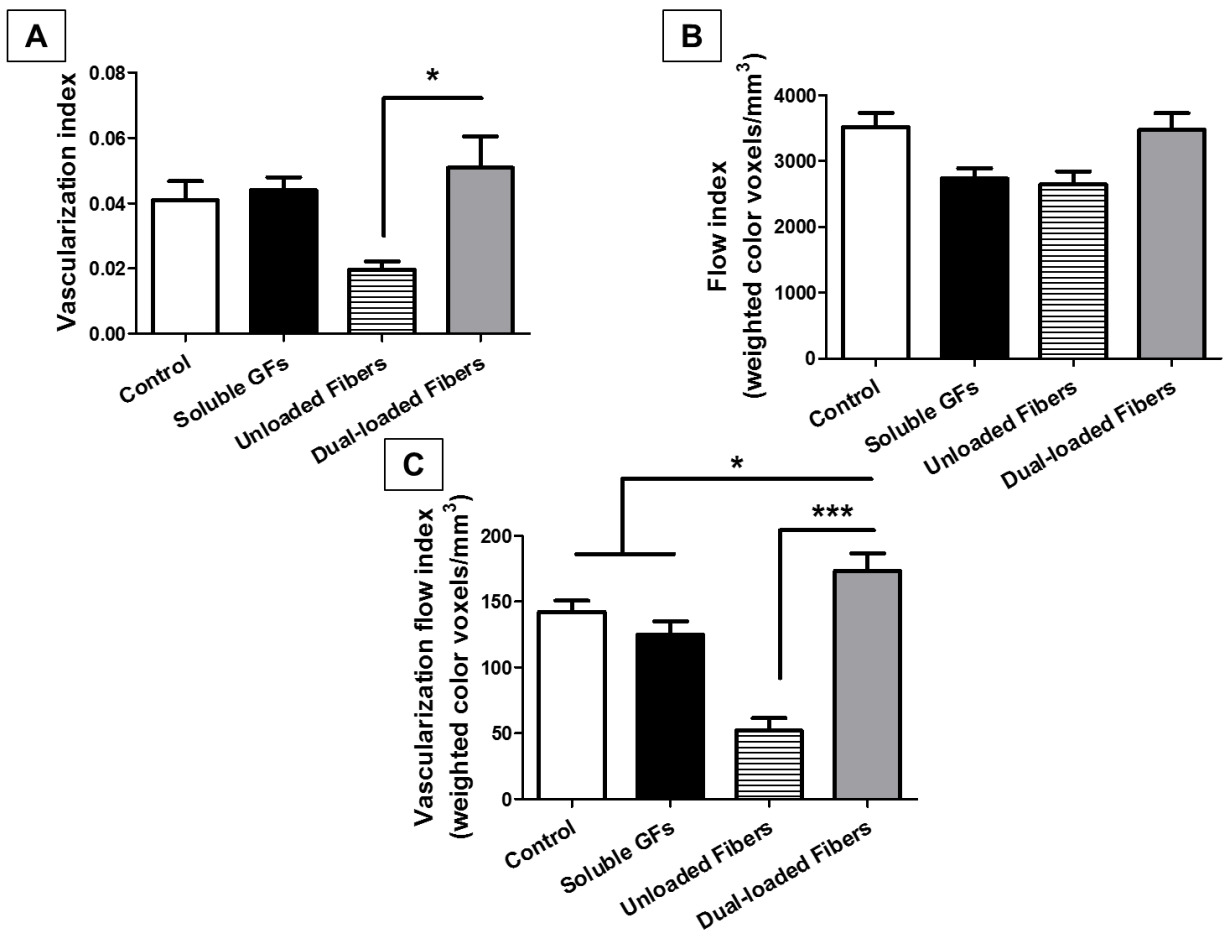


Figure 5-7: Vascular quantification of the power Doppler 3D volumes of the control, and CAMs treated with soluble growth factor, unloaded PEA fibers, and FGF2/FGF9 dual-loaded PEA fibers, acquired at Day 8 (n=3), (* $p < 0.05$, * $p < 0.0001$).**

5.4.2 Controlled Release of FGF9 from PEA Fibers Stimulated Stable Microvessel Formation in Ischemic Hindlimb Mouse model

In order to assess whether the controlled release of FGF9 from PEA fibers promotes neovessel formation and maturation in ischemic conditions, FGF9-loaded PEA fibrous mats were implanted directly onto the TA muscle of B6 mice subjected to femoral artery ligation 3 days post-implantation.

5.4.2.1 Functional Recovery of the Ischemic Hindlimb upon Implantation of FGF9-loaded PEA Fibrous Mats

Functional recovery of the ischemic hindlimb by the controlled delivery of FGF9 was assessed using CatWalk analysis of mice traversing an illuminated glass plate and its foot prints were recorded. At Day 7 post-ischemia, there was no statistically significant difference ($p > 0.05$) between the print intensity, print area and duty cycle of the injured hindlimbs treated with FGF9-loaded fibers compared with those treated with unloaded PEA fibers in terms of usage of the injured limb for weight bearing (Figure 5-8). Detection of significant differences in terms of functional recovery of the injured limbs at Day 7 post-ischemia might be too early, so longer time-point studies (28 days) are proposed in order to evaluate the effect of controlled delivery of FGF9 on reversing ischemia and restoration of function.

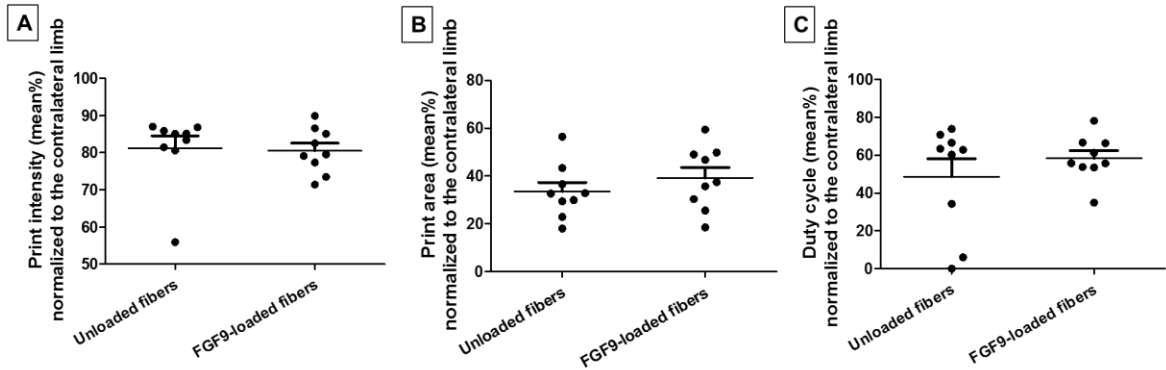


Figure 5-8: CatWalk automated quantitative gait analysis for mice treated with unloaded and FGF9-loaded PEA fibrous mats.

The values for (A) the print intensity, (B) print area and (C) duty cycle for the ischemic limb at Day 7, were normalized to that of the contralateral healthy limb and expressed as mean%, (n = 9) and each dot represents one mouse.

5.4.2.2 Histological Analysis of the TA Muscle Using H&E and Double-immunofluorescent Staining

Histological analysis of tissues harvested 7 days post-ischemia showed enhanced regeneration of the infarcted TA muscle and increased angiogenesis with reduced inflammation and minimal tissue necrosis as illustrated by the H&E photomicrographs (Figure 5-9). Moreover, a reduced presence of interstitial adipocytes in the regenerating skeletal muscle zone was observed for the injured hindlimbs treated with FGF9-loaded fibers.

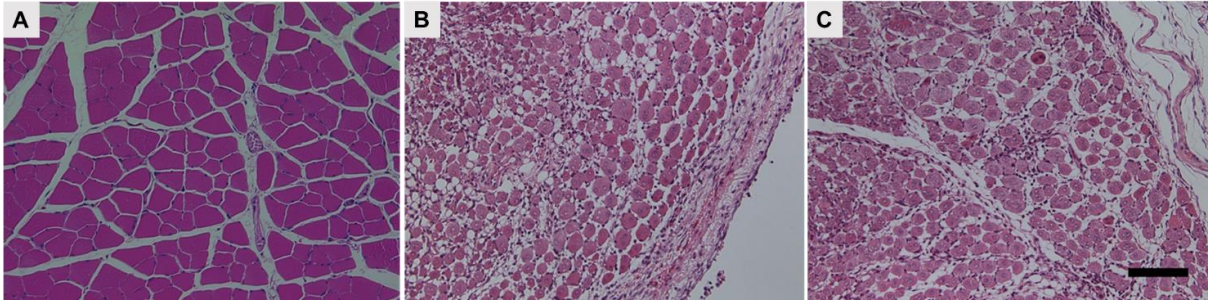


Figure 5-9: H&E staining of the histological sections of the TA muscle.

Photomicrographs of the TA muscle (20× objective) harvested at Day 7, (A) without infarction and after implantation of (B) unloaded PEA fibers and (C) FGF9-loaded PEA fibers 3 days prior to infarction (scale bar = 100 μm).

Fluorescence microscopy images of the TA muscle double-immunolabeled for CD31 and SM α -actin showed no difference in the number of CD31-positive microvessels between the TA muscles treated with unloaded and FGF9-loaded fibers (Figure 5-10). However, controlled delivery of FGF9 resulted in a statistically significant increase ($p < 0.05$) in the proportion of microvessels invested by SM α -actin-containing mural cells (Figure 5-10 B&D).

NG2 is a pericyte cell marker; it is expressed in nascent microvessels by vascular pericytes [30]. While, endomucin is a sialomucin or CD164 that is specifically expressed on the endothelium of adult mice during development of the vascular system [31]. Using NG2 as mural cell marker could give us further insights into the recruitment of mural cells by FGF9 and their investment of the neomicrovessels. Results from the NG2/endomucin double immunostaining of the TA muscle were similar to that observed from the CD31/SM α -actin double immunostaining, showing a statistically significant increase ($p < 0.01$) in the proportion of microvessels invested by NG2-containing mural cells, which confirms the enhanced mural cell wrapping of the microvessels due to the controlled release of the FGF9 (Figure 5-11).

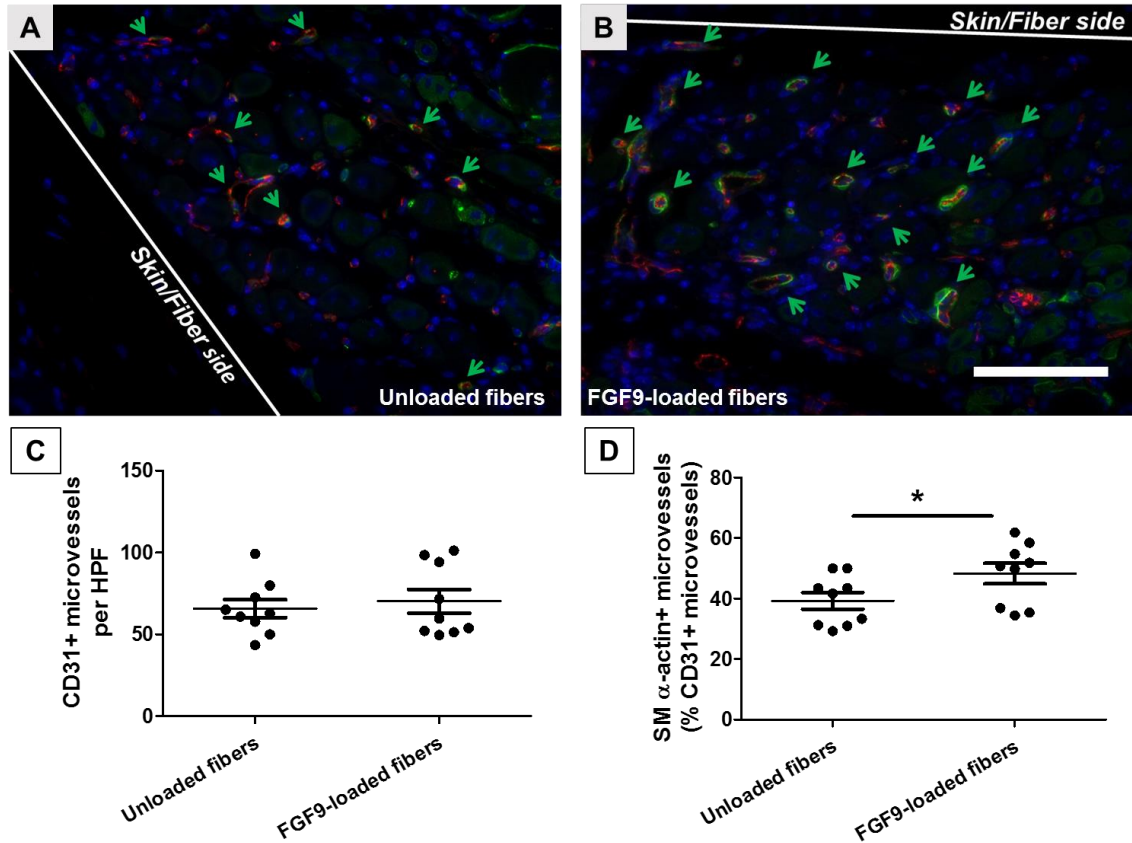


Figure 5-10: CD31/SM α -actin double immunostaining of histological sections of the TA muscle at Day 7 and quantitative estimation of SM α -actin+ microvessels at the skin side.

Fluorescence microscope images of TA muscle (40 \times objective) harvested 7 days after implantation of (A) unloaded PEA fibers and (B) FGF9-loaded PEA fibers, double immunolabeled for CD31 (red) and SM α -actin (green). Quantitative estimation of (C) the number of CD31+ arteriole-like microvessels at the skin side per high power field (40 \times objective), and (D) percentage of SM α -actin+ microvessels normalized to the total number of CD31+ microvessels per field (n = 9). Scale bar = 50 μ m and arrows are pointing to CD31/SM α -actin+ microvessels (* $p < 0.05$).

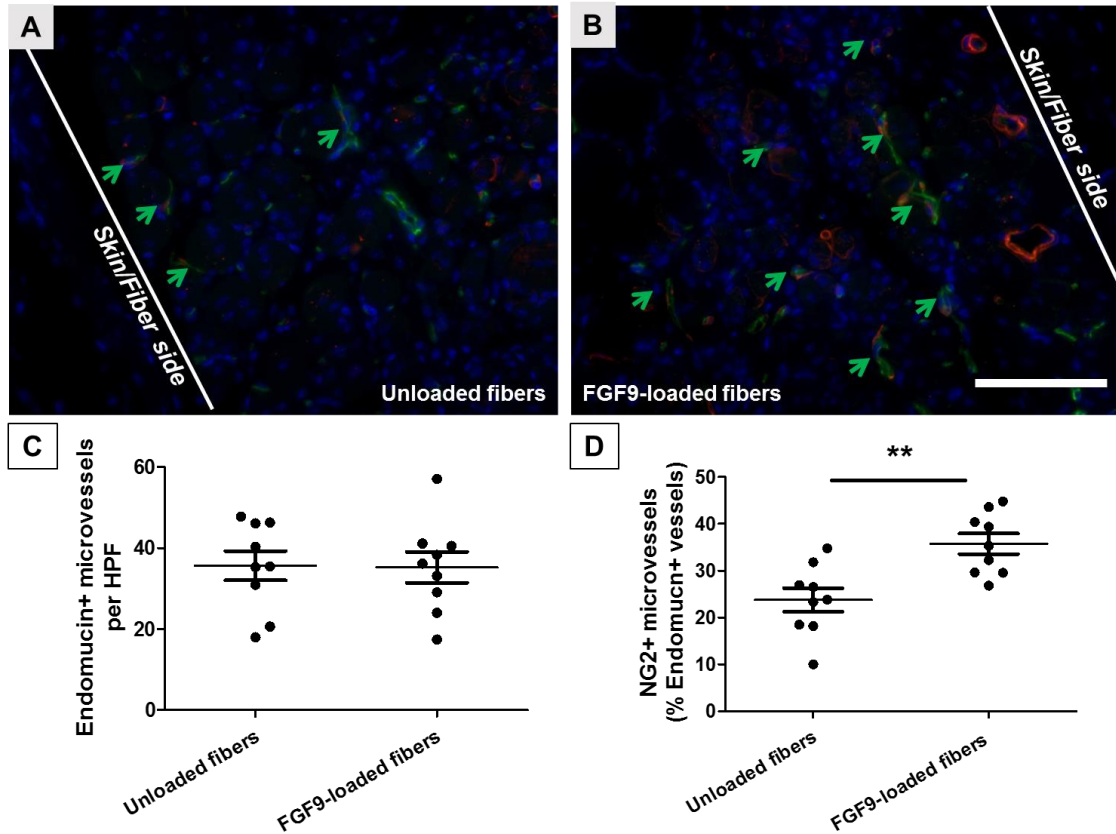


Figure 5-11: Endomucin/NG2 double immunostaining of histological sections of the TA muscle at Day 7 and quantitative estimation of NG2+ microvessels at the skin side. Fluorescence microscope images of TA muscle (40× objective) harvested 7 days after implantation of (A) unloaded PEA fibers and (B) FGF9-loaded PEA fibers, double immunolabeled for endomucin (green) and NG2 (red). Quantitative estimation of (C) the number of endomucin+ arteriole-like microvessels at the skin side per high power field (40× objective), and (D) percentage of NG2+ microvessels normalized to the total number of endomucin+ microvessels per field (n = 9). Scale bar = 50 μm and arrows are pointing to endomucin/NG2+ microvessels (** $p < 0.01$).

Polymer-based delivery vehicles offer great potential to deliver biologically active growth factors in a controlled fashion over a period of days to months to promote neovascularization [32-35]. Mooney and colleagues studied the use of injectable alginate hydrogel with PLGA microspheres for sequential delivery of VEGF and PDGF-BB in a myocardial infarction mouse model [36]. Cao *et al.* investigated the co-delivery of VEGF and PDGF-BB or the co-delivery of FGF2 and PDGF-BB, adsorbed onto heparinized sepharose beads embedded into Matrigel, to ischemic hindlimb model of rat and rabbit [37]. Formation of stable vasculature was observed for the co-delivery of FGF2 and PDGF, while vessel size and maturity was enhanced by sequentially delivering VEGF and PDGF [36-38]. However, VEGF can inhibit vessel maturation during PDGF-mediated angiogenesis [39]. Previous studies has shown that co-delivery of FGF2 and fibroblast growth factor-9 (FGF9) by the means of an osmotic pump to mouse ischemic hindlimb resulted in mature, persistent, and vasoreactive microvessels [40].

As described in Chapter 4, FGF2 and FGF9 were dual-loaded into biodegradable electrospun poly(ester amide) (PEA) fibers, which showed enhanced endothelial tube formation, increased smooth muscle cell migration and improved endothelial cell-smooth muscle cell interaction *in vitro* [22]. Building up on the previous promising results, it was desired to investigate its efficacy in induction of mature neovessel formation using *in vivo* models. FGF9 is a mesenchyme-targeting growth factor that plays a crucial role in the recruitment of mural cells and the formation of physiologically mature and stable neovessels [40]. It acts mainly through sonic hedgehog signaling, an upstream regulator of PDGFR β expression [40], and the PDGF-BB/PDGFR β signaling pathway was reported to be pivotal to recruiting SMCs and pericytes to the developing vasculature [41]. Controlled delivery of FGF9 from PEA fibers will protect FGF9 from rapid degradation and clearance from the application site, which was a major challenge of the delivery of growth factors in a soluble form as a bolus injection or infusion in the systemic circulation or tissue of interest [42-46]. Moreover, controlled delivery of FGF9 from PEA electrospun fibers provides predictable release kinetics of the bioactive agent, which can boost its stability, allow its sustained release in a biologically active form and provide a more efficient means of application at the site of interest [21].

5.5 Conclusion

In this chapter, electrospun PEA fibrous mats as a controlled delivery vehicle for FGF2 and FGF9 for potential therapeutic angiogenesis application, using two *in vivo* models, the CAM model (as a screening platform) and the ischemic hindlimb mouse model (as a pathological preclinical model) were evaluated. Localized angiogenesis was observed at the interface between the FGF-loaded fibrous mat and the CAM surface and there was a significant enhancement in the quality of vasculature in terms of increased amount of perfused blood as detected from the 3D power Doppler vascular quantification metrics (vascularization and vascularization flow indices) of the regions of interest of the CAM underneath the FGF-loaded PEA fibrous mats. Moving forward to a more clinically-relevant model (the ischemic hindlimb model), the implantation of the FGF9-loaded PEA fibrous mats on the surface of infarcted TA muscle resulted in an increased mural cell-wrapping of local microvessels compared to the unloaded fibers group as demonstrated by the H&E and double immunofluorescent staining. Taken together, FGF-loaded PEA electrospun fibers can have promising applications in therapeutic angiogenesis for treatment of ischemic vascular diseases and pre-vascularized tissue engineering.

5.6 References

1. Chow, L.W., R. Bitton, M.J. Webber, D. Carvajal, K.R. Shull, A.K. Sharma, and S.I. Stupp, A bioactive self-assembled membrane to promote angiogenesis. *Biomaterials*, 2011. **32**(6): 1574-82.
2. Zijlstra, A., M. Seandel, T.A. Kupriyanova, J.J. Partridge, M.A. Madsen, E.A. Hahn-Dantona, J.P. Quigley, and E.I. Deryugina, Proangiogenic role of neutrophil-like inflammatory heterophils during neovascularization induced by growth factors and human tumor cells. *Blood*, 2006. **107**(1): 317-27.
3. Rubinstein, A.L., Zebrafish: from disease modeling to drug discovery. *Curr Opin Drug Discov Devel*, 2003. **6**(2): 218-23.
4. Zheng, L., P. Ling, Z. Wang, R. Niu, C. Hu, T. Zhang, and X. Lin, A novel polypeptide from shark cartilage with potent anti-angiogenic activity. *Cancer Biol Ther*, 2007. **6**(5): 775-80.

5. Shan, S. and M.W. Dewhirst, Corneal angiogenesis assay, in *Angiogenesis Assays: A Critical Appraisal of Current Techniques*, C.A. Staton, R. Bicknell, and C.E. Lewis, Editors. 2006, John Willey & Sons: Chichester, UK. p. pp. 203-222.
6. Dragneva, G., P. Korpisalo, and S. Yla-Herttuala, Promoting blood vessel growth in ischemic diseases: challenges in translating preclinical potential into clinical success. *Dis Model Mech*, 2013. **6**(2): 312-22.
7. Gao, E., Y.H. Lei, X. Shang, Z.M. Huang, L. Zuo, M. Boucher, Q. Fan, J.K. Chuprun, X.L. Ma, and W.J. Koch, A novel and efficient model of coronary artery ligation and myocardial infarction in the mouse. *Circ Res*, 2010. **107**(12): 1445-53.
8. Harada, K., W. Grossman, M. Friedman, E.R. Edelman, P.V. Prasad, C.S. Keighley, W.J. Manning, F.W. Sellke, and M. Simons, Basic fibroblast growth factor improves myocardial function in chronically ischemic porcine hearts. *J Clin Invest*, 1994. **94**(2): 623-30.
9. Limbourg, A., T. Korff, L.C. Napp, W. Schaper, H. Drexler, and F.P. Limbourg, Evaluation of postnatal arteriogenesis and angiogenesis in a mouse model of hind-limb ischemia. *Nat Protoc*, 2009. **4**(12): 1737-46.
10. Tang, G.L., D.S. Chang, R. Sarkar, R. Wang, and L.M. Messina, The effect of gradual or acute arterial occlusion on skeletal muscle blood flow, arteriogenesis, and inflammation in rat hindlimb ischemia. *J Vasc Surg*, 2005. **41**(2): 312-20.
11. Adair, T.H. and J.P. Montani, Angiogenesis, in *Integrated Systems Physiology: from Molecule to Function to Disease*, D.N. Granger and J.P. Granger, Editors. 2010, Morgan & Claypool Life Sciences. 1-84.
12. Ribatti, D., *The Chick Embryo Chorioallantoic Membrane in the Study of Angiogenesis and Metastasis*. 2010: Springer Dordrecht Heidelberg London New York 89.
13. Staton, C.A., M.W. Reed, and N.J. Brown, A critical analysis of current in vitro and in vivo angiogenesis assays. *Int J Exp Pathol*, 2009. **90**(3): 195-221.
14. Weiss, A., J.R. van Beijnum, D. Bonvin, P. Jichlinski, P.J. Dyson, A.W. Griffioen, and P. Nowak-Sliwinska, Low-dose angiostatic tyrosine kinase inhibitors improve photodynamic therapy for cancer: lack of vascular normalization. *J Cell Mol Med*, 2014. **18**(3): 480-91.
15. Nowak-Sliwinska, P., T. Segura, and M.L. Iruela-Arispe, The chicken chorioallantoic membrane model in biology, medicine and bioengineering. *Angiogenesis*, 2014. **17**(4): 779-804.
16. Distler, J.H., A. Hirth, M. Kurowska-Stolarska, R.E. Gay, S. Gay, and O. Distler, Angiogenic and angiostatic factors in the molecular control of angiogenesis. *Q J Nucl Med*, 2003. **47**(3): 149-61.

17. Carmeliet, P., Angiogenesis in health and disease. *Nat Med*, 2003. **9**(6): 653-60.
18. Carmeliet, P., Angiogenesis in life, disease and medicine. *Nature*, 2005. **438**(7070): 932-6.
19. Carmeliet, P. and R.K. Jain, Molecular mechanisms and clinical applications of angiogenesis. *Nature*, 2011. **473**(7347): 298-307.
20. Knight, D.K., E.R. Gillies, and K. Mequanint, Strategies in Functional Poly(ester amide) Syntheses to Study Human Coronary Artery Smooth Muscle Cell Interactions. *Biomacromolecules*, 2011. **12**(7): 2475-87.
21. Said, S.S., J.G. Pickering, and K. Mequanint, Controlled Delivery of Fibroblast Growth Factor-9 from Biodegradable Poly(ester amide) Fibers for Building Functional Neovasculature. *Pharm Res*, 2014. **31**: 3335–3347.
22. Said, S.S., C. O'Neil, H. Yin, Z. Nong, J.G. Pickering, and K. Mequanint, Concurrent and Sustained Delivery of FGF2 and FGF9 from Electrospun Poly(ester amide) Fibrous Mats for Therapeutic Angiogenesis. *Tissue Eng Part A*, 2016. **22**(7-8): 584-596.
23. Leong, H.S., N.F. Steinmetz, A. Ablack, G. Destito, A. Zijlstra, H. Stuhlmann, M. Manchester, and J.D. Lewis, Intravital imaging of embryonic and tumor neovasculature using viral nanoparticles. *Nat Protoc*, 2010. **5**(8): 1406-17.
24. Schindelin, J., I. Arganda-Carreras, E. Frise, V. Kaynig, M. Longair, T. Pietzsch, S. Preibisch, C. Rueden, S. Saalfeld, B. Schmid, J.Y. Tinevez, D.J. White, V. Hartenstein, K. Eliceiri, P. Tomancak, and A. Cardona, Fiji: an open-source platform for biological-image analysis. *Nat Methods*, 2012. **9**(7): 676-82.
25. Elfarnawany, M., M.R. Lowerison, M.N. Hague, A.F. Chambers, and J.C. Lacefield. In vivo evaluation of an objective method to select power Doppler wall filter cut-off frequency for microvascular quantification. in *Ultrasonics Symposium (IUS), 2014 IEEE International*. 2014.
26. Elfarnawany, M., Signal Processing Methods for Quantitative Power Doppler Microvascular Angiography (Doctoral of Philosophy Thesis), in *Biomedical Engineering Graduate Program*. 2015, The University of Western Ontario: London. 167.
27. Elfarnawany, M., S.Z. Pinter, and J.C. Lacefield, Improved objective selection of power Doppler wall-filter cut-off velocity for accurate vascular quantification. *Ultrasound Med Biol*, 2012. **38**(8): 1429-39.
28. Pairleitner, H., H. Steiner, G. Hasenoehrl, and A. Staudach, Three-dimensional power Doppler sonography: imaging and quantifying blood flow and vascularization. *Ultrasound Obstet Gynecol*, 1999. **14**(2): 139-43.

29. Masocha, W. and S.S. Parvathy, Assessment of weight bearing changes and pharmacological antinociception in mice with LPS-induced monoarthritis using the Catwalk gait analysis system. *Life Sci*, 2009. **85**(11-12): 462-9.
30. Ozerdem, U., K.A. Grako, K. Dahlin-Huppe, E. Monosov, and W.B. Stallcup, NG2 proteoglycan is expressed exclusively by mural cells during vascular morphogenesis. *Dev Dyn*, 2001. **222**(2): 218-27.
31. Brachtendorf, G., A. Kuhn, U. Samulowitz, R. Knorr, E. Gustafsson, A.J. Potocnik, R. Fassler, and D. Vestweber, Early expression of endomucin on endothelium of the mouse embryo and on putative hematopoietic clusters in the dorsal aorta. *Dev Dyn*, 2001. **222**(3): 410-9.
32. King, T.W. and C.W. Patrick, Jr., Development and in vitro characterization of vascular endothelial growth factor (VEGF)-loaded poly(DL-lactic-co-glycolic acid)/poly(ethylene glycol) microspheres using a solid encapsulation/single emulsion/solvent extraction technique. *J Biomed Mater Res*, 2000. **51**(3): 383-90.
33. Zisch, A.H., M.P. Lutolf, and J.A. Hubbell, Biopolymeric delivery matrices for angiogenic growth factors. *Cardiovasc Pathol*, 2003. **12**(6): 295-310.
34. Cleland, J.L., E.T. Duenas, A. Park, A. Daugherty, J. Kahn, J. Kowalski, and A. Cuthbertson, Development of poly-(D,L-lactide--coglycolide) microsphere formulations containing recombinant human vascular endothelial growth factor to promote local angiogenesis. *J Control Release*, 2001. **72**(1-3): 13-24.
35. Silva, E.A. and D.J. Mooney, Spatiotemporal control of vascular endothelial growth factor delivery from injectable hydrogels enhances angiogenesis. *J Thromb Haemost*, 2007. **5**(3): 590-8.
36. Sun, Q., E.A. Silva, A. Wang, J.C. Fritton, D.J. Mooney, M.B. Schaffler, P.M. Grossman, and S. Rajagopalan, Sustained release of multiple growth factors from injectable polymeric system as a novel therapeutic approach towards angiogenesis. *Pharm Res*, 2010. **27**(2): 264-71.
37. Cao, R., E. Brakenhielm, R. Pawliuk, D. Wariaro, M.J. Post, E. Wahlberg, P. Leboulch, and Y. Cao, Angiogenic synergism, vascular stability and improvement of hind-limb ischemia by a combination of PDGF-BB and FGF-2. *Nat Med*, 2003. **9**(5): 604-13.
38. Chen, R.R., E.A. Silva, W.W. Yuen, and D.J. Mooney, Spatio-temporal VEGF and PDGF delivery patterns blood vessel formation and maturation. *Pharm Res*, 2007. **24**(2): 258-64.
39. Greenberg, J.I., D.J. Shields, S.G. Barillas, L.M. Acevedo, E. Murphy, J. Huang, L. Schepke, C. Stockmann, R.S. Johnson, N. Angle, and D.A. Cheresh, A role for VEGF as a negative regulator of pericyte function and vessel maturation. *Nature*, 2008. **456**(7223): 809-13.

40. Frontini, M.J., Z. Nong, R. Gros, M. Drangova, C. O'Neil, M.N. Rahman, O. Akawi, H. Yin, C.G. Ellis, and J.G. Pickering, Fibroblast growth factor 9 delivery during angiogenesis produces durable, vasoresponsive microvessels wrapped by smooth muscle cells. *Nat Biotechnol*, 2011. **29**(5): 421-427.
41. Lutolf, M.P. and J.A. Hubbell, Synthetic biomaterials as instructive extracellular microenvironments for morphogenesis in tissue engineering. *Nat Biotechnol*, 2005. **23**(1): 47-55.
42. Lee, K.Y., M.C. Peters, and D.J. Mooney, Comparison of vascular endothelial growth factor and basic fibroblast growth factor on angiogenesis in SCID mice. *J Control Release*, 2003. **87**(1-3): 49-56.
43. Freedman, S.B. and J.M. Isner, Therapeutic angiogenesis for coronary artery disease. *Ann Intern Med*, 2002. **136**(1): 54-71.
44. Simons, M. and J.A. Ware, Therapeutic angiogenesis in cardiovascular disease. *Nat Rev Drug Discov*, 2003. **2**(11): 863-71.
45. Cao, L. and D.J. Mooney, Spatiotemporal control over growth factor signaling for therapeutic neovascularization. *Adv Drug Delivery Rev*, 2007. **59**(13): 1340-50.
46. Annex, B.H. and M. Simons, Growth factor-induced therapeutic angiogenesis in the heart: protein therapy. *Cardiovasc Res*, 2005. **65**(3): 649-55.

Chapter 6

6 General Discussion and Conclusions

Overview: This chapter provides a summary of the research work and discusses the strengths and limitations of this work. Overall significance of the research work is highlighted and future directions are recommended.

6.1 Summary

In therapeutic angiogenesis, the use of recombinant protein growth factors is a preferred therapeutic strategy compared with gene therapy, as it potentially offers a more straightforward treatment [1]. Angiogenic growth factors have been delivered either by bolus injection or infusion into the systemic circulation or the tissues of interest. However, the short half-life of these proteins results in a low local availability at the site of interest that represents the major challenge for angiogenic protein therapy [2]. One approach to overcome such limitation is the localized and sustained delivery of growth factors at the desired site from polymer-based delivery systems [3, 4].

Hence, the focus of this research was to develop a controlled delivery system for the sustained release of angiogenic growth factors over a period of weeks to months in order to mimic the normal multifaceted angiogenic process and to exogenously augment it [5]. To that end, 8-Phe-4, a member of the biodegradable poly(ester amide) (PEA) family was utilized to fabricate electrospun nanofibers. The rationale for exploring PEAs is that they combine the favorable properties of both polyesters and polyamides – the tunability in the degradation rate via the ester groups and mechanical strength via the hydrogen bonding of the amide groups. The ester and amide linkages promote both hydrolytic and enzymatic degradation, which should ensure a surface degradation mechanism [6], and this provides better prediction and control over the release profile. In addition, PEAs with tailored degradation rates can be synthesized with the careful selection of the monomers. Their degradation by-products include amino acids, which are found physiologically, limiting their potential systemic toxicity [7]. Unlike polyesters, PEA degradation results in less

acidic by-products, avoiding significant pH decrease in the tissues and thus decreased host immune responses [8].

One or multiple growth factors can be loaded into PEA delivery vehicles, potentially sustaining their release, enhancing their therapeutic efficacy and accelerating favorable cell-material interactions. And the ultimate goal is to support the formation of functional and stable neovasculature. Electrospinning is a versatile technique that can produce delivery vehicles with high surface area-to-volume ratio, which can prolong the angiogenic factor release and overcome difficulties encountered with angiogenic factor incorporation within conventional delivery systems, such as controlling the release profile and retaining growth factor bioactivity. Angiogenic growth factors were previously loaded into electrospun fibers using blending, emulsion and coaxial electrospinning [9-11], or through heparin immobilization onto electrospun scaffolds [12]. Controlled-release biodegradable polymeric fibers can serve as a simple, low-cost and efficient alternative for implantable mini-infusion pumps for the delivery of angiogenic growth factors, without the need of delivery system removal after depletion of the growth factor.

Although stimulating angiogenesis using angiogenic growth factors is an essential first step, it might not be a sufficient condition for producing a stable neovasculature. The absence of mural cell coverage subjects newly formed vessels to regression; however, nascent vessels are stabilized and become resistant to regression once they are invested with pericytes [13]. To mimic the complex angiogenesis process, the delivery of more than one growth factor in a differential and sustained fashion is required in order to pattern neovessel maturation and to achieve functional vascular formation. Fibroblast growth factor-9 (FGF9), an arteriogenic growth factor, was recently reported to play a crucial role in the recruitment of mural cells and the formation of physiologically mature and stable neovessels [14]. It acts mainly through Sonic Hedgehog signaling, an upstream regulator of platelet-derived growth factor receptor- β (PDGFR β) expression [14], and the PDGF-BB/PDGFR β signaling pathway was reported to be pivotal to recruiting mural cells to the developing vasculature [15]. When FGF9 was infused into ischemic mouse hindlimb, the resulting microvessels were found to be invested with more vascular smooth muscle cells than those generated in the absence of FGF-9. In addition, FGF-9 injection had led to

enhanced regeneration of the skeletal muscle, along with restoration of limb function [14, 16]. Hence, FGF9 sustained delivery could potentially drive muscularization of angiogenic sprouts and help regenerate functional neovasculature in ischemic vascular disease patients.

In the current work, a controlled delivery system for the sustained release of FGF9 has been developed utilizing electrospun PEA fibers fabricated by either blend or emulsion electrospinning technique. The morphological properties of the FGF-loaded fibers have been characterized using SEM and TEM. *In vitro* PEA matrix degradation, biocompatibility, *in vitro* FGF9 and FGF2 release kinetics, and bioactivity of the released growth factor were evaluated. RT-qPCR was employed to evaluate PDGFR β gene expression in NIH-3T3 fibroblasts, 10T1/2 cells, and human coronary artery smooth muscle cells cultured on PEA fibers at different FGF9 concentrations. FGF9-loaded PEA fibers exhibited controlled release of FGF9 over 28 days with limited burst effect while preserving the FGF9 bioactivity. Electrospun PEA fibers were found to support the proliferation of fibroblasts for five days even in serum-depleted medium. Cells cultured on FGF9-supplemented PEA mats resulted in upregulation of PDGFR β in concentration and cell type-dependent manner (Chapter 3).

Subsequently, FGF2 and FGF9 were dual-loaded using a mixed blend and emulsion electrospinning technique, and exhibited differential and sustained-release from PEA fibers over 70 days with preserved bioactivity. *In vitro* angiogenesis assays showed enhanced endothelial cell (EC) tube formation and directed-migration of smooth muscle cells (SMCs) to PDGF-BB, and stabilized EC-SMC tube formation. FGF2/FGF9-loaded PEA fibers did not induce significant inflammatory response *in vitro* as shown by the low interleukin-8 mRNA expression of THP-1 human monocytic cell line or *in vivo* after their subcutaneous implantation into mice. Histological examination showed that FGF2/FGF9-loaded fibers induced cell niche recruitment around the site of implantation. Furthermore, controlled *in vivo* delivery of FGF9 to mouse tibialis anterior muscle resulted in a dose-dependent expansion of mesenchymal progenitor-like cell layers and ECM deposition (Chapter 4).

Lastly, FGF-loaded PEA fibers were evaluated using two *in vivo* models, the CAM model as a screening platform and the ischemic hindlimb mouse model as a pathological pre-clinical model (Chapter 5). The CAM assay coupled with 3D power Doppler vascular quantification showed localized angiogenic effects at the regions underneath the FGF-loaded fibrous mats, which could indicate the assembly of stable microvessels and increased blood flow in the CAM owing to the controlled release of FGF2 and FGF9. Moreover, the implantation of the FGF9-loaded PEA fibrous mats on the surface of infarcted tibialis anterior muscle resulted in an enhanced skeletal muscle regeneration and increased abundance of mural-wrapped microvessels compared with the unloaded fibers control group as demonstrated by the histological analysis. At Day 7 post-ischemia, there was no significant difference in terms of usage of the injured limb for weight bearing, between the injured limbs treated with FGF9-loaded fibers compared with those treated with unloaded PEA fibers. Longer time-point studies (28 days) are proposed to evaluate the effect of controlled delivery of FGF9 on reversing ischemia and restoration of function.

6.2 Strengths and Limitations

Firstly, although PEAs have been electrospun previously from alanine and phenylalanine [17, 18], smaller average fiber diameter (~ 250 nm) was achieved with electrospinning of 8-Phe-4, due to the higher molecular weight of the synthesized polymer by interfacial polymerization, and subsequent reduction in the concentration of the polymer required for reaching the optimal viscosity needed for electrospinning. This would impart increased surface area-to-volume ratio, which facilitates improved drug loading. The solution and processing parameters were optimized for fabricating defect-free fibers.

Secondly, although model compounds have been previously loaded into PEA ultrafine fibers [17, 18], this study demonstrated the versatility of PEA electrospun fibers as a controlled delivery vehicle for different bioactive molecules (bovine serum albumin, FGF2 and FGF9) with varying molecular weights (from 14 kD to 60 kD), and dual loading of two growth factors using mixed blend and emulsion electrospinning techniques. Also, the bioactivity of the released growth factors and their *in vitro* release kinetics have been investigated. The surface erosion degradation mechanism of PEA fibers was studied and correlated to the *in vitro* release

profile of the growth factors. The *in vitro* biocompatibility of the developed 3D scaffold have been assessed and the PEA fibrous scaffolds demonstrated positive interaction with different types of cells (NIH 3T3 fibroblasts, C3H 10T1/2 cells and human coronary artery smooth muscle cells (HCASMC)) in terms of attachment, spreading and proliferation.

Another strength of this study is the evaluation of the induced host immune response *in vitro* using human monocytes followed by analysis of gene expression of a targeted inflammatory marker (Interleukin 8), and *in vivo* by subcutaneous implantation of the fibrous mats in mice. PEA fibers neither elicited inflammatory responses nor induced scar formation. Although inflammation is usually associated with a biomaterial implantation in a host and negative outcomes (*e.g.*, fibrosis and implant rejection) might take place, some inflammatory reactions can have positive outcomes that can promote biomaterial-tissue integration and regeneration [19, 20]. Notwithstanding that, severe induced inflammation and host response often preclude many synthetic biomaterials from growth factor delivery applications [21].

Moreover, the angiogenic capacity of the FGF-loaded PEA fibers have been evaluated through *in vitro* angiogenesis assays (Matrigel tube formation and directed migration assays). Treatment with FGF2/FGF9-loaded PEA fibers showed enhanced tube formation and directed migration of HCASMC towards a chemotactic agent PDGF-BB, as well as increased interaction between ECs and SMCs. Also, it was evaluated *in vivo* using two models; the chick chorioallantoic membrane (CAM) assay, as a quick screening platform, and the ischemic hindlimb mouse model as a pathological model. The CAM assay demonstrated a localized angiogenic effect due to the controlled release of FGF2 and FGF9, and 3D power Doppler vascular quantification showed improvement in the quality of microvessels in terms of blood perfusion in the local microenvironment underneath the fibrous mat. In the ischemic hindlimb mouse model, injured limbs treated with FGF9-loaded PEA mats resulted in an enhanced regeneration of the ischemic skeletal muscle with reduced inflammation and minimal tissue necrosis, and increased abundance of mural-covered microvessels.

The CAM model was simple and it provided a better physiological system for *in vivo* analysis than the *in vitro* assays, but it had some limitations in detecting a significant increase in vascular density of the full CAM vasculature due to its rapid vascular growth that outpaced the controlled and relatively slow release of FGF2 and FGF9 from the PEA

fibers. In addition, the released amount of growth factors from the fibers might not have reached the effective therapeutic dose to induce significant angiogenesis in the full CAM surface.

The histological analysis of the ischemic hindlimb mouse model showed promising initial results 10 days after implantation of the FGF9-loaded fibers in terms of enhanced regeneration of the ischemic skeletal muscle and increased abundance of mural-covered microvessels. The CatWalk gait analysis for the mice treated with FGF9-loaded fibrous mats did not show superior restoration of function of the injured limb when compared with the group treated with unloaded fibers. Detection of significant differences at Day 7 post-ischemia in terms of functional recovery of the injured limbs might be early. In view of this, longer time-point studies (28 days) are proposed in order to evaluate the effect of controlled delivery of FGF9 on reversing ischemia and restoration of function.

6.3 Future Directions

This study investigated the utility of electrospun PEA fibers for dual and sustained delivery of FGF2 and FGF9 for therapeutic angiogenesis application and the data collectively indicated that they are promising candidates. In order to advance to the level of angiogenic therapy clinical studies, the aforementioned limitations with the current study, including rapid vascular growth of the CAM model that outpaced the controlled and slow release of FGF2 and FGF9 from the PEA fibers and the CatWalk gait analysis for Day 7 post-ischemia study that was not able to detect superior restoration of injured limb function for the FGF9-loaded fibers treated mice, have to be addressed. And to that end:

- Longer time-point ischemic hindlimb mouse study (28 days) is proposed in order to evaluate the effect of controlled delivery of FGF9 on reversing ischemia and restoration of function.
- Ischemic hindlimb perfusion can be assessed by laser Doppler perfusion imaging and a perfusion ratio can be determined by dividing the mean perfusion value of the dorsal side of the ischemic limb by that of the identical region of the non-ischemic limb of the mouse.

- RT-qPCR analysis can be employed for *in vivo* samples to evaluate the mRNA expression of other inflammatory markers, such as interleukin-6 (IL-6), interleukin-1 (IL-1), tumor necrosis factor alpha (TNF- α) and interferon gamma (IFN-gamma), together with specific immunohistochemical staining of inflammatory cells (such as CD68, CD163 and F4/80).
- Studying the release kinetics and diffusion pattern of FGF9 *in vivo* from the PEA fibers to the infarcted muscle and determining the concentration gradient across different regions of the tibialis anterior muscle from the skin side to the bone side is recommended, which may provide better understanding about the therapeutic efficiency of the released FGF9 *in vivo*.
- Deeper *in vivo* investigation of the signaling pathway *via* which FGF9 controls the mural cell-wrapping of microvessels building on the signaling cascade proposed by Frontini *et al.* [14], by conducting RT-qPCR and Western blot protein analyses of selected signaling molecules other than PDGFR- β .
- The use of alternative ischemic models is also suggested, such as myocardial infarction models of larger animals (*e.g.*, canine and porcine models), in order to better mimic the clinical situation of ischemic vascular disease and have a more comprehensive investigation of the effects of the controlled delivery of FGF9 on targeting neovessel maturation.

6.4 Significance

This study provides a novel strategy of using amino acid-based biodegradable poly(ester amide)s to fabricate electrospun fibrous scaffolds for sustained-release of single or multiple angiogenic growth factors, thus providing a means for minimally invasive revascularisation technique as the next advance in the treatment of ischemic vascular diseases.

6.5 References

1. Renault, M.A. and D.W. Losordo, Therapeutic myocardial angiogenesis. *Microvasc Res*, 2007. **74**(2-3): 159-71.
2. Lee, K.Y., M.C. Peters, and D.J. Mooney, Comparison of vascular endothelial growth factor and basic fibroblast growth factor on angiogenesis in SCID mice. *J Control Release*, 2003. **87**(1-3): 49-56.
3. Roy, R.S., B. Roy, and S. Sengupta, Emerging technologies for enabling proangiogenic therapy. *Nanotechnology*, 2011. **22**(49): 494004.
4. Cao, L. and D.J. Mooney, Spatiotemporal control over growth factor signaling for therapeutic neovascularization. *Adv Drug Delivery Rev*, 2007. **59**(13): 1340-50.
5. Ruel, M. and F.W. Sellke, Angiogenic protein therapy. *Semin Thorac Cardiovasc Surg*, 2003. **15**(3): 222-35.
6. Fan, Y., M. Kobayashi, and H. Kise, Synthesis and specific biodegradation of novel polyesteramides containing amino acid residues. *Journal of Polymer Science Part A: Polymer Chemistry*, 2001. **39**(9): 1318-1328.
7. Knight, D.K., E.R. Gillies, and K. Mequanint, Strategies in Functional Poly(ester amide) Syntheses to Study Human Coronary Artery Smooth Muscle Cell Interactions. *Biomacromolecules*, 2011. **12**(7): 2475-87.
8. Vert, M., S. Li, and H. Garreau, New insights on the degradation of bioresorbable polymeric devices based on lactic and glycolic acids. *Clinical materials*, 1992. **10**(1-2): 3-8.
9. Sahoo, S., L.T. Ang, J.C.-H. Goh, and S.-L. Toh, Growth factor delivery through electrospun nanofibers in scaffolds for tissue engineering applications. *J Biomed Mater Res*, 2010. **93A**: 1539–1550.
10. Yang, Y., T. Xia, W. Zhi, L. Wei, J. Weng, C. Zhang, and X. Li, Promotion of skin regeneration in diabetic rats by electrospun core-sheath fibers loaded with basic fibroblast growth factor. *Biomaterials*, 2011. **32**(18): 4243-54.
11. Rubert, M., J. Dehli, Y.-F. Li, M.B. Taskin, R. Xu, F. Besenbacher, and M. Chen, Electrospun PCL/PEO coaxial fibers for basic fibroblast growth factor delivery. *J Mater Chem B*, 2012. **2**(48): 8538-8546.
12. Leong, N.L., A. Arshi, N. Kabir, A. Nazemi, F.A. Petrigliano, B.M. Wu, and D.R. McAllister, In vitro and in vivo evaluation of heparin mediated growth factor release from tissue-engineered constructs for anterior cruciate ligament reconstruction. *J Orthop Res*, 2015. **33**(2): 229-236.

13. Benjamin, L.E., D. Golijanin, A. Itin, D. Pode, and E. Keshet, Selective ablation of immature blood vessels in established human tumors follows vascular endothelial growth factor withdrawal. *J Clin Invest*, 1999. **103**(2): 159-65.
14. Frontini, M.J., Z. Nong, R. Gros, M. Drangova, C. O'Neil, M.N. Rahman, O. Akawi, H. Yin, C.G. Ellis, and J.G. Pickering, Fibroblast growth factor 9 delivery during angiogenesis produces durable, vasoresponsive microvessels wrapped by smooth muscle cells. *Nat Biotechnol*, 2011. **29**(5): 421-427.
15. Lutolf, M.P. and J.A. Hubbell, Synthetic biomaterials as instructive extracellular microenvironments for morphogenesis in tissue engineering. *Nat Biotechnol*, 2005. **23**(1): 47-55.
16. Niklason, L.E., Building stronger microvessels. *Nat Biotechnol*, 2011. **29**(5): 405-6.
17. Li, L. and C.C. Chu, Nitroxyl radical incorporated electrospun biodegradable poly(ester Amide) nanofiber membranes. *J Biomater Sci Polym Ed*, 2009. **20**(3): 341-61.
18. del Valle, L.J., M. Roa, A. Díaz, M.T. Casas, J. Puiggalí, and A. Rodríguez-Galán, Electrospun nanofibers of a degradable poly(ester amide). Scaffolds loaded with antimicrobial agents. *Journal of Polymer Research*, 2012. **19**(2): 1-13.
19. Crupi, A., A. Costa, A. Tarnok, S. Melzer, and L. Teodori, Inflammation in tissue engineering: The Janus between engraftment and rejection. *Eur J Immunol*, 2015. **45**(12): 3222-36.
20. Padmanabhan, J. and T.R. Kyriakides, Nanomaterials, inflammation, and tissue engineering. *Wiley Interdiscip Rev Nanomed Nanobiotechnol*, 2015. **7**(3): 355-70.
21. Anderson, J.M., A. Rodriguez, and D.T. Chang, Foreign body reaction to biomaterials. *Semin Immunol*, 2008. **20**(2): 86-100.

Appendices

Appendix A: Copyright Permissions

29/06/2016

Rightslink® by Copyright Clearance Center



RightsLink®

Account
Info

Help

KARGER

Title: Advances in Growth Factor Delivery for Therapeutic Angiogenesis
Author: Said Somiraa S., Pickering J. Geoffrey, Mequanint Kibret
Publication: Journal of Vascular Research
Publisher: Karger Publishers
Date: Nov 15, 2012

Logged in as:
Somiraa Said
Account #:
3000506994

LOGOUT

Copyright © 2012, Karger Publishers

Review Order

Please review the order details and the associated [terms and conditions](#).

Last Comment:

Dear Mrs Said,

Thank you for your request. We are pleased to inform you that permission is granted herewith to use your article

Said S.S. et al; Advances in Growth Factor Delivery for Therapeutic Angiogenesis: J Vasc Res 2013;50:35â51 (DOI:10.1159/000345108)

to be reproduced in your PhD thesis. This permission covers the right to have the PhD thesis including the above-mentioned article archived in the university's repository.

Please note that this is a non-exclusive permission, hence any further use, edition, translation or distribution, either in print or electronically, requires written permission again as this permission is valid for the above mentioned purpose only.

Hopefully, we have been of assistance to you.

Best regards,

David Schaub
Legal Advisor
S. Karger AG

No royalties will be charged for this reuse request although you are required to obtain a license and comply with the license terms and conditions. To obtain the license, click the Accept button below.

**NATURE PUBLISHING GROUP LICENSE
TERMS AND CONDITIONS**

Jun 28, 2016

This Agreement between Somiraa Said ("You") and Nature Publishing Group ("Nature Publishing Group") consists of your license details and the terms and conditions provided by Nature Publishing Group and Copyright Clearance Center.

License Number	3897701068992
License date	Jun 28, 2016
Licensed Content Publisher	Nature Publishing Group
Licensed Content Publication	Nature Biotechnology
Licensed Content Title	Building stronger microvessels
Licensed Content Author	Laura E Niklason
Licensed Content Date	May 6, 2011
Licensed Content Volume Number	29
Licensed Content Issue Number	5
Type of Use	reuse in a dissertation / thesis
Requestor type	academic/educational
Format	electronic
Portion	figures/tables/illustrations
Number of figures/tables/illustrations	1
High-res required	no
Figures	Figure 1
Author of this NPG article	no
Your reference number	Chapter 2- 92
Title of your thesis / dissertation	CONTROLLED DELIVERY OF ANGIOGENIC AND ARTERIOGENIC GROWTH FACTORS FROM BIODEGRADABLE POLY(ESTER AMIDE) ELECTROSPUN FIBERS FOR THERAPEUTIC ANGIOGENESIS
Expected completion date	Aug 2016
Estimated size (number of pages)	200
Requestor Location	Somiraa Said Biomedical Engineering Graduate Program The University of Western Ontario London, ON, CANADA London, ON N6A 5B7 Canada Attn: Somiraa Said
Billing Type	Invoice
Billing Address	Somiraa Said Biomedical Engineering Graduate Program The University of Western Ontario London, ON, CANADA

**SPRINGER LICENSE
TERMS AND CONDITIONS**

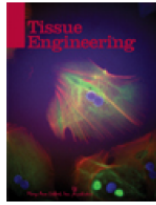
Jun 28, 2016

This Agreement between Somiraa Said ("You") and Springer ("Springer") consists of your license details and the terms and conditions provided by Springer and Copyright Clearance Center.

License Number	3897680246319
License date	Jun 28, 2016
Licensed Content Publisher	Springer
Licensed Content Publication	Pharmaceutical Research
Licensed Content Title	Controlled Delivery of Fibroblast Growth Factor-9 from Biodegradable Poly(ester amide) Fibers for Building Functional Neovasculature
Licensed Content Author	Somiraa S. Said
Licensed Content Date	Jan 1, 2014
Licensed Content Volume Number	31
Licensed Content Issue Number	12
Type of Use	Thesis/Dissertation
Portion	Full text
Number of copies	1
Author of this Springer article	Yes and you are the sole author of the new work
Order reference number	
Title of your thesis / dissertation	CONTROLLED DELIVERY OF ANGIOGENIC AND ARTERIOGENIC GROWTH FACTORS FROM BIODEGRADABLE POLY(ESTER AMIDE) ELECTROSPUN FIBERS FOR THERAPEUTIC ANGIOGENESIS
Expected completion date	Aug 2016
Estimated size(pages)	200
Requestor Location	Somiraa Said Biomedical Engineering Graduate Program The University of Western Ontario London, ON, CANADA London, ON N6A 5B7 Canada Attn: Somiraa Said
Billing Type	Invoice
Billing Address	Somiraa Said Biomedical Engineering Graduate Program The University of Western Ontario London, ON, CANADA London, ON N6A 5B7 Canada Attn: Somiraa Said
Total	0.00 USD
Terms and Conditions	



RightsLink®

[Home](#)
[Account Info](#)
[Help](#)


Title: Concurrent and Sustained Delivery of FGF2 and FGF9 from Electrospun Poly(ester amide) Fibrous Mats for Therapeutic Angiogenesis

Author: Somiraa S. Said, Caroline O'Neil, Hao Yin, et al

Publication: Tissue Engineering Part A

Publisher: Mary Ann Liebert, Inc.

Date: Apr 1, 2016

Copyright © 2016, Mary Ann Liebert, Inc.

Logged in as:

Somiraa Said

Account #:

3000506994

[LOGOUT](#)

Permissions Request

Mary Ann Liebert, Inc. publishers does not require authors of the content being used to obtain a license for their personal reuse of full article, charts/graphs/tables or text excerpt.

[BACK](#)
[CLOSE WINDOW](#)

Copyright © 2016 [Copyright Clearance Center, Inc.](#) All Rights Reserved. [Privacy statement.](#) [Terms and Conditions.](#) Comments? We would like to hear from you. E-mail us at customercare@copyright.com

**SPRINGER LICENSE
TERMS AND CONDITIONS**

Jun 28, 2016

This Agreement between Somiraa Said ("You") and Springer ("Springer") consists of your license details and the terms and conditions provided by Springer and Copyright Clearance Center.

License Number	3897671431335
License date	Jun 28, 2016
Licensed Content Publisher	Springer
Licensed Content Publication	Angiogenesis
Licensed Content Title	The chicken chorioallantoic membrane model in biology, medicine and bioengineering
Licensed Content Author	Patrycja Nowak-Sliwinska
Licensed Content Date	Jan 1, 2014
Licensed Content Volume Number	17
Licensed Content Issue Number	4
Type of Use	Thesis/Dissertation
Portion	Figures/tables/illustrations
Number of figures/tables/illustrations	1
Author of this Springer article No	
Order reference number	Chapter 5-25
Original figure numbers	Figure 8 (A-C)
Title of your thesis / dissertation	CONTROLLED DELIVERY OF ANGIOGENIC AND ARTERIOGENIC GROWTH FACTORS FROM BIODEGRADABLE POLY(ESTER AMIDE) ELECTROSPUN FIBERS FOR THERAPEUTIC ANGIOGENESIS
Expected completion date	Aug 2016
Estimated size(pages)	200
Requestor Location	Somiraa Said Biomedical Engineering Graduate Program The University of Western Ontario London, ON, CANADA London, ON N6A 5B7 Canada Attn: Somiraa Said
Billing Type	Invoice
Billing Address	Somiraa Said Biomedical Engineering Graduate Program The University of Western Ontario London, ON, CANADA London, ON N6A 5B7 Canada Attn: Somiraa Said
Total	0.00 CAD

**NATURE PUBLISHING GROUP LICENSE
TERMS AND CONDITIONS**

Jun 28, 2016

This Agreement between Somiraa Said ("You") and Nature Publishing Group ("Nature Publishing Group") consists of your license details and the terms and conditions provided by Nature Publishing Group and Copyright Clearance Center.

License Number	3897681043409
License date	Jun 28, 2016
Licensed Content Publisher	Nature Publishing Group
Licensed Content Publication	Nature Protocols
Licensed Content Title	Evaluation of postnatal arteriogenesis and angiogenesis in a mouse model of hind-limb ischemia
Licensed Content Author	Anne Limbourg, Thomas Korff, L Christian Napp, Wolfgang Schaper, Helmut Drexler et al.
Licensed Content Date	Nov 5, 2009
Licensed Content Volume Number	4
Licensed Content Issue Number	12
Type of Use	reuse in a dissertation / thesis
Requestor type	academic/educational
Format	electronic
Portion	figures/tables/illustrations
Number of figures/tables/illustrations	1
High-res required	no
Figures	Figure 3
Author of this NPG article	no
Your reference number	Chapter 5- 8
Title of your thesis / dissertation	CONTROLLED DELIVERY OF ANGIOGENIC AND ARTERIOGENIC GROWTH FACTORS FROM BIODEGRADABLE POLY(ESTER AMIDE) ELECTROSPUN FIBERS FOR THERAPEUTIC ANGIOGENESIS
Expected completion date	Aug 2016
Estimated size (number of pages)	200
Requestor Location	Somiraa Said Biomedical Engineering Graduate Program The University of Western Ontario London, ON, CANADA London, ON N6A 5B7 Canada Attn: Somiraa Said
Billing Type	Invoice
Billing Address	Somiraa Said Biomedical Engineering Graduate Program

Curriculum Vitae

Name: Somiraa Said

Post-secondary Education and Degrees: Alexandria University
Alexandria, Egypt
Bachelor of Pharmaceutical Sciences
2000-2005

Alexandria University
Alexandria, Egypt
Master of Science in Pharmaceutical Sciences (Pharmaceutics)
2007-2010

Honors and Awards: CIHR Strategic Training Program in Vascular Research fellowship
The University of Western Ontario,
London, ON, Canada
2011-2013

Related Work Experience: Teaching Assistant (Pharmaceutics Department)
Alexandria University
2005-2010

Assistant Lecturer (Pharmaceutics Department)
Alexandria University
2010-present (Study Leave for Doctoral Studies)

Teaching Assistant (Chemical and Biochemical Engineering)
The University of Western Ontario
2012-2015

Publications:

6- Somiraa S. Said, Caroline O'Neil, Hao Yin, Zengxuan Nong, J. Geoffrey Pickering and Kibret Mequanint. *Concurrent and Sustained delivery of FGF2 and FGF9 from Poly(ester amide) Fibers for Therapeutic Angiogenesis*, **Tissue Engineering Part A (2016), 22(7-8): 584-596. (Research article)**

5- Somiraa S. Said, J. Geoffrey Pickering and Kibret Mequanint. *Controlled Delivery of Fibroblast Growth Factor-9 from Biodegradable Poly(ester amide) Fibers for Building Functional Neovasculature*. **Pharmaceutical Research (2014), 31(12); 3335-3347. (Research article)**

4- Lisa Rogers, Somiraa S. Said, and Kibret Mequanint. The Effects of Fabrication Strategies on 3D Scaffold Morphology, Porosity, and Smooth Muscle Cell Response. **J. Biomater. Tissue Eng., 3 (2013); 300-311. (Research article)**

3- Somiraa S. Said, J. Geoffrey Pickering and Kibret Mequanint. *Advances in growth factor delivery for therapeutic angiogenesis*. **J. Vasc. Res., (2013), 50; 35-51. (Review article)**

2- Somiraa S. Said, Omar M. El-Halfawy, Hanan M. El-Gowell, Affaf K. Aloufy, Nabila A. Boraie, and Labiba K. El-Khordagui. *Bioburden-responsive antimicrobial PLGA ultrafine fibers for wound healing*. **Eur. J. Pharm. Biopharm., 80 (2012); 85-94. (Research article)**

1- Somiraa S. Said, Affaf K. Aloufy, Omar M. El-Halfawy, Nabila A. Boraie, and Labiba K. El-Khordagui. *Antimicrobial PLGA ultrafine fibers: Interaction with wound bacteria*. **Eur. J. Pharm. Biopharm., 79 (2011); 108-118. (Research article)**

Patents:

Somiraa S. Said, Omar M. El-Halfawy, Affaf K. Aloufy, Nabila A. Boraie, and Labiba K. El-Khordagui. *Smart antimicrobial polymeric ultrafine fibres for the preparation of novel wound dressings*. **National Patent Pending** applied for to the Patent office, Egyptian Ministry of Scientific Research, **Application No. 2010060999**.